ACTION POTENTIAL DISCHARGE IN SOMATA AND DENDRITES OF CA1 PYRAMIDAL NEURONS OF MAMMALIAN HIPPOCAMPUS: AN ELECTROPHYSIOLOGICAL ANALYSIS

by

RAY W. TURNER

B.Sc., University of British Columbia

A THESIS SUBMITTED IN PARTIAL FULFILLMENT OF

THE REQUIREMENTS FOR THE DEGREE OF

DOCTOR OF PHILOSOPHY

in

THE FACULTY OF GRADUATE STUDIES

(Department of Physiology)

We accept this thesis as conforming

to the required standard

THE UNIVERSITY OF BRITISH COLUMBIA

August, 1985

In presenting this thesis in partial fulfilment of the requirements for an advanced degree at the University of British Columbia, I agree that the Library shall make it freely available for reference and study. I further agree that permission for extensive copying of this thesis for scholarly purposes may be granted by the head of my department or by his or her representatives. It is understood that copying or publication of this thesis for financial gain shall not be allowed without my written permission.

Department of Physiology

The University of British Columbia
1956 Main Mall
Vancouver, Canada
V6T 1Y3

Date August 15, 1985

ABSTRACT

The electrophysiological properties of somatic and dendritic membranes of CA1 pyramidal neurons were investigated using the rat *in vitro* hippocampal slice preparation. A comprehensive analysis of extracellular field potentials, current-source density (CSD) and intracellular activity has served to identify the site of origin of action potential (AP) discharge in CA1 pyramidal neurons.

1) Action potential discharge of CA1 pyramidal cells was evoked by suprathreshold stimulation of the alveus (antidromic) or afferent synaptic inputs in stratum oriens (SO) or stratum radiatum (SR). Laminar profiles of the "stimulus evoked" extracellular field potentials were recorded at 25μm intervals along the dendro-somatic axis of the pyramidal cell and a 1-dimensional CSD analysis applied.

2) The shortest latency population spike response and current sink was recorded in stratum pyramidale or the proximal stratum oriens, a region corresponding to somata and axon hillocks of CA1 pyramidal neurons. A biphasic positive/negative spike potential (current source/sink) was recorded in dendritic regions, with both components increasing in peak latency through the dendritic field with distance from the border of stratum pyramidale.

3) A comparative intracellular analysis of evoked activity in somatic and dendritic membranes revealed a basic similarity in the pattern of AP discharge at all levels of the dendro-somatic axis. Stimulation of the alveus, SO, or SR evoked a single spike while injection of depolarizing current evoked a repetitive

train of spikes grouped for comparative purposes into three basic patterns of AP discharge.

4) Both current and stimulus evoked intracellular spikes displayed a progressive decline in amplitude and increase in halfwidth with distance from the border of stratum pyramidale.

5) The only consistent voltage threshold for intracellular spike discharge was found in the region of the cell body, with no apparent threshold for spike activation in dendritic locations.

6) Stimulus evoked intradendritic spikes were evoked beyond the peak of the population spike recorded in stratum pyramidale, and aligned with the biphasic extradendritic field potential shown through laminar profile analysis to conduct with increasing latency from the cell body layer.

The evoked characteristics of action potential discharge in CA1 pyramidal cells are interpreted to indicate the initial generation of a spike in the region of the soma-axon hillock and a subsequent retrograde spike invasion of dendritic arborizations.

ACKNOWLEDGEMENTS

For support and guidance over the course of my graduate program I am indebted to Dr. James J. Miller. I would also like to express my sincere thanks to Thomas L. Richardson for data analysis programs, recording equipment and technical advice, and for the endless hours of discussion, support and collaborative effort that made this work possible. Thanks also to other members of the laboratory and department whose contributions and comments were greatly appreciated.

I gratefully acknowledge the expert assistance of Kurt Henze and Rob Andersen in photography and preparation of figures. I also wish to thank the members of the advisory committee and Dr. P. Carlen, the external examiner for reviewing this thesis. Finally, I would like to acknowledge the award of a Studentship by the Medical Research Council of Canada.

TABLE OF CONTENTS

LIST OF FIGURES

LIST OF TABLES

1-0. INTRODUCTION

1-1. Anatomy

The Hippocampal Formation

The hippocampus is a forebrain cortical structure found as a small gyrus beneath the inferior horn of the lateral ventricle. Primitive homologues of the hippocampus can be traced as far back as the cyclostomes (Angevine 1975), with a progressive development of the structure through vertebrate phylogeny. Although comprising a major portion of lower mammalian cortical tissue, the expansion of neocortex and development of the corpus callosum has reduced the relative size of the hippocampus in more advanced vertebrate forms. For instance, in the rat, the hippocampus forms a long tube-like structure from a dorso-anterior septal pole to a postero-lateral temporal pole beneath the floor of the lateral ventricle. In man, the hippocampus is confined primarily to the temporal lobe, forming the floor of the inferior horn of the lateral ventricle and extending from within a few centimeters of the temporal pole to the splenium of the corpus callosum.

In coronal section, the hippocampal formation appears to arise as an extension of the entorhinal cortex folded back on itself to form two interlocking gyri, the hippocampus proper (hereafter referred to as hippocampus), and dentate gyrus (Fig 1.1). Ramon y Cajal (1911) divided the hippocampus into regio superior and regio inferior, in reference to the organization of the principle cell type of the structure, the pyramidal neuron (Fig 1.1). Lorente de No (1934) further subdivided the

hippocampus into four fields abbreviated by the letters CA (Cornu Ammonis). Of these the CA1 and CA3 areas were divided into regions designated a, b, and c according to cytological features or efferent projections of pyramidal neurons in each field. The CA1 region defines the dorsal aspect of pyramidal cells, CA2 and CA3 the giant pyramidal cells in the ventral aspect of the hippocampus, and CA4 the "modified" pyramidal cells located within the hilar region. The boundary between CA2 and CA1 is taken as the limit between regio superior and regio inferior. As the present study was confined to pyramidal cells in the CA1 region of the hippocampus, further anatomical description will be restricted to regio superior.

Laminae and Neuronal Elements of Regio Superior (CA1)

Regio superior can be divided into six strata running parallel to the cell layer extending from the ventricular epithelial surface to the hippocampal fissure (Cajal 1911). The most obvious stratum is the stratum pyramidale, a layer of packed pyramidal cell somata three to four cells deep with the basal and apical dendritic shafts of pyramidal cells extending perpendicular to the cell layer (Fig 1.1). One or more dendrites arise from the basal portion of the pyramidal cell and one large dendrite from the apical region, giving the cell a triangular or "pyramidal" appearance. The basal dendrites undergo profuse branching a short distance from their origin and extend into the stratum oriens and occasionally into the alvear region. The apical dendrite projects radially through the stratum radiatum, lacunosum and moleculare, the latter two often referred to as stratum lacunosum-moleculare in the rat (Fig 1.1; Cajal 1911).

FIG. 1.1 Ultrastructural anatomy of the transverse hippocampal slice. Recordings were restricted to the CA1 field of Regio Superior. Notations:

S.Ori. = stratum oriens

S.Pyr. = stratum pyramidale

S.Rad. = stratum radiatum

S.Lac. = stratum lacunosum

S.Mol. = stratum moleculare

S.C. = Schaffer collaterals

B.C. = basket cell

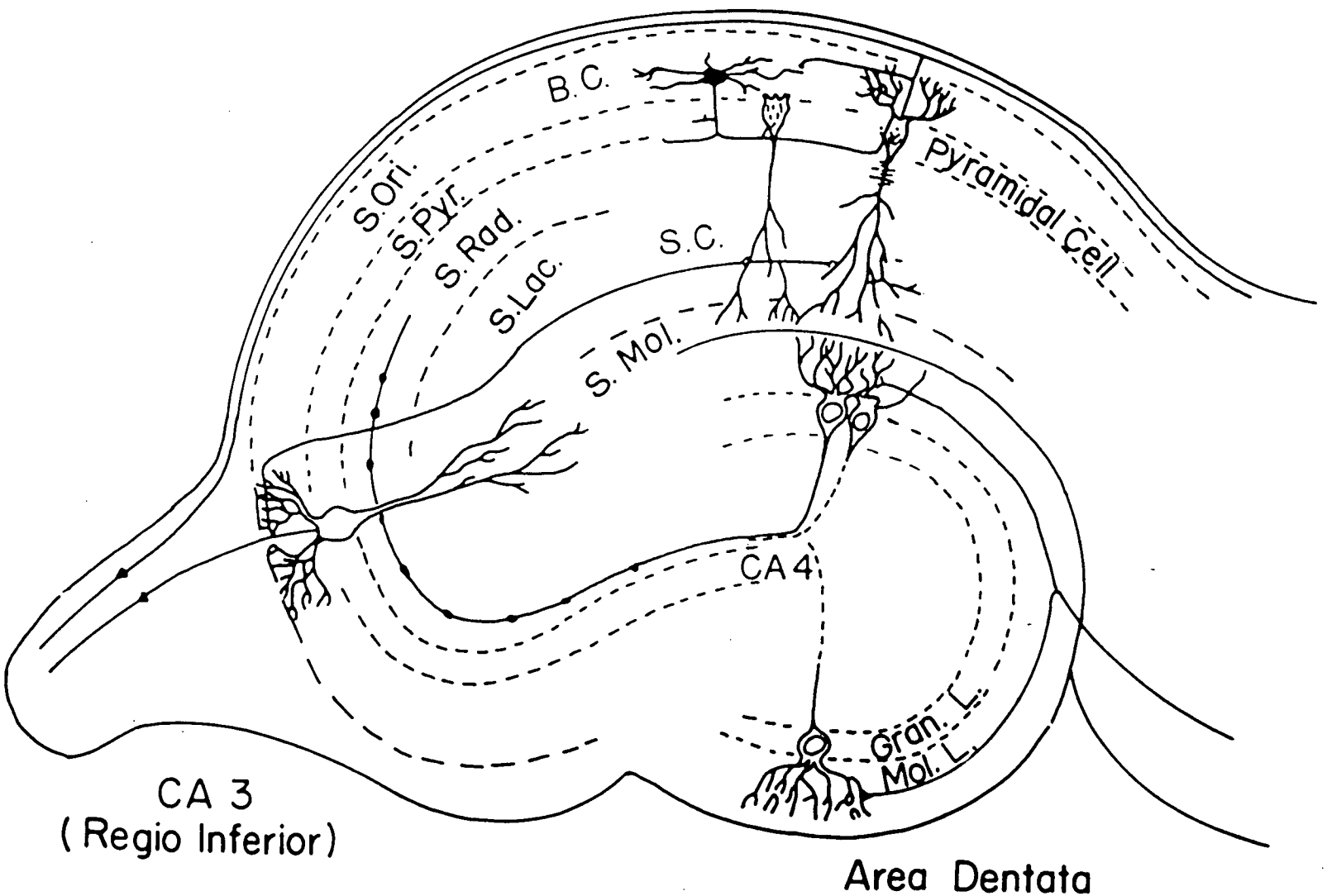
CA I
(Regio Superior)
B.C.
S.Ori.
S.Pyr.
S.Rad.
S.Lac.
S.C.
S.Mol.
Pyramidal Cell
CA 4
Gran. L.
Mol. L.
CA 3
(Regio Inferior)
Area Dentata

The apical dendrite is characterized by a thick proximal shaft in stratum radiatum with a greater degree of arborization occurring in the mid-distal stratum radiatum. In the rat hippocampus, many apical dendrites exhibit profuse lateral branching at the border of stratum lacunosum-moleculare, although the maximal limit of dendritic extension is found at the hippocampal fissure. Dendritic spines are relatively sparse on the proximal apical dendritic shaft but are profusely distributed on dendritic branches, increasing in number toward stratum lacunosum-moleculare (Westrum and Blackstad 1962).

The axons of CA1 pyramidal neurons course radially through stratum oriens and consolidate within the alvear white matter to project to the subicular pyramidal cell layer or to join efferent fibers of the fimbria (Knowles and Schwartzkroin 1981b; Lorente de No 1934).

Ramon y Cajal (1911) and Lorente de No (1934) described at least thirteen neuronal cell types in regio superior distinct from the pyramidal neuron. However, the most common of these are the basket cells, a set of interneurons believed to mediate recurrent inhibition of pyramidal cells (Allen et al. 1977; Andersen et al. 1964,1969; Dingledine and Langmoen 1980; Knowles and Schwartzkroin 1981a; Tombol et al. 1979). Although cytological features can be used to distinguish between several subtypes of basket cells (Lorente de No 1934), certain characteristics can be considered common to each class. The cell bodies of basket cells are generally larger than adjacent pyramidal neurons, and are located within stratum pyramidale or stratum oriens. Most have a basal and apical dendritic tree extending parallel to pyramidal cell dendrites within stratum

oriens and stratum radiatum, respectively. The axon extends into stratum radiatum and lacunosum-moleculare, sending several collaterals back to form horizontal projections in the proximal stratum radiatum, with final termination in the form of a basket-like plexus around pyramidal cell somata and proximal dendrites (Lorente de No 1934). A major source of excitatory synaptic input to these cells is derived from collateral projections of CA1 pyramidal cell axons.

Basket cell interneurons are thought to be inhibitory in nature, each providing a potent recurrent inhibition of somata, proximal dendrites and axon hillocks of as many as 500 pyramidal neurons (Andersen et al. 1969; Knowles and Schwartzkroin 1981a; Somogyi et al. 1983). In addition, interneurons with anatomical and physiological characteristics similar to that of basket cells have also been proposed to bring about a feed-forward inhibition of pyramidal neurons in the CA1 region (Alger and Nicoll 1982; Andersen et al. 1969; Ashwood et al. 1984; Knowles and Schwartzkroin 1981a; Schwartzkroin and Mathers 1978). Thus, through formation of extensive synaptic contact with pyramidal neurons, basket cells are believed to be responsible for the major balance of inhibitory influence in the region.

Afferent Synaptic Inputs to Regio Superior

A characteristic feature of the hippocampus is the lamellar organization of afferent synaptic inputs and the laminar distribution of terminal projections onto basal and apical dendritic structures (Andersen et al. 1971a; Raisman et al. 1965). For instance, the majority of afferent synaptic inputs enter the hippocampus approximately perpendicular to the

septo-hippocampal pole, and project in a laminar fashion to form synaptic contact along discrete regions of the dendro-somatic axis (Raisman et al. 1965). Although a wide variety of anatomically and chemically defined projection systems innervate the CA1 region, the present study was confined to two of the major afferents, the Schaffer collateral and the commissural inputs to regio superior.

1)Schaffer Collaterals

A major input from regio inferior of the hippocampus to CA1 was first described by Schaffer in 1892. This system originates as an axon collateral projection of CA3 pyramidal cells shortly before the efferent fiber enters the fimbria. These course back through stratum oriens and pyramidale of CA2 and then turn down to project through stratum radiatum of regio superior (Lorente de No 1934). There, en-passage excitatory synaptic contacts are formed on the apical dendrites of CA1 pyramidal neurons (Andersen and Lomo 1966; Westrum and Blackstad 1962).

2)Commissural Projections

Commissural inputs to the CA1 region of the dorsal hippocampus arise in large part from the CA3 field of the contralateral hippocampus (Raisman et al. 1965). Efferent CA3 fibers enter the fimbria and proceed in a rostral direction to cross the midline in the ventral psalterium. There the fibers turn and progress caudad through the contralateral fimbria and alveus to enter regio superior and form excitatory synaptic contact upon the basal and apical dendrites of the CA1 pyramidal neuron (Blackstad 1956; Raisman et al. 1965).

1-2. The Hippocampal Slice Preparation

The laminar organization of the hippocampus and the anatomical specificity of synaptic inputs onto pyramidal neurons make this system an ideal model for the study of the electrophysiological characteristics of cortical neurons in the mammalian CNS. Original investigations into the evoked electrical activity of the hippocampus were performed through stereotaxic implantation of stimulating and recording electrodes in the acute, anesthetized animal. Although a great deal of information has been gained in this way, there are several drawbacks to this approach, including the effects of anesthetics on evoked potentials, and difficulties in determining the exact site of recording and stimulating electrodes. Many of these problems have been overcome through development of the *in vitro* slice preparation (Skrede and Westgaard 1971). With this technique, small sections of neuronal tissue can be maintained *in vitro* in the absence of anesthetic, and are found to exhibit electrophysiological characteristics comparable to those observed in the intact animal (Schwartzkroin 1975,1977). The laminar organization of the hippocampus makes this structure particularly well suited to the application of the slice technique. For example, a slice taken perpendicular to the longitudinal axis of the hippocampus preserves the majority of afferent synaptic inputs, and stimulating and recording electrodes can be accurately placed within the major strata of regio superior under direct microscopic observation. Therefore, through use of the slice preparation all strata of the CA1 region become accessible to electrophysiological analysis,

permitting a characterization of evoked activity along the entire dendro-somatic axis of the pyramidal neuron. For these reasons, the hippocampal slice technique was used in the present study.

1-3. Electrophysiological Characteristics of CA1 Pyramidal Neurons

1) Evoked Extracellular Field Potentials

The characteristics of extracellular field potentials of CA1 pyramidal neurons evoked by stimulation of afferent or efferent pathways have been described in detail in previous investigations (Andersen 1960; Andersen et al. 1966a,b; Andersen and Lomo 1966; Cragg and Hamlyn 1955; Gloor et al. 1963; Leung 1979a,b,c; Sperti et al. 1967).

Electrical stimulation of pyramidal cell axons within the alvear region evokes an antidromic response within pyramidal neurons, characterized by a sharp, short latency negative-going potential in stratum pyramidale (Fig 1.2A). This waveform represents the summed synchronous discharge of a population of pyramidal neurons, and is referred to as an antidromic "population spike" (Andersen et al. 1971b).

Activation of Schaffer collateral/commissural (Sch/Comm) afferent inputs in stratum radiatum evokes a small biphasic negative/positive deflection superimposed on the rising edge of a larger, longer duration negativity in stratum radiatum (Fig 1.2B). The initial component is graded in nature and independent of extracellular calcium (arrows in Fig 1.2B,C), evident as a triphasic potential in low calcium medium (expanded in Fig

FIG.1.2 Characteristics of evoked extracellular potentials in the CA1 region. A. An antidromic population spike recorded in stratum pyramidale evoked through stimulation of efferent pyramidal cell axons in the alvear region, shown for increasing intensities of stimulation. B. The excitatory postsynaptic potential (EPSP) and population spike evoked through stimulation of afferent synaptic inputs in stratum radiatum. Both the somatic (St. Pyr.) and apical dendritic response (St. Rad.) are shown for increasing stimulus intensities. The arrow denotes the fiber potential associated with activity of afferent axonal projections in stratum radiatum. C. The effect of lowering the extracellular Ca+2 concentration from 1.6mM to .1mM on stratum radiatum evoked somatic (St. Pyr.) and apical dendritic potentials (St. Rad.). Note the gradual decline in amplitude of the EPSP and population spike, revealing a Ca+2-independent fiber potential in the apical dendritic region (arrow).
D. An expanded view of the fiber potential in C shown at a higher stimulus intensity, illustrating the triphasic nature of the fiber potential in the absence of an extracellular EPSP.

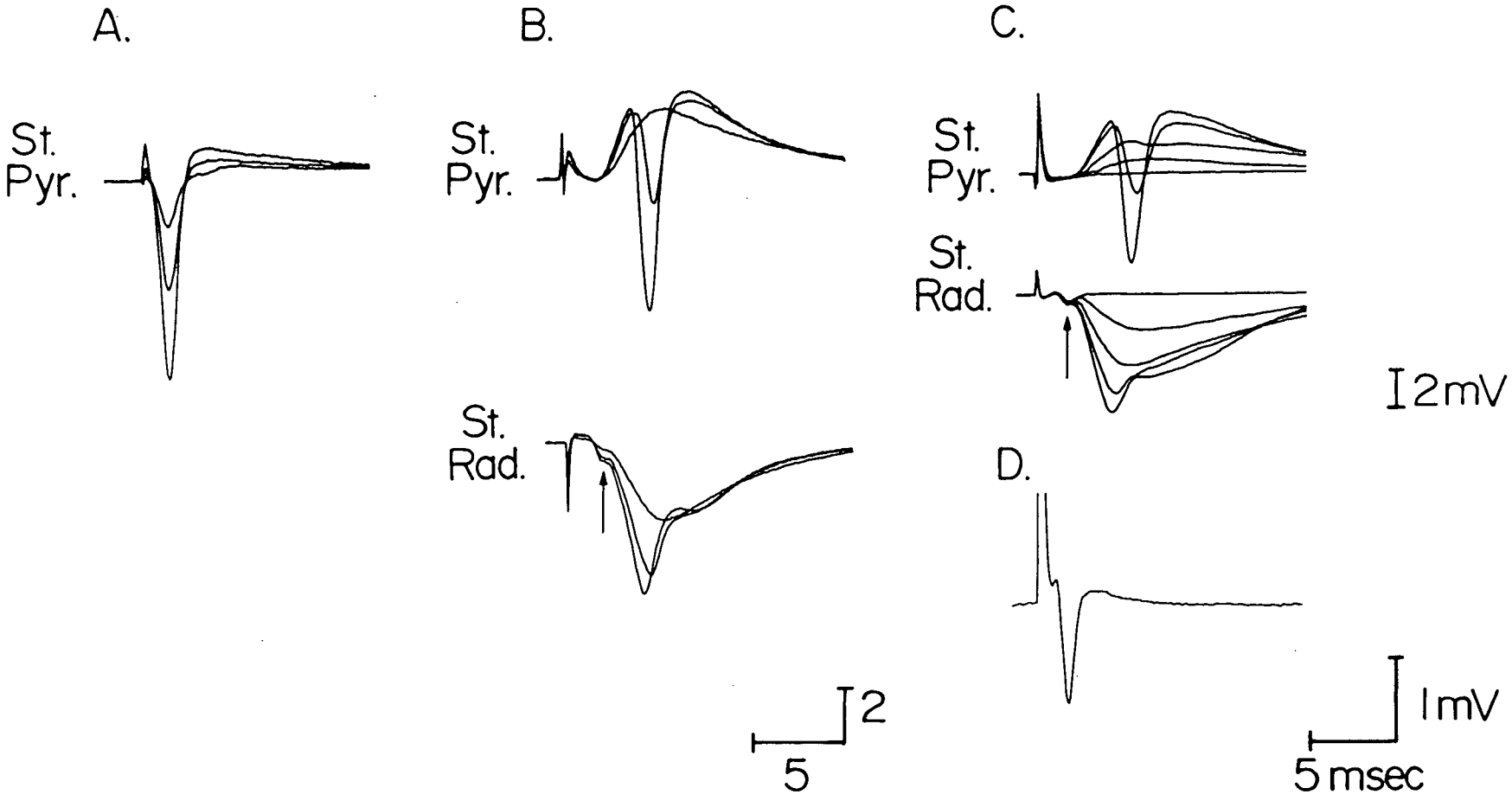
A.
St.
Pyr.
B.
St.
Pyr.
St.
Rad.
C.
St.
Pyr.
St.
Rad.
2mV
D.
2
5
1mV
5 msec

1.2D). This waveform is the compound action potential associated with the activity of Sch/Comm axons in stratum radiatum and is referred to as a "fiber potential". The second component is a smooth graded negative waveform with a maximal negativity in the region of Sch/Comm afferent inputs (Andersen 1960; Andersen et al. 1966a; Andersen and Lomo 1966; Leung 1979c). This potential is calcium-dependent (Fig 1.2C) and represents the extracellular reflection of the excitatory postsynaptic potential (EPSP) associated with synaptic depolarization of pyramidal cell apical dendrites (Andersen 1960; Andersen and Lomo 1966; Leung 1979c). The EPSP conducts electrotonically through the dendritic field, declining in amplitude and reversing in polarity just proximal to the cell layer to appear as a positive-going potential in stratum pyramidale (Fig 1.2B). With higher stimulus intensities, a sharp negative-going "population spike" is evoked upon the positive-going synaptic waveform in stratum pyramidale, reflecting the synchronous discharge of pyramidal neurons following synaptic depolarization of the cell population (Andersen et al. 1971b; Fig 1.2B).

Activation of commissural afferents in stratum oriens evokes a similar sequence of potentials along the basal dendritic axis of the pyramidal neuron (not shown). Stimulation of stratum oriens evokes a fiber potential and a negative-going extracellular EPSP in the basal dendritic region (Gessi et al. 1966; Leung 1979c). The EPSP negativity is maximal in the region of afferent synaptic inputs, declines in amplitude through the dendritic tree, and inverts to a positive potential near stratum pyramidale (Leung 1979c). Higher intensities of stimulation can then bring about neuronal discharge and the generation of a

population spike at the cell layer.

2) Evoked Action Potential Discharge

According to the traditional model of neuronal function, all-or-none action potential (AP) discharge could occur only in the region of the soma-axon hillock. The dendritic arborization of a cell served as the principle site for termination of afferent excitatory synaptic inputs, and for the passive electrotonic conduction of synaptic currents to the soma-axon hillock region. However, this view has been substantially modified in recent years with the knowledge that dendritic membrane can also exhibit electroresponsive properties, and that regional variations in the distribution of ionic channels can lead to regenerative action potential discharge in the dendritic tree (Llinas 1975; Llinas and Sugimori 1980b; Wong et al. 1979).

The evoked activity of somatic and dendritic membranes of a neuron has been most thoroughly examined in the Purkinje cell of the cerebellum (Ekerot and Oscarrson 1981; Llinas and Nicholson 1971; Llinas and Sugimori 1980a,b, 1984; Nicholson and Llinas 1971). In these neurons, voltage-dependent Na+ channels in the region of the axon hillock give rise to fast Na+-dependent spikes in response to stimulation of climbing fiber afferent inputs. However, synaptic depolarization of the dendritic tree can also evoke prolonged all-or-none Ca+2-dependent spikes within the dendritic arborization through the action of intrinsic voltage-dependent Ca+2 channels (Llinas and Sugimori 1980a,b). Ca+2 spikes may arise at one or more locations within the dendritic tree at presumed "hot spots" of low threshold dendritic membrane, and can determine the pattern of

Na+-dependent spike discharge in the Purkinje cell soma (Llinas 1975; Llinas and Nicholson 1971). For instance, Ca+2 spikes can propagate to the somatic region, summating within the dendritic tree to form a prolonged depolarization capable of evoking repetitive Na+ spike discharge at the somatic level. In this way, the dendritic spike can serve to "boost the weight" of afferent synaptic inputs by ensuring a reliable dendro-somatic transfer of synaptic currents to the region of the axon hillock (Llinas 1975).

A differential distribution of ionic channels can thus confer a non-uniformity to the excitability of membrane along the dendro-somatic axis of a neuron. In the case of the Purkinje cell, voltage-dependent Ca+2 channels give rise to regenerative Ca+2 spikes in the dendrites, while voltage-dependent Na+ channels and Na+-dependent spike activation are restricted to the somatic region. The distribution of Na+ and Ca+2 channels are in fact so pronounced in this neuron that somatic Na+ spikes cannot actively reinvade the dendritic arborization, but electrotonically decay through the proximal portion of the dendritic tree (Llinas 1975; Llinas and Sugimori 1980b). Active, all-or-none responses can thus be evoked at both the somatic and dendritic level of a cell, but the exact form and characteristics of the evoked potential depend upon the specific distribution and properties of intrinsic voltage-dependent ionic channels.

A second cortical neuron thought to exhibit a non-uniform membrane excitability is the pyramidal neuron of mammalian hippocampus. The properties of spike discharge at the level of the pyramidal cell soma were first characterized <u>in vivo</u> through

the analysis of extracellular field potentials (Andersen 1960; Andersen et al. 1966a,b; Andersen and Lomo 1966; Leung 1979a,b; Sperti et al. 1977), extracellular single unit discharge (Andersen et al. 1971b; Green et al. 1961; Kandel et al. 1961; Euler and Green 1960) and intracellular recordings in the vicinity of the pyramidal cell soma (Andersen et al. 1966a,b; Andersen and Lomo 1966; Kandel et al. 1961; Kandel and Spencer 1961; Spencer and Kandel 1961a,b). The evoked characteristics of spike discharge in pyramidal cell somata have also been examined in the in vitro preparation through both extra- and intracellular recording techniques (Richardson et al. 1984a; Schwartzkroin 1975,1977; Schwartzkroin and Prince 1980; Schwartzkroin and Slawsky 1977). Stimulation of efferent pyramidal cell axons in the alveus evokes an antidromic spike invasion of pyramidal cell somata, as indicated by a short latency intracellular action potential corresponding in time to the extracellular population spike in stratum pyramidale. Stimulation of afferent synaptic inputs impinging upon either basal or apical dendritic structures also evokes a single spike superimposed upon the underlying EPSP in pyramidal cell somata (Schwartzkroin 1975,1977). As with antidromic responses, the latency of the orthodromic intracellular spike is found to coincide with the negative-going extracellular population spike in stratum pyramidale, revealing a close correspondence between intracellular spike discharge and the extracellular waveform (Richardson et al. 1984a; Schwartzkroin and Prince 1980; Turner et al. 1984).

Given the laminar organization of the hippocampus, an electrophysiological analysis of evoked activity can also be

carried out at the dendritic level of the pyramidal cell. The characteristics of dendritic activity were first examined in vivo through an analysis of laminar profiles of evoked extracellular field potentials along the dendro-somatic axis of the CA1 pyramidal cell (Andersen 1959; Andersen 1960; Cragg and Hamlyn 1955; Fujita and Sakata 1962). These early studies reported the possible occurrence of spike generation in the pyramidal cell apical dendrite following stimulation of afferent synaptic inputs. Dendritic spikes were detected as a sharp negative-going extracellular potential in the dendritic region (presumably Na+-dependent) and were thought to actively propagate from a dendritic site of origin along the pyramidal cell axis (Andersen 1960; Cragg and Hamlyn 1955; Fujita and Sakata 1962). In agreement with this, intracellular recordings in the region of pyramidal cell somata revealed the presence of all-or-none Na+-dependent "fast pre-potentials" (FPPs), thought to be the somatic representation of dendritic spike discharge (Andersen and Lomo 1966; Schwartzkroin 1977; Spencer and Kandel 1961b). With the recording stability afforded by the slice preparation, a limited number of investigators have now succeeded in obtaining microelectrode impalements of pyramidal cell dendrites, and have reported the presence of evoked Na+ and Ca+2-dependent action potentials in the dendritic region (Benardo et al. 1982; Masukawa and Prince 1984; Wong and Prince 1979; Wong et al. 1979).

The generation of dendritic spikes in pyramidal neurons is thought to exert considerable influence on the pattern of cell discharge in both normal and pathological states. According to the prevailing hypothesis, synaptic activation of the pyramidal

cell under normal conditions gives rise to a single fast (Na+-dependent) dendritic spike that conducts to the cell body to appear as a small fast pre-potential in the somatic region. Through summation with underlying dendritic postsynaptic potentials, the dendritic Na+ spike may serve to "boost the weight" of synaptic inputs by increasing the probability for AP discharge at the axon hillock (Andersen and Lomo 1966; Schwartzkroin 1977; Spencer and Kandel 1961). In contrast, the activation of excitatory synaptic inputs in the presence of pharmacological agents known to reduce the efficacy of inhibitory feedback networks can evoke a burst discharge of both Na+ and Ca+2-dependent dendritic spikes (Wong and Prince 1979). The dendritic depolarization evoked in this way can elicit repetitive Na+ spike discharge in the cell body, leading to the proposal that dendritic spike activation may underly the multiple spike discharge characteristic of epileptiform activity in the hippocampus (Schwartzkroin and Prince 1980; Schwartzkroin and Wyler 1979; Wong and Prince 1979; Wong et al. 1979).

1-4. THE PRESENT STUDY

Previous investigations of the characteristics of evoked activity in the hippocampus have reported evidence for action potential discharge at both the somatic and dendritic level of the CA1 pyramidal neuron. Dendritic spike activation may play an important role in determining the final output of the pyramidal cell, and aberrant dendritic discharge may even contribute to the pathology of epilepsy in mammalian cortical structures. Identification of the factors responsible for generation of dendritic spikes would thus be an important step in understanding the discharge patterns of a cortical neuron in the mammalian CNS.

Much information has been gained about the properties of the fast Na+-dependent dendritic spike, as these spikes are reliably evoked under the more physiological conditions of synaptic depolarization (Andersen 1960; Andersen and Lomo 1966; Andersen et al. 1966a,b; Cragg and Hamlyn 1955; Fujita and Sakata 1962; Masukawa and Prince 1984; Schwartzkroin 1977; Spencer and Kandel 1961b). Based on intracellular recordings at the somatic level, the site for generation of the Na+ spike was tentatively proposed to exist at branchpoints of the dendritic tree at "hot spots" of dendritic membrane (Spencer and Kandel 1961b), analagous to that proposed for Ca+2 spike generation in the cerebellar Purkinje neuron (Llinas 1975). However, despite extensive analysis of action potential discharge in the pyramidal cell, the exact site of generation of a dendritic spike has not yet been identified.

The present study was therefore undertaken to characterize

and compare the electrophysiological properties of somatic and dendritic membranes of CA1 pyramidal neurons in order to identify the site of origin of evoked fast action potentials in pyramidal cell apical dendrites.

The results to be described are divided into three stages of experimentation. The first is a laminar profile analysis of evoked extracellular field potentials in the CA1 region, and determination of current-source density relationships along the dendro-somatic axis of the pyramidal cell (Chapter 3). The second is an intracellular investigation of the membrane properties, synaptic potentials, and spike characteristics of the soma and apical dendrites of CA1 pyramidal neurons (Chapter 4). The final set of experiments examine various parameters of intracellular spike discharge at all levels of the pyramidal cell axis, and assess the relationship between intracellular activity and extracellular field potentials (Chapter 5). A general summary and discussion of the data and conclusions derived from these experiments are presented in Chapter 6.

2-0. Methods

2-1. Surgical Procedure

Experiments were performed on the hippocampal formation of male Wistar rats (150-250g; Charles River, Montreal) using the *in vitro* slice preparation. The animals were decapitated and the skin and connective tissue overlying the skull removed by scalpel. Cranial bones were removed with rongeurs and the dura mater cut with fine surgical scissors and removed with forceps. A cold (1-4 degrees centigrade) modified Ringer's solution consisting of 124mM NaCl, 3mM KCl, 0.75mM KH_2PO_4, 1.6mM $CaCl_2$, 1.2mM $MgSO_4$, 24mM $NaHCO_3$, 10mM D-glucose (Sigma) preoxygenated with 95% O_2 / 5% CO_2 was poured over the exposed cortex to cool and oxygenate the tissue. Complete coronal cuts were made between the occipital cortex and cerebellum and across the frontal cortex. The cerebellum was discarded and the remaining brain lifted out with a spatula and placed in a petri dish filled with cold oxygenated medium. The right and left hemispheres were separated by a sagittal scalpel cut and one hemisphere immersed in a beaker of cold oxygenated medium for later dissection. The remaining hemisphere was tipped up onto the coronal surface of the frontal cortex and the midbrain separated from the cortical tissue, leaving the ventro-medial surface of the hippocampus exposed. A spatula was placed beneath the curvature of the fimbria and fornix to carefully "roll" the hippocampus away from the subicular cortex, and the remaining cortex cut away. The hippocampus was then placed on the cutting stage of a Sorvall tissue chopper and slices of 400um thickness

were cut 10 degrees oblique to the longitudinal axis of the hippocampus. Each slice was lifted from the blade with a OOO brush, placed in a small petri dish of medium, and transferred to a nylon net within the recording chamber. Slices were then allowed at least 45 min for recovery and equilibration to the recording bath environment.

Once the tissue had been placed in cold oxygenated medium, it was found that the time required for dissection was not as critical to the health of a slice as the care taken during dissection. Therefore, following a dissection time of 5-7 min, slices could be cut from the second hemisphere with no apparent detriment to slice viability (as determined by electrophysiological characteristics).

2-2. Recording Chamber

The recording chamber is designed to create an artificial environment resembling the *in vivo* condition so as to maintain neuronal tissue in a viable state for extended periods of time following removal from the animal. Briefly, this is accomplished by providing slices with an oxygenated artificial cerebrospinal fluid warmed to body temperature and an atmosphere of warmed, humidified oxygen/carbon dioxide gas.

The chamber is constructed from plexiglass and consists of an outer circular water jacket and a separate inner circular recording well. The outer water jacket is partially filled with distilled water and warmed by a heating coil to maintain an inner recording chamber temperature of 35 +/- 0.5 degrees centigrade. Plastic tubing connected to the ouside of the bath

runs through the outside water jacket and delivers warmed, preoxygenated medium to the inner chamber via gravity feed at a rate of 2-3 ml/min (Dial-a-Flo, Sorenson Research Co., Utah). Excess medium is then drawn off by suction through a piece of plastic tubing in a well connected to the recording chamber. Media of altered ionic constituency can be introduced without interruption of flow through a three-way valve outside of the chamber.

Slices are placed on a nylon net within the recording chamber and illuminated by reflected light from below the chamber. A 95% oxygen / 5% carbon dioxide gas mixture is then passed through the outer chamber to superfuse slices with a warm, humidified gas mixture.

2-3. Stimulating and Recording Techniques

Bipolar stimulating electrodes constructed from twisted 62um nichrome wire were mounted on a micro-manipulator (Narishige) and positioned in major strata of the hippocampal slice under direct observation with the aid of a 4X dissecting microscope (Carl Zeiss). Square wave pulses of 0.1 msec duration and 1-70V intensity were delivered from isolation units (Medical Systems Corp., Model DS2) controlled by a four channel pulse generator (Digitimer, Medical Systems Corp.). Stimuli were delivered at a baseline rate of stimulation of 1/7 secs and minimal stimulus intensities used whenever possible to avoid any long-term alterations in the characteristics of evoked potentials (Turner et al. 1982).

All recordings in the present work were carried out in the

CAlb region of the mid-dorsal rat hippocampus. Extracellular recordings were obtained along the entire extent of the pyramidal cell axis, while intracellular impalements of neuronal elements were restricted to stratum pyramidale and stratum radiatum.

Recording electrodes were constructed using either a Narishige or Frederick Haer microelectrode puller. Extracellular electrodes of 2-6 megohm impedance were pulled from either glass capillary tubing (Frederick Haer, Omega Dot Tubing , 1.5mm O.D.) or from 2.0mm glass tubing and filled with 2M NaCl. Fiber filled electrodes were backfilled with a 31 gauge hypodermic needle while the tips of non-capillary electrodes were broken back under microscopic observation (Leitz Wetzler, Germany) to a diameter of 1-2um before backfilling with electrolyte. Intracellular electrodes of 30-80 megohm impedance were constructed from glass capillary tubing (Frederick Haer, 1.5mm O.D.) and backfilled with 1M K+-acetate. Extracellular electrodes were mounted on a micro-manipulator (Narishige) and intracellular electrodes to a manipulator equipped with a variable speed piezoelectric advance (Burleigh Inchworm PZ-550).

Recording electrodes were connected to the preamplifier headstage of a dual microprobe (WPI, Model KS700) and potentials recorded in reference to a silver-silver chloride bath ground. Extracellular field potentials were filtered using a 0.1Hz-10kHz bandpass and intracellular responses a DC-10kHz bandpass. Recorded electrical activity was displayed on a dual beam storage oscilloscope (Tektronix) and photographed or led to a PDP 11/23 computer for storage and subsequent analysis.

Microelectrodes of 30-80 megohm impedance were found to be

satisfactory for obtaining impalements of either somata or apical dendrites of pyramidal cells. The current passing capability of an electrode was first examined by immersing the tip of the electrode into the artificial CSF of the recording chamber. Command pulses to the probe were provided by a custom-made "probe-driver", and electrodes balanced through use of a conventional Wheatstone bridge circuit while monitoring the electrode voltage response to a square wave current pulse of up to 1.5 nA. Electrodes were considered acceptable for intracellular work if capable of passing .75 nA of inward or outward current with minimal voltage deflection (< 2.0mV).

Intracellular electrodes were placed within stratum pyramidale or stratum radiatum under direct microscopic observation, and advanced slowly through the slice. Impalements of the pyramidal cell were obtained by applying brief (0.5 sec) bursts of high-frequency capacitance feedback through the electrode. Penetration of the cell membrane was signified by a sharp drop of the voltage response in the order of -30 to -60mV, and a hyperpolarizing current of 0.25-0.75nA was immediately applied to aid recovery of the cell resting membrane potential. The penetration was considered stable if the resting potential was maintained following gradual removal of hyperpolarizing current over 1-2min following initial cell penetration. The cell was then allowed 5-15min to recover from the procedure of microelectrode impalement. Pyramidal cell impalements obtained in this manner could be maintained in a stable state for up to 4hrs, with minimal change in membrane characteristics (ie. resting potential) or evoked potentials over the duration of the recording period.

The quality of electrode penetration and extent of membrane recovery was estimated by calculating the input resistance of the membrane, as determined by the membrane response to a series of square wave current pulse injections. The electrode was first balanced, and six to twelve inward and outward square wave current pulse injections of up to 1.0nA (100 msec duration) applied across the membrane. The membrane response was recorded, and a current/voltage (I/V) graph later constructed by plotting the amplitude of the membrane voltage against that of the corresponding current pulse. A best-fit straight line was drawn through the linear range of membrane voltage deflections, and the slope of the line taken as the value of the cell input resistance (Ri). Alternatively, the input resistance could be estimated by the amplitude of the membrane voltage shift in response to a single 0.5 or 1.0nA inward current pulse. Although the Ri value calculated in this manner was not as accurate as that obtained through construction of an entire current/voltage plot, this method was commonly used in distal dendritic impalements as the application of a full range of current pulse injections (particularly over 1.5nA) could lead to a decline in the quality or sudden loss of the dendritic impalement. Data was collected from cells exhibiting an input resistance of at least 18 megohm or more, with the Ri value of impalements used in the present study ranging from 18-37 megohm.

The membrane potential baseline was continuously monitored using a digital voltage display, and the absolute value of the resting potential taken as the baseline voltage shift observed upon withdrawal of the electrode from the intracellular to the extracellular compartment.

Further information on recording arrangements for specific experiments are provided in the METHODS section of relevant chapters.

3-0. CURRENT-SOURCE DENSITY ANALYSIS OF ACTION POTENTIAL DISCHARGE IN THE CA1 REGION OF THE HIPPOCAMPUS

3-1. Introduction

Of paramount importance to the understanding of neuronal function is the identification of the actual site for action potential (AP) generation, the final output of a neuron following integration of excitatory and inhibitory synaptic potentials. In most cells, the conductance mechanism responsible for spike generation is thought to exist in the axon hillock, a region under the influence of currents passively conducting from the point of synaptic termination (Edwards and Ottoson 1958; Kado 1973; Ringham 1971; Smith et al. 1982; Smith 1983). However, it is now thought that neuronal membrane can display a non-uniform excitability along the dendro-somatic axis, giving rise to action potential discharge at both the somatic and dendritic level. This characteristic could be a significant factor in the integration of synaptic inputs if the dendritic spike should summate with synaptic currents and increase the probability for AP discharge at the axon hillock (Andersen and Lomo 1966; Kandel and Spencer 1961; Llinas 1975; Llinas and Sugimori 1980b; Wong et al. 1979)

One neuron thought to exhibit Na+-dependent spike discharge in both somatic and dendritic locations is the pyramidal neuron of mammalian hippocampus. Evidence for spike generation in the pyramidal cell apical dendrite came from early investigations into the characteristics of extracellular field potentials evoked through stimulation of afferent excitatory synaptic

inputs (Andersen 1959; Andersen 1960; Cragg and Hamlyn 1955; Fujita and Sakata 1962). These studies reported an evoked negative spike potential at all levels of the pyramidal cell axis, suggesting the activation of a spike in dendritic membrane that subsequently propagated in both directions along the pyramidal cell structure (Andersen 1960; Andersen and Lomo 1966; Andersen et al. 1966; Cragg and Hamlyn 1955; Fujita and Sakata 1962). Further support for dendritic spike activation came from intracelluar recordings in pyramidal cell somata of small Na+-dependent "fast pre-potentials" inferred to represent an electrotonically decayed spike arising from within the dendritic tree (Andersen and Lomo 1966; Schwartzkroin 1977; Spencer and Kandel 1961b). Microelectrode impalements of the pyramidal cell apical dendrite finally confirmed that stimulation of afferent synaptic inputs gave rise to spike activation (Na+-dependent) in pyramidal cell dendritic membrane (Wong et al. 1979). However, the actual site for generation of the Na+-dependent dendritic spike is presently unknown.

Since extracellular potentials are generated through the activation of ionic channels in neuronal membrane, the site for spike generation in the dendrite might be detected in the characteristics of extracellular field potentials along the pyramidal cell axis. Several laminar profile analyses of evoked field potentials have been carried out in the CA1 region. However, the site of origin of spikes evoked through stimulation of afferent synaptic inputs has been placed at various points along the pyramidal cell structure. For instance, some investigators have assigned the lowest threshold for spike generation to proximal dendritic membrane (Andersen 1959;

Andersen 1960; Fujita and Sakata 1962), while other studies have reported initial spike activation in either somatic (Andersen et al. 1961) or distal dendritic regions of the pyramidal cell (Andersen 1960; Andersen et al. 1966a,b; Andersen and Lomo 1966; Cragg and Hamlyn 1955).

The variabilty in these results may relate to the fact that the majority of extracellular investigations into the characteristics of spike discharge in the pyramidal cell have relied solely upon the interpretation of extracellular potential waveforms. Although much information has been gained in this way, the low resistivity of the extracellular medium results in a dissipation of voltage over space through volume conduction, reducing the accuracy by which field potential analysis can locate the true site of ionic channels underlying the evoked potential (Gloor et al. 1963; Leung 1979b; Mitzdorf 1985; Nicholson 1973). A more accurate resolution of neuronal activity is obtained through current-source density (CSD) analysis, in which the ionic channels responsible for generation of an evoked potential can be spatially localized in terms of a net loss (sink) or accumulation (source) of current with respect to the extracellular medium (Pitts 1952). Unlike field potentials, the density of current in the extracellular space can be well localized, with the result that CSD profiles provide a far superior estimate of the location, magnitude and time course of transmembrane currents as compared to that obtained through field potential analysis (Freeman and Stone 1969; Mitzdorf 1980; Nicholson 1973; Nicholson and Freeman 1975).

At the present time, a current-source density analysis of spike discharge in the CA1 pyramidal cell has only been

performed for potentials evoked by antidromic stimulation of pyramidal cell axons (Leung 1979a,b). In these studies, the site for initial spike activation in pyramidal cells was found in the region of the soma-axon hillock, as indicated by a short latency current sink in proximal stratum oriens or the stratum pyramidale. Both the basal and apical dendritic regions were subsequently invaded by a short duration source/sink, providing strong evidence that a spike evoked at the cell layer can conduct in a retrograde manner through the dendritic arborization of pyramidal neurons.

Comparable studies have not yet been performed for spike discharge in the pyramidal cell following stimulation of afferent excitatory synaptic inputs. Therefore, a current-source density analysis of evoked extracellular field potentials was carried out in the CA1 region for the purpose of locating the origin of the evoked dendritic spike of pyramidal neurons.

3-2. Methods

Current-Source Density Calculations

Current-source density analysis is a means by which ionic movements across the membranes of cells within a population can be localized in terms of current movement with respect to the extracellular space (Pitts 1952). A movement of current from the extracellular to the intracellular compartment is detected as a net loss or sink of current, a result most often signifying a depolarization of neuronal membrane. In contrast, the flow of current from the intracellular to the extracellular compartment is observed as a net accumulation or source of current in the extracellular space.

Current-source density can be estimated from the spatial distribution of extracellular voltage deflections and the resistivity of the extracellular medium. The extracellular resistance to current flow (conductivity) is in large part determined by the anatomical structure of neuronal tissue (Freeman and Stone 1969; Mitzdorf 1985; Nicholson and Freeman 1975). Most tissues are found to exhibit different values of conductivity in at least two planes of a rectangular coordinate system. This can be attributed to the presence of neuronal elements running transverse to the direction of current flow (ie. myelinated fibers; Freeman and Stone 1969; Haberly and Shepherd 1973) or to an alignment of core conductors (ie. dendrites) parallel to the axis of current flow (Freeman and Stone 1969; Mitzdorf 1985; Nicholson and Freeman 1975). Variations in the structure of a cellular aggregate can also lead to a lack of homogeneity of extracellular resistance along

a principle coordinate axis, with a change in conductivity observed at the border of cell layers or fiber bundles (Haberly and Shepherd 1973; Mitzdorf 1985).

Experimentally, current-source density is approximated as the second spatial derivative of evoked potentials recorded at equidistant locations in neuronal tissue. Under ideal conditions, a real-time analysis of CSD is obtained by simultaneously recording potentials from a 3-dimensional array of electrodes, taking into account the conductivity of the extracellular space in all three dimensions (Freeman and Nicholson 1975; Freeman and Stone 1969). In this case, the current density at time t for point x,y,z of a rectangular coordinate system is given by:

$$S(t,x,y,z) = -\left[\sigma x \frac{d^2V(t)}{dx^2} + \sigma y \frac{d^2V(t)}{dy^2} + \sigma z \frac{d^2V(t)}{dz^2} \right]$$

where σx, σy, σz are the conductivity values for the x,y,z dimensions, and V(t) the extracellular voltage for time t at point x,y,z (Nicholson and Freeman 1975). However, in neuronal tissue displaying a high degree of laminar organization, the calculation of current-source density can be simplified to a 1-dimensional analysis (Haberly and Shepherd 1973). Such a condition is commonly found in cortical structures of the mammalian CNS, where neuronal tissue is comprised of one or a few principle cell types arranged in a serial laminar fashion. In this case, the laminar organization of neuronal elements results in a relatively high conductivity along the

dendro-somatic axis of the principle cell type, and during synchronous activation of the cell population, the majority of extracellular current flow is restricted to the laminar plane of the tissue (Haberly and Shepherd 1973). Relatively little current flow is found normal to this axis, and errors introduced into the calculation of current-source density by excluding extracellular conductivity estimates in these dimensions are found to be of a quantitative rather than qualitative nature (Haberly and Shepherd 1973). In other words, the use of a 1-dimensional CSD analysis may affect the absolute value of the current-source density measurement, but the polarity and time course of current sinks and sources are preserved. The measured values of variation in the conductivity along the principle axis of a laminated structure have also been found to exert a minor influence on the qualitative aspects of CSD profiles, and the extracellular conductivity is usually treated as a constant (Freeman and Stone 1969; Haberly and Shepherd 1973; Mitzdorf 1980,1985; Nicholson and Freeman 1975).

Therefore, given the conditions of:

1) large scale synchronous activation of a laminated structure

2) equidistant recording of evoked potentials parallel to the dendro-somatic axis of the principle cell type

3) a homogeneous conductivity tensor, where $\sigma x = \sigma y = \sigma z$

the calculation of current-source density can be reduced to a 1-dimensional analysis given by:

$$S(t,x) = \sigma \frac{d^2V(t)}{dx^2} = \frac{(V_1 - V_2) - (V_2 - V_3)}{(\Delta X)^2}$$

$$= \frac{V_1 + V_3 - 2V_2}{(\Delta X)^2}$$

where V1, V2, V3 represent the field potentials recorded at three consecutive locations along the dendro-somatic axis separated by a distance of ΔX.

Anatomically, the CA1 region of the hippocampus satisfies the requirements of a 1-dimensional CSD analysis, with symmetric organization of dendritic structures perpendicular to the pyramidal cell body layer. Through use of the slice preparation the placement of stimulating and recording electrodes can be visually confirmed, and the pyramidal cell population activated by stimulation of afferent or efferent fiber projections. Synchronous discharge of the cell population also gives rise to large voltage gradients along the dendro-somatic axis of the pyramidal cell (up to 120 mV/mm; Richardson et al. 1984b), reducing the degree of current flow normal to the laminar plane of the tissue. Although a slight increase in resistivity has been found in the region of stratum pyramidale (1.5 - 3X dendritic resistivity; Jefferys 1984), this slight variation in conductivity will only affect the absolute value of current-source density measurements, and a homogeneous extracellular conductivity can be assumed. Therefore, given a synchronous activation of the pyramidal cell population, a 1-dimensional current-source density analysis can be appropriately applied in the CA1 region of the hippocampus.

Stimulating and Recording Procedures

Synchronous activation of the pyramidal cell population was achieved through stimulation of three distinct pathways in the hippocampal slice. The first was suprathreshold activation of pyramidal cell efferent fibers in the alveus (S1; Fig 3.1), known to result in antidromic invasion of the pyramidal cell and recurrent activation of inhibitory interneurons in the region of stratum pyramidale. The second employed stimulation of afferent excitatory inputs to the basal dendritic arborization of pyramidal cells through stimulation of stratum oriens (S2; Fig 3.1). A third stimulating electrode was placed in stratum radiatum to activate Schaffer collateral/commissural excitatory inputs synapsing directly upon pyramidal cell apical dendrites (S3; Fig 3.1).

Laminar profiles of extracellular field potentials evoked from each of the above pathways (usually one profile for each slice) were constructed by recording extracellular potentials at 25um intervals parallel to the dendro-somatic axis of the pyramidal cell. To ensure that recording positions were located along a straight line parallel to the dendritic structure, the recording electrode manipulator was secured in a position with the horizontal travel of the electrode oriented perpendicular to stratum pyramidale. Consecutive movements of the electrode could then be made without visual estimation of the recording axis, and the distance of the recording location along the pyramidal cell measured directly from the micrometer scale of the manipulator. Evoked potentials were always recorded during withdrawal of the electrode from the maximum depth of the electrode track in order to avoid any alteration of the

FIG. 3.1 Schematic diagram of the rat pyramidal cell and strata of the CA1 region of the hippocampus, illustrating the placement of stimulating electrodes for activation of the pyramidal cell population. Stimulation of the alveus (S1) was used to evoke an antidromic response through stimulation of pyramidal cell axons. A second electrode in stratum oriens (S2) was used to stimulate afferent synaptic inputs to the basal dendritic tree, and a third in stratum radiatum (S3) for synaptic activation of the apical dendritic arborization. Stimulus evoked potentials were recorded parallel to the dendro-somatic axis at all levels of the pyramidal neuron.

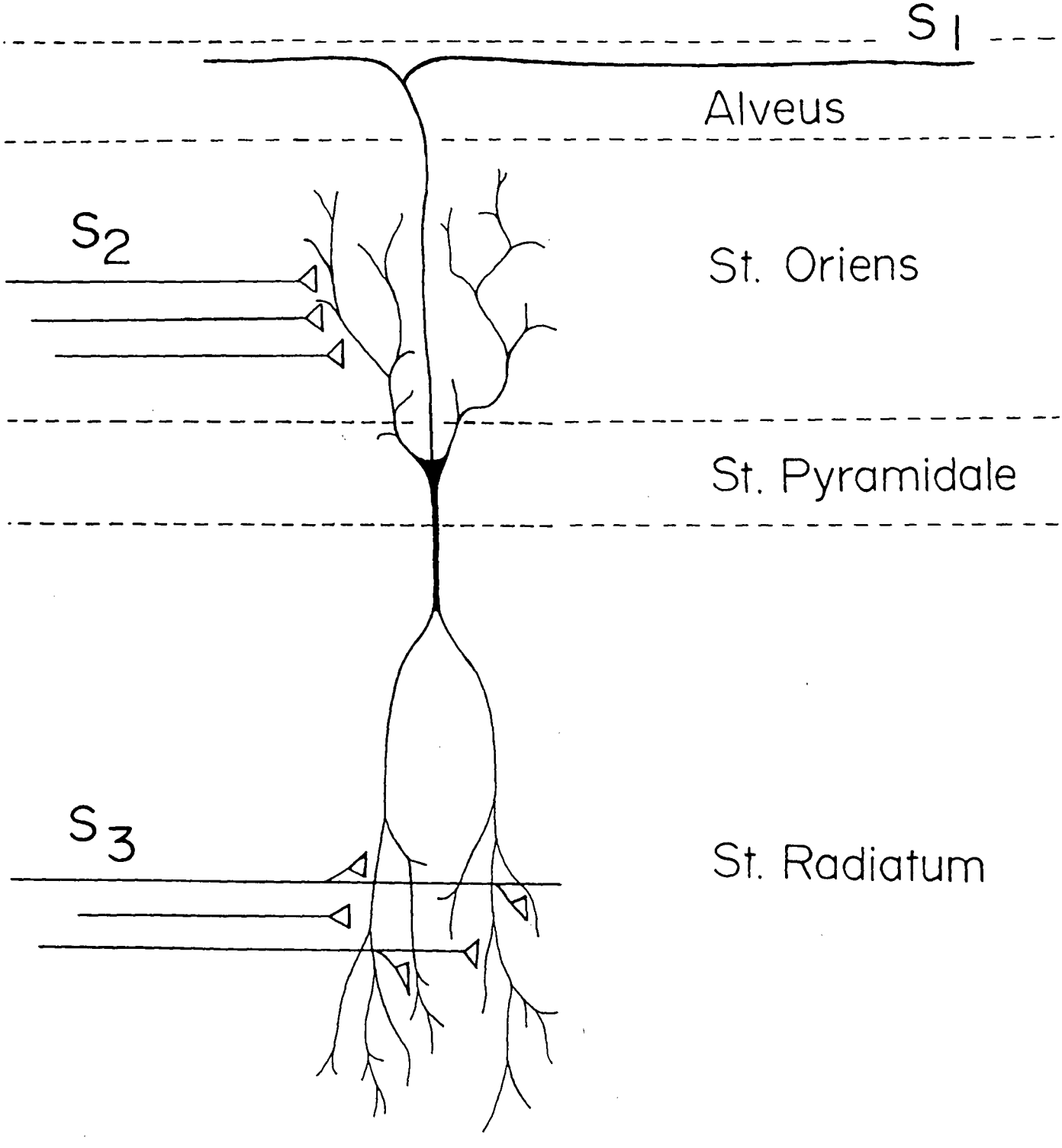
S1
Alveus
S2
St. Oriens
St. Pyramidale
S3
St. Radiatum

extracellular waveform that might accompany compression of tissue during forward electrode advancement.

Profiles of field potentials within a single recording electrode track revealed that the peak amplitude of an evoked potential could vary with the recording depth, and that the depth at which peak amplitude was attained could differ at various points along the cell axis. Since minor variations in waveform characteristics could be of serious consequence to the accuracy of current-source density measurements, evoked potentials were collected at 20μm intervals of depth up to 100μm above and below the approximate depth of maximal waveform (determined prior to serial profile measurements). Potentials along each electrode tract were then averaged by computer (four to eleven sweeps), avoiding the problem of potential variation with recording depth and providing the equivalent of an average value of current-source density over a "column" of tissue perpendicular to the dendro-somatic axis of the pyramidal cell. The stability of field potentials were continuously monitored with a second recording electrode placed in stratum pyramidale, and laminar profiles omitted from data analysis in the event of any change in the control population spike during the course of the experiment.

Current-source density analysis was performed in one dimension as a continuous function of time for each 25μm interval along the pyramidal cell axis. The resolution of current-source density was optimized by varying the value of delta X used in each calculation according to the slope of the voltage gradient along different regions of the pyramidal cell. In general, a delta X of 75μm was used in dendritic regions, but

was shortened to 25μm in areas with a steep voltage gradient, such as in the vicinity of stratum pyramidale. In order to increase the signal-noise ratio, potentials were collected on-line at a sampling frequency of up to 25kHz, and could be averaged and digitally filtered before applying current-source density calculations. Since current-source density was calculated in one dimension, and the value of the extracellular conductivity was not determined in the present study, CSD waveforms cannot be considered absolute quantitative estimates of current density, and units are not provided on CSD profiles. Rather, current-source density profiles are used to compare the qualitative characteristics of sink-source relationships in the CA1 region following stimulation of major efferent or afferent pathways in the hippocampal slice.

3-3. Results

Morphological Characteristics of the Rat CA1 Pyramidal Neuron

In order to correlate current-source density relationships to specific anatomical locations of the pyramidal cell, a detailed knowledge of both the structure and relationship of the cell to various strata within the CA1 region is required. Almost all measurements of the length and branching pattern of pyramidal cell structures have been carried out in the mouse, guinea-pig or rabbit (Cajal 1911, Cragg and Hamlyn 1955; Green and Maxwell 1961; Lorente de No 1934; Turner and Schwartzkroin 1980). An exception is Westrum and Blackstad's (1962) electron microscopic study of CA1 pyramidal neurons in the rat. Although the general morphology of the pyramidal cell is similar between species, the exact dimension of cell processes can vary considerably. For instance, the length of the proximal shaft and dimension of neuronal elements in the rat are said to be "considerably smaller" than those in the rabbit (Green and Maxwell 1961). The size of the pyramidal cell can also vary according to the hippocampal subfield and along the septo-temporal pole, with the dorsal CA1b region containing some of the smallest pyramidal cells of the hippocampal formation (Lorente de No 1934).

Attempts were thus made to obtain quantitative estimates of the width of strata and of the length and branching pattern of pyramidal cell dendrites in the CA1 region. This was accomplished through light microscopic examination of cresyl violet stained hippocampal slices or of pyramidal cells in thin sections of hippocampal tissue stained immunohistochemically for

calcium-binding protein (CaBP; Baimbridge and Miller 1982). Since subsequent intradendritic recordings were confined to the apical dendrite, attention was focused primarily upon apical dendritic elements in stratum radiatum, with measurements of dendritic diameter taken from the study of Westrum and Blackstad (1962).

Measurements of the width of strata in rat hippocampus gave values for the alveus of 70 +/- 17.8 μm (n=5; mean +/- sem), stratum oriens 160 +/- 18.1 μm (n=5), stratum pyramidale 44 +/- 2.9μm (n=34), stratum radiatum 303 +/- 7.8μm (n=18), and stratum lacunosun-moleculare 102 +/- 4.4μm (n=18). Pyramidal cells spanning the distance from the deep edge of stratum oriens to stratum lacunosum-moleculare would therefore exhibit a maximal overall length of 600μm. This contrasts with a length of up to 1mm in golgi-stained pyramidal cells of the guinea-pig (Turner and Schwartzkroin 1980).

Delineation of the boundary between somatic and dendritic membrane is often difficult as the cell body tapers gradually into the apical dendritic shaft, but the width and depth of pyramidal cell somata fall within the range of 10-15μm and 15-20μm, respectively. Although the length of the proximal apical dendritic shaft can vary considerably, most are within a range of 25-100μm. The diameter of the rat pyramidal cell dendrite is greatest in the proximal shaft (3-4μm) gradually tapering to a width of 2-3μm at the first branch point (Westrum and Blackstad 1962). Secondary branches progress radially at a slight angle towards the hippocampal fissure, tapering to a diameter of 0.5-1μm (Westrum and Blackstad 1962). The degree of transverse spread of dendritic branching from the region of the

soma can be as great as 225μm, but is more usually within a range of 50-100μm.

Laminar Profiles of Evoked Activity in CA1 Pyramidal Neurons

The characteristics of evoked extracellular field potentials and sink-source relationships in the CA1 region were examined over the entire axis of the pyramidal neuron. However, most attention was focussed upon evoked electrical activity and current-source density in stratum pyramidale and stratum radiatum, regions corresponding to the somata and apical dendrites of the pyramidal cell population, respectively.

Antidromic Population Spike Response

The laminar profiles of extracellular field potentials (voltage) and associated current-source density (CSD) evoked through antidromic activation of CA1 pyramidal cells are shown in Fig 3.2. In this and all subsequent figures, the reference point for the distance of the recording electrode along the neuronal axis is taken as the ventral border of stratum pyramidale (0μm).

The characteristics of the antidromic field potential were found to vary according to the recording position along the pyramidal cell structure (Fig 3.2A). At the level of stratum pyramidale, alvear stimulation evoked a short latency negative-going potential characteristic of an antidromic population spike response (Fig 3.2A; Leung 1979a,b; Sperti et al. 1967). A similar response was recorded approximately 100μm on either side of stratum pyramidale, but the negativity of the potential was of shortest peak latency in stratum pyramidale or

the proximal stratum oriens. The population spike then progressively declined in amplitude and increased in latency along the apical dendrite with distance from the border of stratum pyramidale. In stratum radiatum, the negativity of the spike was continuous with the negative component of a positive/negative dendritic potential (Fig 3.2A, 150μm). The peak latency of both the positive and negative potentials of the dendritic waveform continued to increase with distance along the dendritic tree, giving rise in distal dendritic locations to a monophasic positive field potential.

Calculation of current-source density from laminar profiles of antidromic field potentials also revealed a transition in the characteristics of current sources and sinks along the pyramidal cell axis (Fig 3.2B). Alvear stimulation evoked a large amplitude current sink with shortest peak latency within stratum pyramidale or the proximal region of stratum oriens, indicating the movement of current from the extra- to the intracellular compartment. A biphasic current source/sink could be observed in the proximal-mid stratum radiatum, revealing an outward followed by an inward flow of current in the region of pyramidal cell apical dendrites. Both the source and sink of the dendritic response displayed a gradual increase in peak latency with distance from the border of stratum pyramidale. In distal stratum radiatum, the source component of the dendritic waveform progressively increased in duration coincident with a decline of the current sink, eventually forming a monophasic current source in distal apical dendritic locations.

The shift in peak latency of the field potential negativity and current sink along the pyramidal cell axis is

FIG. 3.2 A,B. Laminar profiles of extracellular field potentials (voltage) and current-source density (CSD) evoked through suprathreshold alvear antidromic stimulation. A. Evoked potentials were collected at 25μm steps parallel to the dendro-somatic axis of the pyramidal cell, and B, current-source density calculated in 1 dimension for each 25μm interval. CSD measurements are displayed with a zero line to facilitate comparison of sink-source relationships. A scaled schematic diagram of the rat pyramidal cell is interposed between profiles with the borders of stratum pyramidale denoted by dotted lines. Distance along the cell axis is taken from the ventral border of stratum pyramidale (0μm). C,D. A comparison of extracellular field potentials (C) and associated CSD measurements (D) at the level of pyramidal cell somata (-20μm) and apical dendrites (160μm) in response to alvear antidromic stimulation (waveforms taken from laminar profiles in A,B). Voltage polarity negative down in this and all subsequent figures.

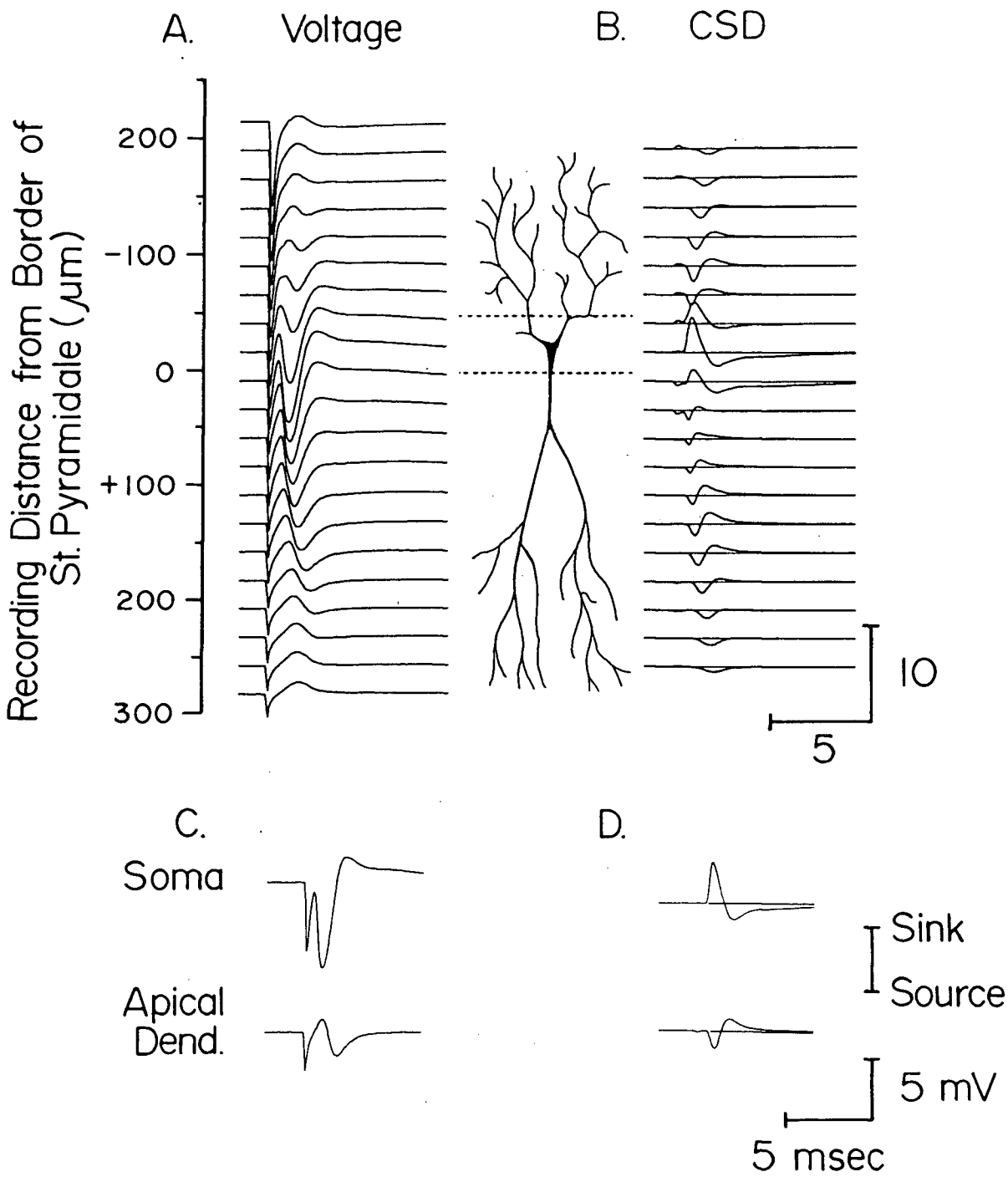
A.
Voltage
B.
CSD
Recording Distance from Border of St. Pyramidale (μm)
200
-100
0
+100
200
300
10
5
C.
Soma
Apical Dend.
D.
Sink
Source
5 mV
5 msec

more clearly distinguished by comparing the evoked antidromic response at the level of stratum pyramidale and radiatum (Fig 3.2C,D). The negativity of the antidromic field potential was evoked at a peak latency of 1.1msec in the cell body layer (Fig 3.2C) and 1.96msec in the apical dendritic region 160um from the border of stratum pyramidale (Fig 3.2C). A shift in peak latency of the evoked current sink is also apparent, with peak latency measurements of .9msec in stratum pyramidale and 2.1msec at the 160μm dendritic recording location (Fig 3.2D).

Therefore, both voltage and current-source density profiles indicate that alvear stimulation results in the initial activation of an antidromic spike in the region of pyramidal cell somata, as shown by the presence of a short-latency population spike and current sink in the vicinity of the cell body layer. The conduction of a biphasic potential and current source/sink through stratum radiatum further suggests a subsequent antidromic spike invasion of the apical dendritic arborization. In fact, a similar sequence of potentials could often be observed in stratum oriens following alvear stimulation, indicating that an antidromically evoked spike can conduct through both the basal and apical dendritic tree of the pyramidal cell. Similar results were obtained in previous analyses of alvear evoked potentials in the in vivo hippocampus (Gessi et al. 1966; Leung 1979a,b; Sperti et al. 1967), all evidence supporting the interpretation that an antidromically evoked action potential can sequentially invade the soma and dendritic arborizations of the CA1 pyramidal neuron.

Antidromic activation also evoked a long duration (7-15msec) positive-going potential immediately following the

population spike in stratum pyramidale and the proximal region of stratum oriens and radiatum (Fig 3.2B; -90 - 60μm). This potential was associated with a current source in the region of the cell layer (Fig 3.2B, -25 - 25μm) and a current sink in mid-dendritic locations. The sink component of this potential could thus overlap with that of the dendritic antidromic spike, preventing a comparison of the amplitude of action potential current sinks along the apical dendritic axis (Fig 3.2B, 50 - 150μm). This potential was not extensively examined in the present study, but most likely corresponds to the recurrent activation of inhibitory synaptic inputs in the region of stratum pyramidale (Andersen et al. 1969: Dingledine and Langmoen 1980; Leung 1979a,b,c; Sperti et al. 1967).

Subthreshold Excitatory Synaptic Potentials

Field potentials evoked through subthreshold stimulation of either stratum oriens or stratum radiatum displayed characteristics reflecting the activation of excitatory postsynaptic potentials (EPSPs) in dendritic locations of the pyramidal cell population (Fig 3.3). Stratum oriens (SO) stimulation evoked a graded negative-going potential of approximately 20msec duration in the region of pyramidal cell dendrites and a positive-going potential at the level of the cell body layer and apical dendrites (Fig 3.3A). The negativity of the SO evoked potential was maximal in stratum oriens (3.5mV at -100μm, Fig 3.3A), decreasing in amplitude towards the pyramidal cell layer to invert to a positive potential just proximal to or within stratum pyramidale. The positivity was often largest in amplitude in the proximal apical dendritic

region, progressively declining in amplitude but retaining a positive polarity throughout the apical dendritic field (Fig 3.3A). In some slices, the SO evoked dendritic negativity was followed by a second potential of positive polarity that increased in amplitude with proximity to stratum pyramidale (Fig 3.3A). This potential was observed as a positive-going deflection just beyond the peak of the negative dendritic waveform in proximal stratum oriens (-75μm - -125μm, Fig 3.3A), with both potentials evident in the form of a biphasic negative/positive waveform in the vicinity of stratum pyramidale (-50μm, Fig 3.3A). In this case, the peak latency of the basal dendritic negativity could appear to decrease with proximity to the pyramidal cell layer as the late positive potential increased in amplitude towards stratum pyramidale.

Current-source density analysis indicated that the negative -going wave in stratum oriens was associated with a graded long lasting current sink, indicating an inward movement of current in the region of pyramidal cell basal dendrites (Fig 3.3B). The current sink was maximal in the stratum oriens and decreased in amplitude with proximity to the cell layer, inverting to a current source in stratum pyramidale and the proximal apical dendritic region. The duration of the dendritic current sink was found to decline in the proximal region of the basal dendrite coincident with the increase in amplitude of the late positive-going potential (Fig 3.3B), suggesting that the latter was associated with the development of a late current source in the region of the pyramidal cell layer.

Subthreshold stimulation of stratum radiatum evoked a long duration negative-going potential with maximal amplitude in

FIG. 3.3 Laminar profiles of extracellular field potentials (voltage) and current-source density (CSD) evoked through subthreshold stimulation of stratum oriens (A,B) or stratum radiatum (C,D). A,C. Evoked potentials were collected at 25μm steps parallel to the dendro-somatic axis of the pyramidal cell, and B,D, current-source density calculated in 1 dimension for each 25μm interval. CSD measurements are displayed with a zero line to facilitate comparison of sink-source relationships. A scaled schematic diagram of the rat pyramidal cell is interposed between profiles with the borders of stratum pyramidale denoted by dotted lines. Distance along the cell axis is taken from the ventral border of stratum pyramidale (0μm).

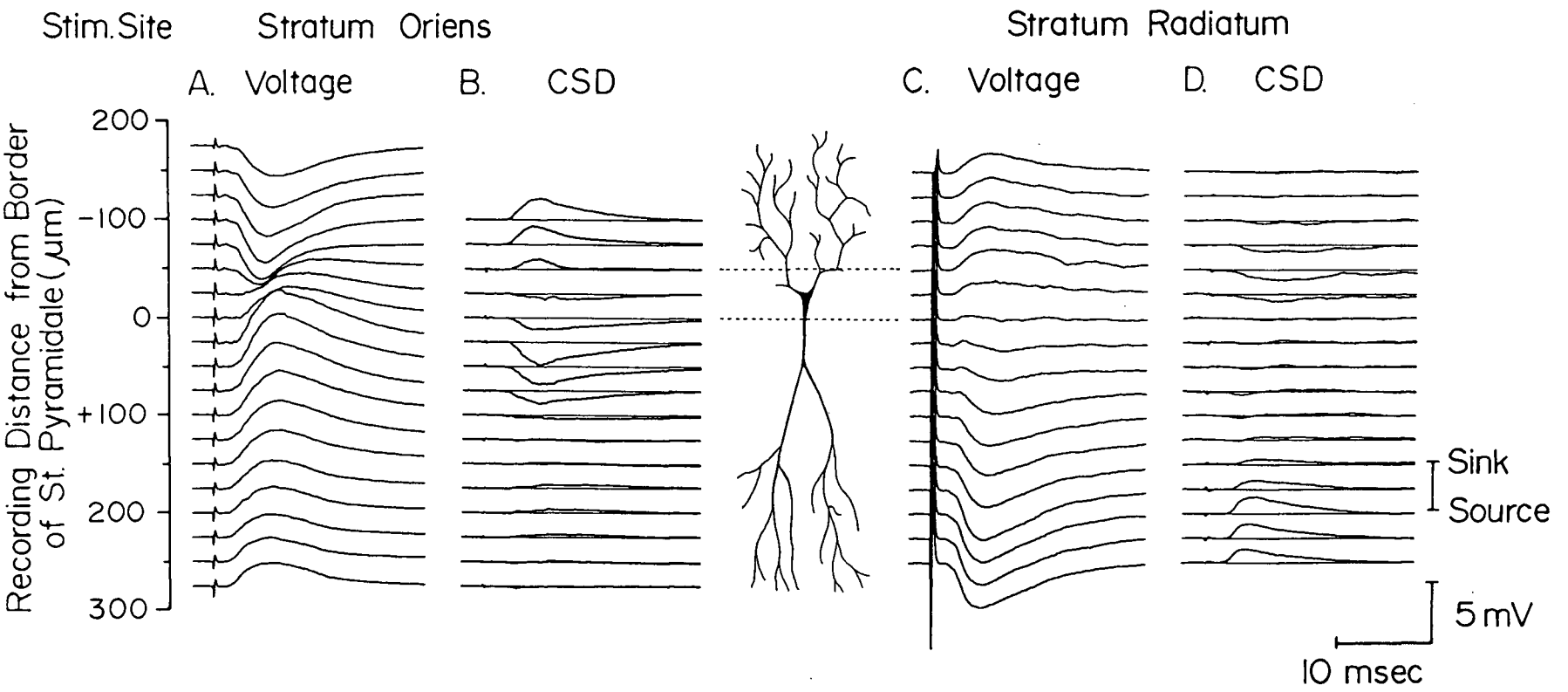
Stim.Site
Stratum Oriens
Stratum Radiatum
A. Voltage
B. CSD
C. Voltage
D. CSD
Recording Distance from Border of St. Pyramidale (μm)
200
-100
0
+100
200
300
Sink
Source
5 mV
10 msec

stratum radiatum 150 - 250μm from the border of stratum pyramidale (3.8mV in amplitude and 22msec in duration at 200μm, Fig 3.3C). This potential declined progressively in amplitude and increased in peak latency with proximity to stratum pyramidale, inverting to a positive polarity in the region of the cell layer. The positive-going potential was of similar duration as the dendritic negativity and attained a maximal amplitude in the proximal-mid stratum oriens.

Current-source density analysis revealed that the negative potential evoked in stratum radiatum was associated with a graded, long duration current sink in the region of the mid-distal apical dendrite (Fig 3.3D). The majority of current sourcing was found in stratum pyramidale or proximal stratum oriens, a region corresponding to the positive-going potential at the level of somata and proximal basal dendritic extensions of pyramidal neurons (Fig 3.3D).

Therefore, activation of synaptic afferents in stratum oriens or radiatum gave rise to an extracellular negativity and current sink restricted to the zone of stimulated afferent inputs, indicating a synaptic depolarization of pyramidal cell basal and apical dendrites, respectively. The decline in amplitude of the EPSP and current sink and the presence of a current source in stratum pyramidale suggest that evoked EPSPs were conducted electrotonically towards the pyramidal cell layer. The fact that synaptic currents were found to source beyond stratum pyramidale further indicate a conduction of the EPSP past the somatic region and through at least the proximal portion of the opposing dendritic tree.

The late positive-going potential and current source

observed in the proximal stratum oriens and pyramidale following SO stimulation likely represent an inhibitory synaptic potential evoked in the pyramidal cell through the action of inhibitory interneurons near the cell body layer (Andersen et al. 1969; Dingledine and Langmoen 1980; Leung 1979a,b,c). This is supported by the finding that the extracellular positivity correlates in time to an inhibitory potential recorded from intrasomatic impalements of the pyramidal neuron (data not shown). The means by which interneurons were activated was not determined, and the late inhibitory potential was not further examined in the present study.

Orthodromic Population Spike Responses

The laminar profiles of extracellular field potentials and current-source density evoked through suprathreshold SO stimulation are illustrated in Fig 3.4A,B. To aid comparison of somatic and apical dendritic activity of the pyramidal cell population, field potentials and corresponding CSD measurements recorded in stratum pyramidale and radiatum (125μm) are shown in Fig 3.4C,D.

The properties of the SO evoked population spike response were found to vary in a characteristic manner according to the recording position along the apical dendritic axis. At the level of stratum pyramidale, SO stimulation evoked a sharp negative population spike upon the underlying positivity of the synaptic waveform (Fig 3.4A,C). The shortest latency population spike was most often found in stratum pyramidale or the proximal stratum oriens, displaying a gradual increase in latency through the proximal apical dendrite. Approximately 150μm from the border of

FIG. 3.4 Laminar profiles of extracellular field potentials (voltage) and current-source density (CSD) evoked through suprathreshold stimulation of stratum oriens. A. Evoked potentials were collected at 25μm steps parallel to the dendro-somatic axis of the pyramidal cell, and B, current-source density calculated in 1 dimension for each 25μm interval. CSD measurements are displayed with a zero line to facilitate comparison of sink-source relationships. A scaled schematic diagram of the rat pyramidal cell is interposed between profiles with the borders of stratum pyramidale denoted by dotted lines. Distance along the cell axis is taken from the ventral border of stratum pyramidale (0μm). C,D. A comparison of extracellular field potentials (C) and associated CSD measurements (D) at the level of pyramidal cell somata (-25μm) and apical dendrites (125μm) in response to stratum oriens stimulation. (waveforms taken from profiles in A,B). Note that the onset of the dendritic spike response can be detected as a break on the rising edge of the positive-going dendritic potential recorded 125μm from stratum pyramidale.

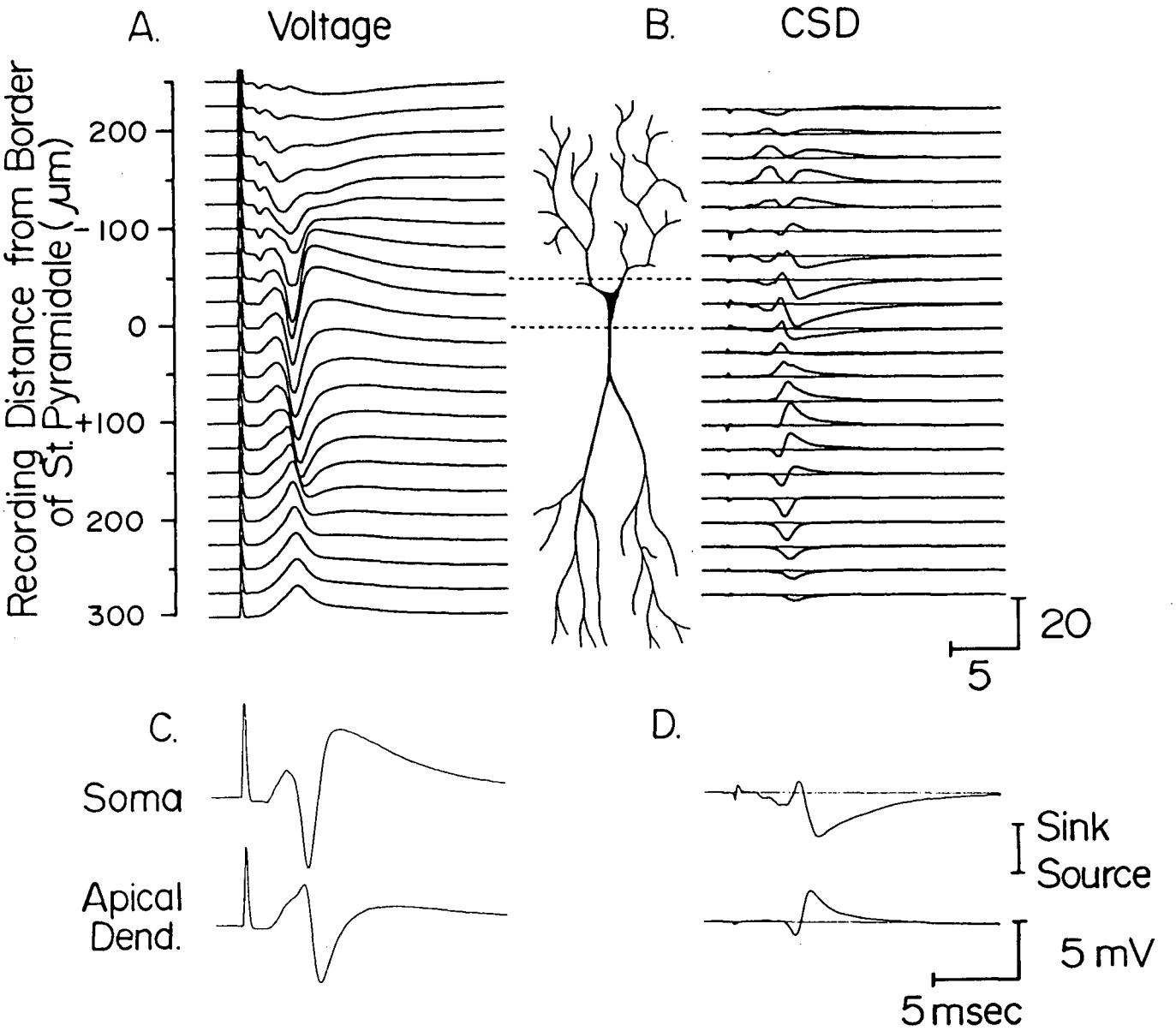
A.
Voltage
B.
CSD
Recording Distance from Border of St. Pyramidale (μm)
200
100
0
+100
200
300
20
5
C.
Soma
Apical Dend.
D.
Sink
Source
5 mV
5 msec

stratum pyramidale, the population spike response consisted of a biphasic positive/negative potential, distinguished from the underlying waveform by a break on the rising edge of the positive-going synaptic potential (see Fig 3.4C). The positive and negative component of the dendritic potential then continued to increase in latency through the mid-dendritic region, with the negativity "dropping out" in distal dendritic locations to leave a pure monophasic positive-going potential.

Calculation of current-source density uncovered a sharp current sink of shortest peak latency in the region of stratum pyramidale superimposed upon the source of current associated with synaptic activation of the basal dendrite (Fig 3.4B, -25μm; Fig 3.4D). The current sink gradually increased in latency through the proximal apical dendrite and was continuous with the sink component of a source/sink in the mid-dendritic region (Fig 3.4B, 125μm; Fig 3.4D). Both the source and sink of the dendritic response increased in latency with distance from stratum pyramidale, with the current sink gradually declining to give rise to a monophasic current source in distal dendritic membrane. The possible "contamination" of the dendritic sink by current flow associated with the large current source following the population spike response at the cell layer is particularly evident in Fig 3.4B (50 - 125μm).

A population spike response could also be detected at all levels of the pyramidal cell axis following suprathreshold stimulation of afferent synaptic inputs in stratum radiatum (Fig 3.5). In the region of the pyramidal cell layer, SR stimulation evoked a large population spike upon the positive-going apical dendritic synaptic potential (Fig 3.5A, -50μm; Fig 3.5C). The

largest amplitude and shortest latency population spike evoked by SR stimulation was most often found in stratum pyramidale or proximal stratum oriens. The peak negativity of the population spike then increased in latency and decreased in amplitude through the proximal apical dendritic field. Beyond 50 - 100μm from the ventral border of stratum pyramidale, the spike response continued through the mid stratum radiatum as a positive/negative waveform superimposed upon the extracellular negativity of the apical dendritic EPSP (Fig 3.5A,C). The latency of both the positive and negative components of the dendritic spike response increased through stratum radiatum, converting in distal dendritic locations to a monophasic positive-going deflection at a latency beyond the peak of the extracellular EPSP.

Current-source density profiles revealed that SR stimulation evoked a large amplitude short latency current sink in the region of stratum pyramidale (Fig 3.5A, -50μm) that gradually increased in peak latency through the proximal stratum radiatum. This waveform continued as the sink component of a dendritic source/sink, with both the source and sink progressively increasing in latency through the dendritic tree to superimpose upon the long lasting current sink in the region of synaptic termination (Fig 3.5B, 200μm; Fig 3.5D). A similar sequence of potentials and current source/sink(s) were also found to conduct through the basal dendritic region of pyramidal cells following stimulation of stratum radiatum afferent inputs (Fig 3.5).

Thus, the characteristics of the SR evoked population spike response along the pyramidal cell axis are not unlike those

FIG. 3.5 Laminar profiles of extracellular field potentials (voltage) and current-source density (CSD) evoked through suprathreshold stratum radiatum stimulation. A. Evoked potentials were collected at 25μm steps parallel to the dendro-somatic axis of the pyramidal cell, and B, current-source density calculated in 1 dimension for each 25μm interval. CSD measurements are displayed with a zero line to facilitate comparison of sink-source relationships. A scaled schematic diagram of the rat pyramidal cell is interposed between profiles with the borders of stratum pyramidale denoted by dotted lines. Distance along the cell axis is taken from the ventral border of stratum pyramidale (0μm). C,D. A comparison of extracellular field potentials (C) and CSD measurements (D) at the level of pyramidal cell somata (-50μm) and apical dendrites (200μm) in response to stratum radiatum stimulation (waveforms taken from laminar profiles in A,B).

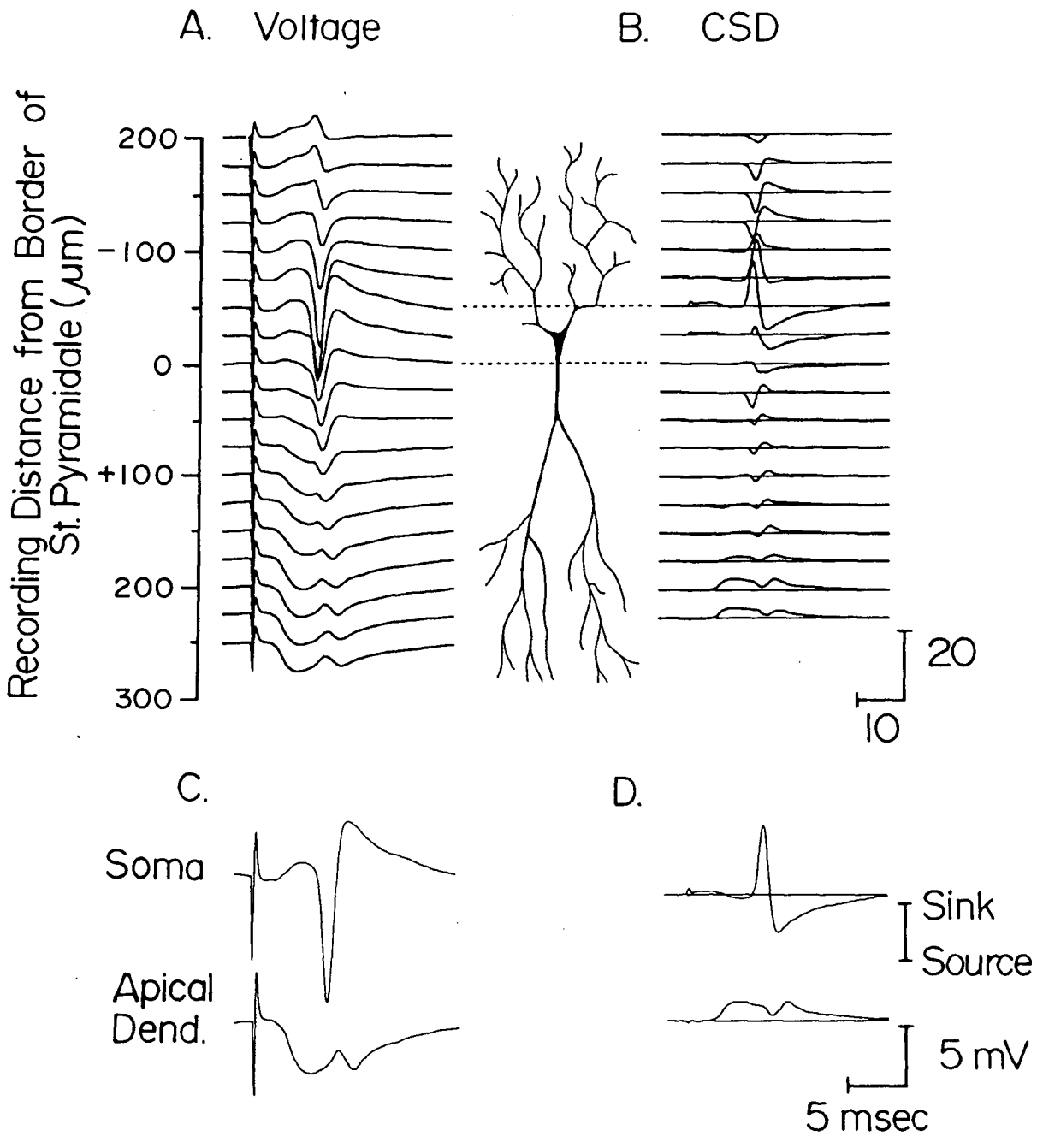
A. Voltage
B. CSD
Recording Distance from Border of St. Pyramidale (μm)
200
100
0
+100
200
300
20
10
C.
Soma
Apical Dend.
D.
Sink
Source
5 mV
5 msec

evoked through antidromic activation or synaptic depolarization of the basal dendritic tree (cf 3.2 and 3.4). This point is more clearly illustrated in Fig 3.6, where evoked field potentials in stratum pyramidale and radiatum are aligned with associated current-source density measurements to provide a direct comparison of responses evoked by SR and alvear stimulation (records taken from Figs 3.2 and 3.5). In stratum pyramidale the falling edge and peak of both the alvear and SR evoked population spike align with the rising edge and peak of the evoked current sink (Fig 3.6A,C). Similarly, in stratum radiatum, the positive and negative components of the dendritic spike potential evoked through stimulation of either pathway correspond in onset and duration to the dendritic current source and sink, respectively (Fig 3.6B).

The similarity between the alvear and SR evoked population spike response is further emphasized by comparing the peak latency of the negative field potential and current sink at various points along the pyramidal cell axis (Fig 3.7; measurements taken from Figs 3.2 and 3.5). Both the negativity of the field potential and the current sink evoked by alvear or SR stimulation were of shortest peak latency in stratum pyramidale, progressively increasing in latency through both the basal and apical dendritic regions. Although the latency of the evoked population spike and current sink were similar along most of the pyramidal cell axis, some deviation in the peak latency of the current sink was found in proximal dendritic regions as a result of current flow towards the late source of current following population spike discharge in stratum pyramidale (Fig 3.7).

FIG. 3.6 A comparison of the timing relationship between evoked extracellular field potentials and associated current-source density (CSD) measurements at the level of pyramidal cell somata (pop spike) and apical dendrites (extra-dend). A,B. Somatic (A) and dendritic response (B, 160μm) to suprathreshold stimulation of pyramidal cell axons in the alveus. C,D. Somatic (C) and dendritic response (D) to suprathreshold stimulation of afferent synaptic inputs in stratum radiatum. Zero lines are included on CSD measurements to facilitate comparison of sink-source relationships.

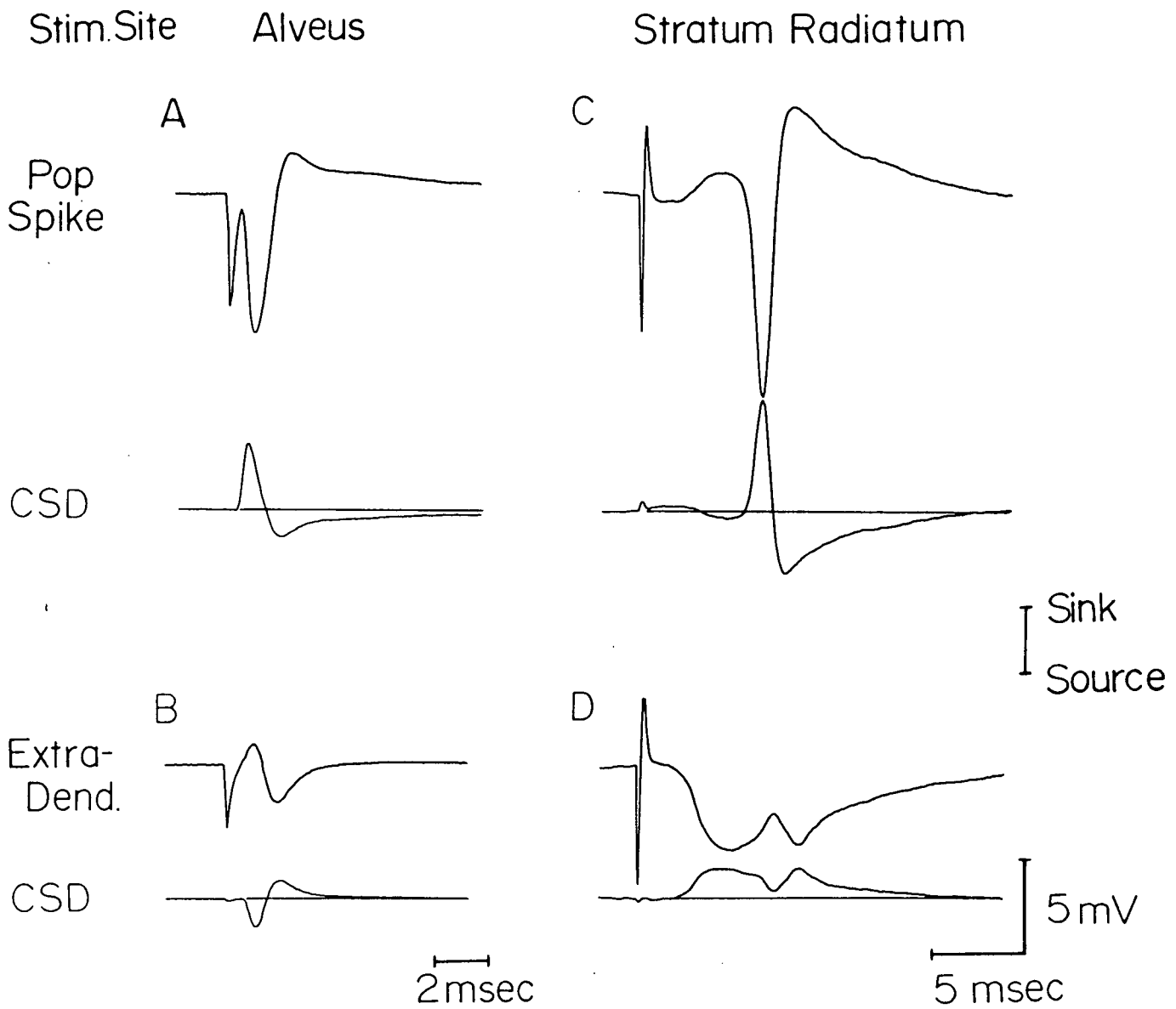
Stim.Site
Alveus
Stratum Radiatum
A
C
Pop Spike
CSD
Sink
Source
B
D
Extra-Dend.
CSD
5 mV
2 msec
5 msec

FIG. 3.7 Peak latency measurements of the extracellular population spike negativity (voltage) and current sink (CSD) at 25μm intervals along the dendro-somatic axis of the pyramidal cell in response to alvear antidromic stimulation (A) or stimulation of afferent synaptic inputs in stratum radiatum (B). Latency measurements were calculated by computer from the laminar profiles of Figs 3.2 and 3.5, with distance along the pyramidal cell axis taken from the ventral border of stratum pyramidale (0μm). A schematic diagram of the rat pyramidal cell drawn to scale is shown for comparison and the borders of stratum pyramidale for each slice are denoted by dotted lines.

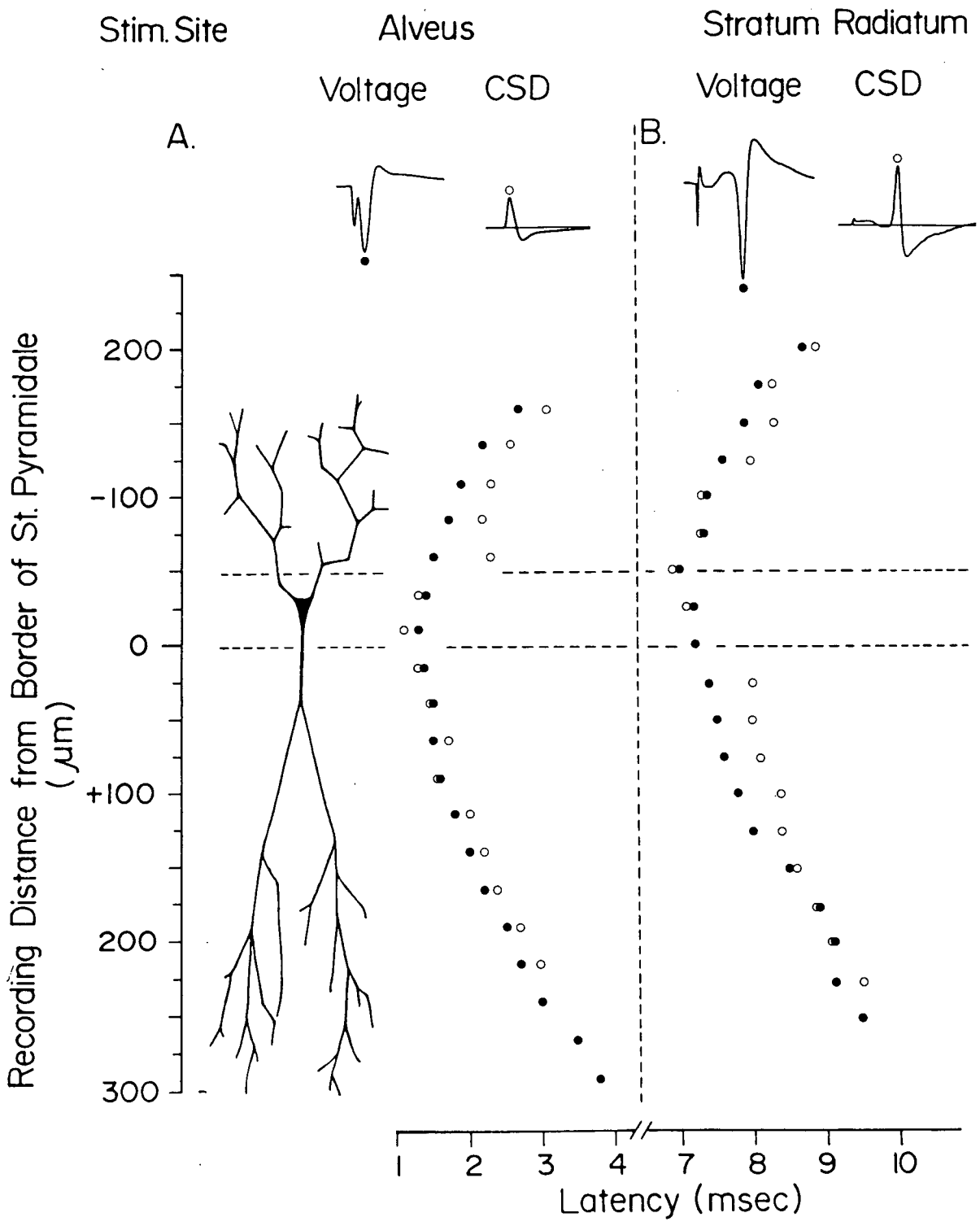
Stim. Site
Alveus
Stratum Radiatum
Voltage
CSD
Voltage
CSD
A.
B.
200
-100
0
+100
200
300
Recording Distance from Border of St. Pyramidale (μm)
1
2
3
4
7
8
9
10
Latency (msec)

Both the alvear and orthodromic evoked response were also found to display a non-uniform increase in the peak latency of the spike waveform through the dendritic field of the pyramidal cell population. In proximal stratum radiatum, the negativity of the population spike displayed little shift in peak latency over the initial 100μm distance from stratum pyramidale. However, the peak latency of the negativity increased in the approximate region of transition of the spike waveform to a biphasic positive/negative potential, with both components exhibiting a greater degree of latency shift through mid stratum radiatum. The greatest shift in peak latency of the negative potential was found in distal dendritic regions, just prior to loss of the negative component of the dendritic spike response.

3-4. Discussion

Current-source density analysis of evoked extracellular field potentials along the pyramidal cell axis has served to identify the site of origin of evoked excitatory synaptic potentials and spike discharge in CA1 pyramidal neurons.

Stimulation of stratum oriens (SO) or radiatum (SR) evoked an extracellular negativity and current sink spatially localized to regions of the pyramidal cell structure consistent with the known distribution of afferent synaptic projections to regio superior. In the case of SO stimulation, the negativity and current sink was maximal in the stratum oriens, a region corresponding to the point of termination of commissural inputs upon the pyramidal cell basal dendritic tree (Blackstad 1956; Raisman et al. 1965). SR stimulation evoked a maximal negativity and current sink in the mid-distal stratum radiatum, an area encompassing the terminal projections of Schaffer collateral and commissural afferent inputs (Lorente de No 1934; Raisman et al. 1965; Westrum and Blackstad 1962). In either case, the synaptically evoked dendritic negativity and current sink declined in amplitude with proximity to stratum pyramidale, and was associated with a source of current within and beyond the region of the cell layer.

The amplitude, spatial distribution and polarity of evoked synaptic potentials along the pyramidal cell axis indicate an active synaptic depolarization of dendritic membrane and electrotonic conduction of EPSPs from the point of synaptic termination towards the pyramidal cell layer. In addition, synaptic potentials were found to conduct beyond the somatic

level and through some portion of the opposing dendritic arborization, as indicated by the presence of an extracellular positivity and current source beyond stratum pyramidale . In fact, the presence and gradual decline in amplitude of the SO evoked EPSP along the apical dendrite has now been confirmed through intradendritic recording procedures (Chapter 5). Therefore, synaptic currents evoked within one dendritic tree of the pyramidal neuron (as with SO stimulation) are found to conduct electrotonically through the majority of the pyramidal cell structure, a result emphasizing the short electrotonic length of the CA1 pyramidal neuron (Brown et al. 1981; Turner 1984; Turner and Schwartzkroin 1980).

A synchronous antidromic population spike response was evoked by suprathreshold stimulation of the alveus, as shown by the generation of a short latency population spike in the region of the pyramidal cell layer. This response was associated with the immediate onset of a current sink, indicating an inward flow of current and the generation of action potentials in the presumed region of the soma and axon hillock of CA1 pyramidal neurons. Antidromic stimulation also evoked an extracellular spike response in the apical dendritic region, observed as a biphasic positive/negative potential in the mid stratum radiatum. This waveform was found through current-source density analysis to correspond to a current source/sink conducting from the cell layer through the apical dendritic field. Such a response would be expected for the case of an action potential conducting towards a recording location, where a local circuit depolarization preceding spike activation would give rise to an initial source of current followed by a current sink at the time

of spike generation at the recording site.

Thus, the evoked characteristics of the antidromic response indicate the initial generation of an action potential in the region of the pyramidal cell body and a sequential depolarization of dendritic membrane, resulting in a retrograde invasion of the spike through the apical dendritic arborization. As mentioned, a similar sequence of current source/sink relationships was observed in stratum oriens following alvear stimulation, suggesting an antidromic spike invasion of both the basal and apical dendritic tree. The above results agree with those of previous investigators, in which alvear evoked potentials in the in vivo hippocampus were interpreted to indicate a sequential spike invasion of axon hillock, soma, and basal and apical dendritic structures (Gessi et al. 1966; Leung 1979a,b; Sperti et al. 1967).

Activation of afferent synaptic inputs terminating upon either the basal or apical dendritic tree also evoked a population spike response at all levels of the pyramidal cell axis. Suprathreshold stimulation of stratum oriens or radiatum evoked a population spike and current sink of shortest peak latency in stratum pyramidale or the proximal stratum oriens. These waveforms were continuous with a biphasic positive/negative potential or current source/sink that progressively increased in latency through both basal and apical dendritic fields. The pattern of spike generation following stimulation of afferent synaptic inputs was thus very similar to that found for antidromically evoked spike discharge. In each case, the shortest latency population spike was found in the region of the pyramidal cell layer, with anti- and orthodromic

spike responses exhibiting a shift in peak latency with distance from stratum pyramidale. In addition, a direct comparison of alvear and SR evoked potentials revealed a similar relationship between extracellular field potentials and current-source density waveforms at both the somatic and apical dendritic level of pyramidal neurons.

Therefore, the sequence of spike generation in the pyramidal cell following activation of afferent synaptic inputs would appear indistinguishable from that found for an action potential evoked through antidromic stimulation. Specifically, synaptic depolarization of either dendritic tree results in the initial generation of a spike in the region of the pyramidal cell layer, with a subsequent retrograde spike invasion of both the basal and apical dendritic arborizations.

Occasionally, short latency current sinks could be found in both the proximal stratum oriens and stratum pyramidale following suprathreshold activation of any of the three stimulus pathways. These current sinks might represent sequential AP discharge in the axon hillock and somatic region of the pyramidal cell, corresponding to the initial segment (IS) and soma-dendritic (SD) components of spike discharge proposed for the spinal motoneuron (Coombs et al. 1957a,b). However, the relative size and tight packing of pyramidal neurons within stratum pyramidale does not permit a reliable dissociation between the activity of initial segment and somatic membranes of pyramidal cells through current-source density analysis. The site for initial spike generation in the pyramidal cell can thus only be referred to the region of the soma - axon hillock.

Regardless of the form of activation, conduction of the

spike through the apical dendritic tree was found to occur in a non-uniform manner. Over approximately the initial 100μm of the dendritic field, the extracellular spike response displayed a minimal shift in latency and a conduction velocity of 0.33 m/sec (peak latency measurements taken from the antidromic field potential negativity). In the mid-distal dendrite, the spike potential increased markedly in latency and slowed in conduction velocity (0.1 m/sec) to eventually terminate at a variable level in the distal dendritic region as a monophasic positivity and current source. These values compare to a conduction velocity of .36m/sec for the fibers of the Schaffer collateral/commissural projection and 1.2m/sec for myelinated pyramidal cell axons in the alvear region (Tielen et al. 1981).

There would thus appear to be two transition points of spike conduction through the apical dendrite, as judged by the change in shape and conduction velocity of the extracellular spike waveform. Of interest is the fact that these points correlate to the approximate location of major branchpoints of the rat pyramidal cell apical dendrite. As described earlier, the proximal shaft of the apical dendrite bifurcates in the range of 25-100μm from the pyramidal cell soma, with more extensive secondary branching in distal stratum radiatum or lacunosum-moleculare. The fast initial conduction velocity in the proximal stratum radiatum might then correspond to spike conduction through the thick proximal dendritic shaft, with a slowing of conduction velocity in the relatively thin secondary dendritic branches. The presence of a monophasic positive-going potential in distal stratum radiatum may further indicate a loss of spike conduction in the region of secondary dendritic

branching.

Previous investigations have reported that stimulation of afferent synaptic inputs in stratum radiatum results in the initial activation of a spike from within the pyramidal cell apical dendrite (Andersen 1960; Andersen and Lomo 1966; Cragg and Hamlyn 1955; Fujita and Sakata 1962). The first evidence for dendritic spike discharge came from laminar profile analyses of evoked extracellular field potentials, and consideration of the latency of field potential components along the pyramidal cell axis. Some of these studies reported an evoked negative spike potential of shortest peak latency in the proximal stratum radiatum, suggesting a proximal dendritic origin for the evoked spike (Andersen 1960; Fujita and Sakata 1962). In the present study, the population spike of shortest peak latency was in fact located in some slices in the proximal region of stratum radiatum. However, subsequent current-source density analysis revealed that the shortest latency current sink was to be found in stratum pyramidale or proximal stratum oriens. Since a more accurate spatial localization of transmembrane current flow can be achieved through current-source density analysis, the site for AP generation can again be taken as within the soma-axon hillock region of pyramidal neurons.

The above result serves to illustrate the difficulties that can arise when attempting to identify the site of origin of an evoked response from the spatial distribution of extracellular field potentials. Indeed, the ambiguity of field potential interpretation of current density was revealed in one slice, where peak latency measurements of the population spike appeared to indicate a different site of origin for spikes evoked from

each of the three stimulus pathways. However, examination of current-source density profiles demonstrated a common site of origin for all evoked spikes in the region of stratum pyramidale, as indicated by a short latency current sink.

Others have reported a distal dendritic site of origin for the pyramidal cell dendritic spike following stimulation of afferent synaptic inputs (Andersen et al. 1966a,b; Andersen and Lomo 1966; Cragg and Hamlyn 1955). In these studies, the extracellular representation of a dendritic spike was often taken as the peak negativity of the evoked response at all levels of the pyramidal cell axis. However, in the present study, the negativity of the SR evoked dendritic spike response was found to be preceded by a positive potential in mid-distal stratum radiatum, with both the positive and negative components conducting from the cell body layer. Furthermore, the positive/negative spike potential would often fall beyond the peak of the EPSP in stratum radiatum, with the result that the negative synaptic waveform was in many cases greater in peak amplitude than the negative component of the dendritic spike (see Fig 3.5A, 225 and 250μm). Measurement of a short latency negativity on evoked dendritic potentials would therefore represent the peak latency of the synaptic potential, giving the impression of initial spike generation in distal dendritic regions.

One factor contributing to the difficulty in identifying the extradendritic spike is the fact that the negative component of the spike potential could at times be difficult to distinguish from the underlying negativity of the SR evoked EPSP. In this case, the dendritic spike would appear as a

monophasic positive potential, even though stimulation of the alveus or stratum oriens in the same slice would evoke a distinct positive/negative spike potential at the same dendritic recording site. This result is not completely understood at the present time, but may relate to the fact that SR stimulation results in an active synaptic depolarization of the apical dendrite, a form of membrane activation not brought about through stimulation of the alveus or stratum oriens. A spike invading the apical dendrite following SR stimulation may thus encounter membrane of relatively high conductance in the region of synaptic termination, distorting the extracellular waveform of the dendritic spike. This interpretation is supported by the fact that the negative component of the basal dendritic spike could also be difficult to distinguish on the extradendritic potential during SO stimulation and synaptic depolarization of the basal dendritic tree. However, regardless of the exact form of the extradendritic spike potential, current-source density analysis would confirm that the positive-going spike response had conducted from the cell body layer through the dendritic field.

Therefore, the results of the present study do not support the contention of a dendritic origin for evoked spikes within the apical dendritic field of the CA1 pyramidal neuron. Rather, the initial site for generation of a spike was localized through current-source density analysis to the cell body layer of the pyramidal cell population. The pyramidal cell dendritic spike would thus appear to arise through a retrograde invasion of the dendritic arborization by a spike initiated in the region of the soma-axon hillock.

4-0. COMPARATIVE INTRACELLULAR ANALYSIS OF SOMATIC AND DENDRITIC ELECTROPHYSIOLOGY OF CA1 PYRAMIDAL NEURONS

4-1. Introduction

Regional variations in the density and spatial distribution of ionic channels in neuronal membrane can result in a non-uniform excitability along the dendro-somatic axis of a cell (Llinas 1975; Traub and Llinas 1979). The hippocampal pyramidal cell is one neuron of the mammalian CNS thought to exhibit a regional variation in electroresponsive properties, with the pattern of evoked activity varying according to the form of activation and between somatic and dendritic recording sites. For instance, stimulation of afferent synaptic inputs is found to evoke a single fast (Na+-dependent) action potential (AP) at both the somatic and apical dendritic level of the pyramidal cell (Benardo et al. 1982; Kandel et al. 1961; Schwartzkroin 1975,1977; Wong et al. 1979). In contrast, a combination of both Na+ and Ca+2-dependent potentials can be evoked in the pyramidal cell by intracellular injection of depolarizing current (Benardo et al. 1982; Schwartzkroin and Slawsky 1977; Wong et al. 1979). However, Ca+2-dependent potentials are more predominant in dendritic than somatic membrane, with the generation of large Ca+2 spikes at the dendritic level (Benardo et al. 1982; Wong et al. 1979).

The differential electroresponsive properties of somatic and dendritic membranes are thought to be of important consequence to the final output of the pyramidal cell. According to the results of previous studies, selective regions of dendritic membrane exhibit a low threshold for Na+ spike

activation (hot spots), and spike generation in the dendrite can precede that at the axon hillock following stimulation of afferent synaptic inputs (Spencer and Kandel 1961b; Traub and Llinas 1979). The dendritic spike then conducts to the cell body, appearing at the somatic level as a small fast pre-potential superimposed upon the synaptic depolarization (Andersen and Lomo 1966; Schwartzkroin 1977; Spencer and Kandel 1961b). Thus, a spike originating from within the dendrite can summate with synaptic currents, and in this way increase the probability for generation of a spike at the soma-axon hillock. However, a major question that remains unanswered is the actual site for generation of the Na+-dependent dendritic spike. Most studies have reported evidence to suggest a dendritic site of origin for the spike recorded in the apical dendritic region of pyramidal neurons (Andersen 1960; Andersen and Lomo 1966; Cragg and Hamlyn 1955; Fujita and Sakata 1962; Schwartzkroin 1977; Spencer and Kandel 1961b; Traub and Llinas 1979; Wong et al. 1979). However, results obtained through current-source density analysis of evoked extracellular field potentials would not appear to support this hypothesis (Chapter 3). According to this study, the initial site for spike generation in the pyramidal cell is in the region of the soma-axon hillock, with dendritic spike discharge occurring through a retrograde spike invasion of the dendritic arborization.

Given the conflicting nature of the above hypotheses, it would seem necessary to further characterize the electroresponsive properties of the pyramidal cell in order to understand the factors responsible for spike generation at the somatic and dendritic level. The present study therefore

represents a comparative intracellular analysis of membrane properties, synaptic potentials, and action potential discharge in the soma and apical dendrites of CA1 pyramidal neurons.

4-2. Methods

Intracellular impalements of neuronal elements were restricted to stratum pyramidale and stratum radiatum of the CA1b subfield of regio superior. Intracellular potentials recorded in these strata could correspond to activity of the somata or dendritic extensions of either pyramidal or non-pyramidal neurons (Cajal 1911; Lorente de No 1934). However, several lines of evidence would suggest that the results to be presented were obtained from the somata and apical dendrites of pyramidal neurons.

Firstly, the pyramidal neuron is by far the most common cell type in the CA1 region, with stratum pyramidale and radiatum comprised largely of tightly packed pyramidal cell somata and apical dendrites, respectively. Non-pyramidal neurons are mainly localized above stratum pyramidale, although some are found scattered through the pyramidal cell layer. Even fewer numbers of non-pyramidal neurons are found in stratum radiatum (Cajal 1911; Lorente de No 1934). Therefore, the relative abundance and distribution of pyramidal cell structures suggest that intracellular recordings in CA1 would in high probability correspond to impalements of pyramidal cells.

Secondly, previous investigators have compared the membrane properties and discharge patterns of pyramidal somata (Knowles and Schwartzkroin 1981a; Turner and Schwartzkroin 1980) and apical dendrites (Benardo et al. 1982; Schwartzkroin and Mathers 1978; Wong et al. 1979) to that of non-pyramidal neurons (Ashwood et al. 1984; Knowles and Schwartzkroin 1981a; Schwartzkroin and Mathers 1978; Turner and Schwartzkroin 1980). These studies indicate that pyramidal and non-pyramidal cell

elements can be distinguished on the basis of electrophysiological characteristics. In the present study, impaled neuronal structures displayed evoked patterns of activity characteristic of pyramidal cell somata and apical dendrites, while cellular elements with properties ascribed to non-pyramidal neurons were very infrequently encountered.

Finally, previous investigators have anatomically verified that neuronal elements impaled in stratum pyramidale or radiatum with evoked characteristics very similar to those reported here correspond to impalements of somata (Turner and Schwartzkroin 1980) and apical dendrites of pyramidal neurons (Wong et al. 1979).

Therefore, the intracellular potentials to be described are considered representative of somatic and apical dendritic activity of CA1 pyramidal neurons. Considering the dispersion of cell bodies within the boundary of stratum pyramidale (Lorente de No 1934), the possibility exists that intracellular impalements within this layer may include recordings from the proximal portion of either basal or apical dendrites of pyramidal cells. However, with these limitations in mind, recordings from within stratum pyramidale will be designated as "somatic" in origin.

The results of the present study were obtained from over 165 somatic and 81 apical dendritic recordings. All intracellular potentials to be described were recorded from single microelectrode impalements of either the soma or dendrite, and were not obtained from dual impalements of a single pyramidal neuron. Membrane characteristics defined as satisfactory for inclusion of data were resting potentials of at

least -55mV and input resistance of 18 megohm or more. The amplitudes of evoked potentials were not used as acceptance criteria since this characteristic was found to vary according to the recording position along the pyramidal cell axis (Chapter 5). The term "current evoked spike" is used to refer to an action potential evoked through intracellular injection of depolarizing current, while "stimulus evoked spikes" are those activated through stimulation of afferent or efferent pathways in the hippocampal slice. Spike amplitude and halfwidth (width at half amplitude) was measured with respect to the resting potential baseline preceding the stimulus artefact. Amplitude, width, and voltage threshold measurements for current evoked spikes were taken from the first current evoked action potential. Voltage threshold for synaptically evoked AP discharge was taken as equivalent to the average peak amplitude of the underlying EPSP for stimulus intensities just threshold for spike activation.

The reference point from which the recording distance along the pyramidal cell axis was measured was taken as the ventral border of stratum pyramidale. The distance of the dendritic recording electrode from this point was measured with a graticule within the objective lens of the microscope, or estimated as a fraction of the distance from stratum pyramidale to the hippocampal fissure. This was done by visually dividing the 400um distance from the cell layer to the fissure in half, and subsequently dividing either half into thirds, thereby partitioning the total distance into sections approximating 65um. Any impalements falling between 65μm divisions were given a value intermediate to the distance of adjacent division

points. This technique proved to be a reasonably accurate method of judging the distance of a recording electrode from stratum pyramidale, and estimates made in this way were found to be comparable to those obtained by measurement with the graticule. Unless otherwise stated, dendritic impalements were obtained at least 150μm from the ventral border of stratum pyramidale.

4-3. Results

Membrane Characteristics

The membrane potential response of pyramidal cell somatic and dendritic impalements to a series of square wave current pulse injections are shown in Fig 4.1A,B. Current/voltage (I/V) profiles exhibit a linear displacement of membrane potential at both locations over a range of potentials extending from approximately -80mV to -55mV. For hyperpolarizing pulses beyond this range, a time-dependent sag of the membrane potential could be observed in both somatic and dendritic impalements, a response referred to as "anomalous rectification" (Hotson et al. 1979). Anomalous rectification was also observed for depolarizing current pulse injections as an increase in the slope of the I/V relation at potentials depolarized from resting value. Examples of somatic and dendritic recordings in which this form of rectification was particularly evident are shown in Fig 4.1C,D.

Somatic and dendritic membranes had comparable values of resting potential, with an average value of 62.5 +/- .73mV (n=83; mean +/- sem) in intrasomatic recording sites, and 64.3 +/- .55mV (n=27) for dendritic impalements (Table 1). Input resistance at the somatic and dendritic level were also similar, calculated as 25.9 +/- .57megohm (n=92; mean +/- sem) and 24.4 +/- 2.06megohm (n=14) for intrasomatic and -dendritic recording locations, respectively (Table 1).

FIG. 4.1 Pyramidal cell somatic (A) and apical dendritic (B) membrane potential responses to a range of square wave hyperpolarizing and depolarizing current pulse injections. The corresponding current/voltage (I/V) plot and calculated input resistances (Ri) for somatic and dendritic responses are shown below. Anomalous rectification of membrane potential in the depolarizing range is shown for another somatic (C) and dendritic (D) impalement. Action potentials truncated. In this and all subsequent figures, the intrasomatic and intradendritic response from separate pyramidal neurons are presented for comparison.

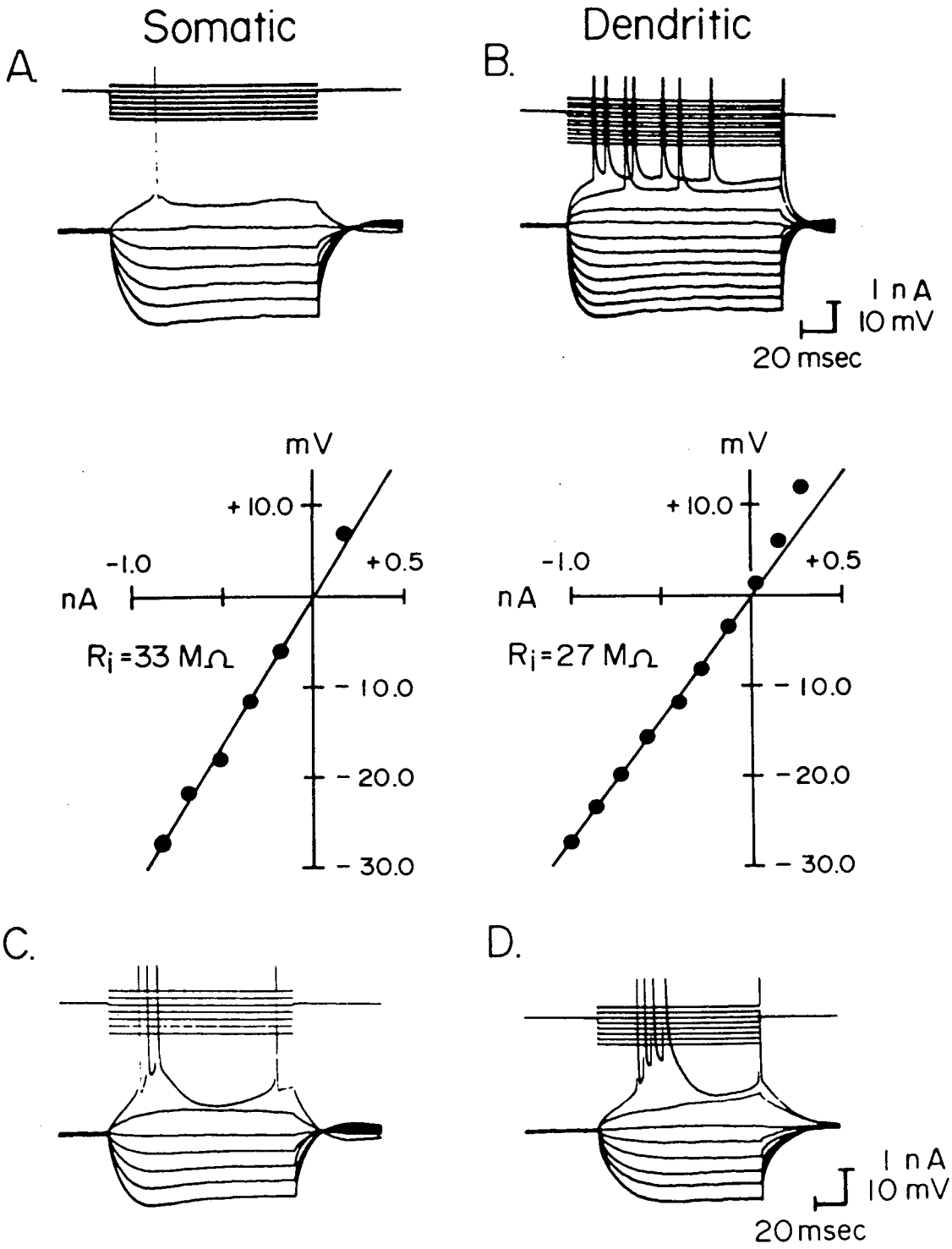
Somatic
Dendritic
A.
B.
1 nA
10 mV
20 msec
mV
+10.0
-1.0
+0.5
nA
Ri=33 MΩ
-10.0
-20.0
-30.0
mV
+10.0
-1.0
+0.5
nA
Ri=27 MΩ
-10.0
-20.0
-30.0
C.
D.
1 nA
10 mV
20 msec

TABLE 1 Average resting membrane potential (RMP) and input resistance (Ri) of CA1 pyramidal cell somatic and apical dendritic impalements obtained at least 150um from the border of stratum pyramidale (mean +/- sem; number of impalements shown in brackets). The average value of input resistance was calculated only for those recordings in which full current/voltage profiles had been constructed.

TABLE 1

	SOMATIC	DENDRITIC (≥150 μM)
RMP (mV)	62.5 ± .73 (83)	64.3 ± .55 (27)
R_I (MΩ)	25.9 ± .57 (92)	24.4 ± 2.06 (14)

Current Evoked Suprathreshold Responses

Depolarizing currents reliably evoked repetitive spike discharge in somatic and dendritic membranes of the pyramidal neuron. In general, current evoked action potential (AP) discharge in each location was very similar and could be assigned to either of two basic patterns, referred to as "Type 1" and "Type 2" for the purpose of comparison. A third but less common form of burst discharge appeared to be restricted to dendritic membrane (Type 3).

The Type 1 response was the most common form of spike discharge in both somatic (12/16) and dendritic impalements (21/36). In these cells, depolarizing current evoked a repetitive sequence of fast spikes for all levels of depolarizing current injection (Fig 4.2). Higher levels of depolarizing current evoked an initial high frequency "burst" of three to four action potentials followed by repetitive spike activation, with a progressive decrease in interspike interval as current injection was increased. The characteristics of evoked spikes within the burst varied in a predictable manner, displaying a rapid decline in amplitude and increase in halfwidth (width at half amplitude), with each spike in the burst arising from a slightly greater level of depolarization.

While the basic pattern of Type 1 discharge was recorded at all levels of the pyramidal cell axis, differences in the characteristics of current evoked somatic and dendritic spikes were detected. For instance, spikes evoked in the somatic region of the pyramidal cell were of greater amplitude and shorter halfwidth than those recorded within the apical dendrite. The recovery of spike amplitude following the initial burst of AP

FIG 4.2 The "Type 1" response of a CA1 pyramidal neuron to increasing levels of depolarizing current applied to a somatic (A-C) and dendritic impalement (D-F). Note difference in voltage calibration between somatic and dendritic recordings.

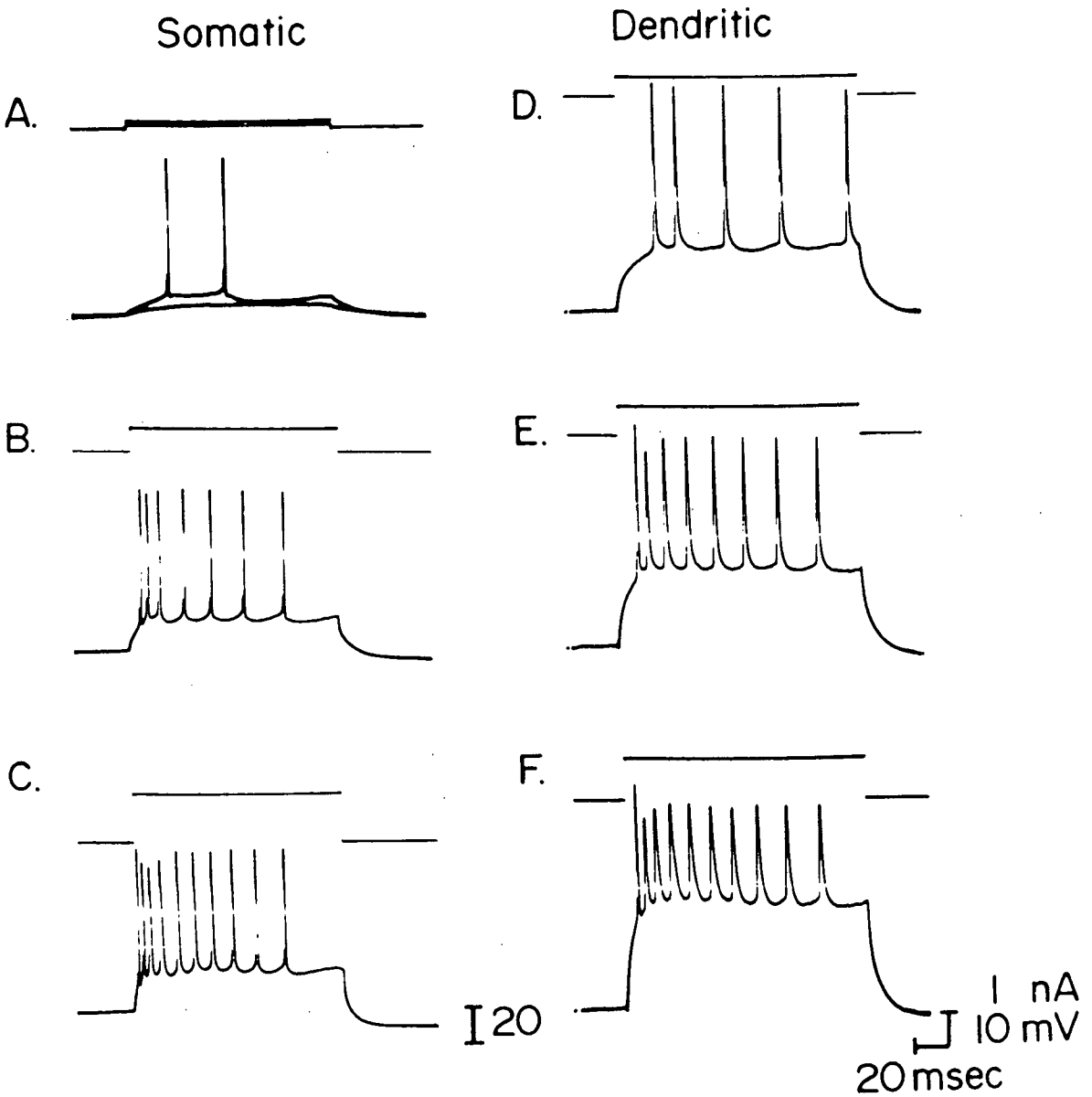
Somatic
Dendritic
A.
B.
C.
D.
E.
F.
I 20
1 nA
10 mV
20 msec

discharge could also differ between somatic and dendritic recording sites. In the soma, spike amplitude usually recovered from the initial decline within the burst by approximately the fifth to eighth action potential of the repetitive spike train. In contrast, the recovery of spike amplitude in the dendrite could depend upon the degree of current injection (7/12), with less recovery observed the greater the amplitude of the depolarizing current pulse (Fig 4.2 D-F). In addition, somatic spikes were evoked from a consistent voltage threshold, with the first evoked action potential arising from a similar level of depolarization regardless of the amplitude of the depolarizing current pulse (Fig 4.2A-C; voltage threshold measured as the absolute voltage of the breakpoint of spike discharge). However, dendritic membrane displayed no apparent threshold for AP discharge, with the voltage breakpoint for spike activation increasing directly with the level of current injection (Fig 4.2D-F).

Type 2 spike discharge was characterized by an initial high frequency burst of fast spikes followed by an afterhyperpolarization (AHP) and repetitive single spike discharge (Fig 4.3A-G). This pattern of activity was less commonly observed in both somatic (4/16) and dendritic (10/36) impalements and appeared to be most prevalent in membrane displaying an obvious anomalous rectification in the depolarizing range of current injection (cf 4.1C,D). Near threshold for AP discharge, current injection evoked the Type 2 response in full form, including an initial burst of spikes, an AHP, and repetitive spike discharge (Fig 4.3A,D). However, the pattern of activity varied with the degree of depolarization,

with repetitive spikes encroaching upon the AHP at higher levels of current injection (Fig 4.3A-C and D-G).

Once again, certain characteristics of the evoked spike differed between somatic and dendritic recording locations. In the soma, spikes within the initial burst of Type 2 discharge were evoked upon an underlying depolarization, exhibitng a rapid decline in amplitude and increase in halfwidth. However, the underlying depolarization and change in spike characteristics during the burst were more accentuated in dendritic impalements. Although spike amplitude following the initial burst could recover in somatic recordings during the current pulse, the amplitude of dendritic spikes could depend upon the level of current injection, displaying a greater degree of depression with higher depolarizing currents (Fig 4.3D-F). In some dendritic impalements (3/10), the third to fifth spike of the initial burst merged on top of a particularly large underlying depolarization to form a larger and broader spike, similar to the "intermediate spike" of Benardo et al. (1982) (Fig 4.3G). Component action potentials could then be detected as small inflections on the rising or falling edge of the intermediate spike (Fig 4.3G). Once again, spikes recorded in the somatic region were evoked from a similar voltage threshold for all levels of current injection (Fig 4.3A-C; measurements refer to the first evoked spike), while the voltage threshold for dendritic spike activation could appear to increase directly with the amplitude of the current pulse (Fig 4.3D-F).

Several of the evoked characteristics of Type 2 discharge were similar to that of Type 1 spike activation. For instance, the amplitude, halfwidth and voltage threshold of the first

FIG. 4.3 The "Type 2" response of CA1 pyramidal neurons to increasing levels of depolarizing current applied to a somatic (A-C) and dendritic impalement (D-F). The Type 2 response of G was taken from a separate dendritic impalement from that in D-F. H-K. "Type 3" responses of dendritic recordings illustrating the current evoked and spontaneous discharge of two separate dendritic impalements in H,I and J,K.

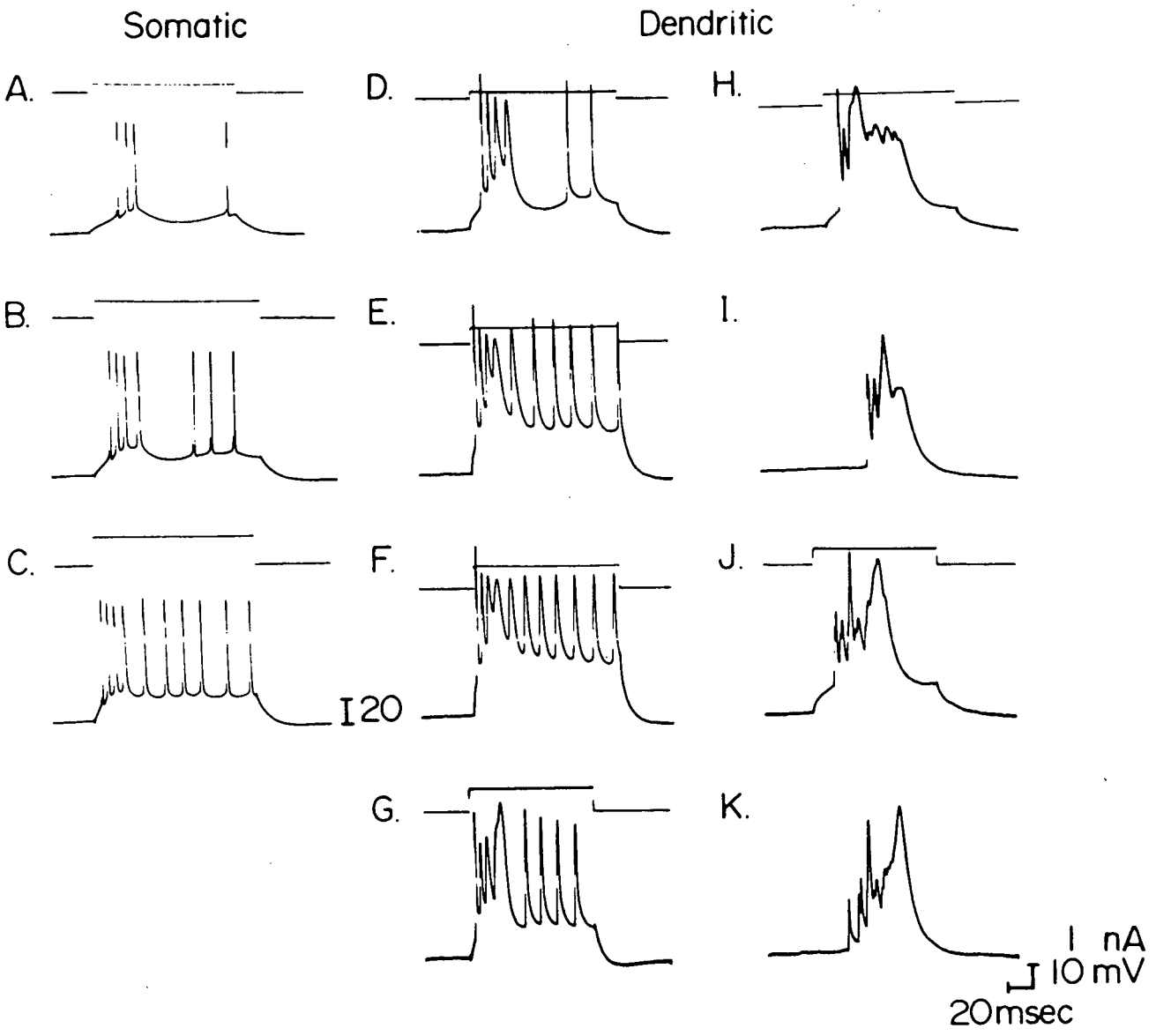
Somatic
Dendritic
A.
B.
C.
D.
E.
F.
G.
H.
I.
J.
K.
I20
1 nA
10 mV
20msec

current evoked spike were comparable in both Type 1 and 2 discharge. However, two major distinguishing features were the larger depolarization underlying the initial burst of spikes and the subsequent afterhyperpolarization observed in the Type 2 pattern of AP discharge. Type 1 and 2 activity were therefore most readily distinguished near threshold for spike activation, where the AHP of Type 2 discharge was most apparent.

A third and infrequent form of spike activiity (5/36) was only encountered in dendritic recording locations. The current evoked and spontaneous discharge of two separate dendritic impalements illustrating this type of response are shown in Fig 4.3H,I and J,K for comparison. The current evoked response in these dendrites consisted of a low threshold all-or-none burst of fast spikes on a rising depolarization with a "slow" spike evoked from the third or subsequent fast spike (Fig 4.3H and J). This pattern of spike generation appeared to be a distinct form of discharge, although one dendrite changed from Type 2 to Type 3 activity during the course of recording. The exact pattern and amplitude of initial fast spikes in Type 3 activity could vary from one dendritic impalement to another, but was generally constant over the time of recording from a given dendritic impalement. In contrast, slow spike characteristics varied from one depolarizing pulse to the next, evoked for example with an amplitude in the range of 50-75mV and halfwidth between 9-20msec in one dendritic recording. Type 3 activity was often accompanied by gradual depolarizing shifts of membrane potential that led to spontaneous all-or-none bursts of spike discharge, the form of which was very similar to that evoked through current injection in the same dendritic impalement (Fig 4.3H,I

and J,K). In contrast, spontaneous activity was not a common feature of cells displaying Type 1 or 2 discharge.

Stimulus Evoked Subthreshold Synaptic Potentials

Graded synaptic potentials were recorded at all levels of the pyramidal cell axis in response to stimulation of the alveus, stratum oriens or stratum radiatum (Fig 4.4). Alvear stimulation was used to activate inhibitory synaptic inputs to the pyramidal cell through recurrent activation of inhibitory interneurons in the region of stratum pyramidale (Fig 4.4A,D). Stimulation of the alveus at intensities subthreshold for antidromic spike discharge evoked a graded inhibitory potential (IPSP) at both somatic and dendritic recording sites. The peak latency of the IPSP differed between somatic and dendritic locations, displaying an average peak latency of 17.7 +/- 1.35msec (n=6; mean +/- sem) in the soma and 25.6 +/- 1.72msec (n=8) in dendritic recordings ($p \leq .014$ Students t-test). The dendritic inhibitory potential was often low in amplitude, and in many cases appeared as a slight depolarizing potential. However, the dendritic IPSP could be reversed to a hyperpolarizing potential through slight membrane depolarization (5-10 mV), and was equally effective in blocking the discharge of orthodromically evoked dendritic spikes regardless of polarity at resting potential (data not shown).

Stimulation of afferent synaptic inputs coursing through stratum oriens (SO) evoked a graded excitatory potential (EPSP) in both somata and apical dendrites of pyramidal cells (4.4B,E). The SO evoked EPSP was of largest amplitude in the somatic region, displaying an average peak amplitude of 14 +/- 2.48mV

FIG. 4.4 Stimulus evoked subthreshold synaptic potentials recorded in pyramidal cell soma (A-C) and dendrites (D-F) 200um from the border of stratum pyramidale superimposed at increasing intensities of stimulation. Potentials were evoked by stimulation of the alveus (A,D), stratum oriens (B,E), or stratum radiatum (C,F). All somatic recordings (A-C) were obtained from the same impalement (membrane slightly depolarized in A), while the recordings of D and F were taken from a single dendritic impalement. All potentials are averaged records of five single sweeps.

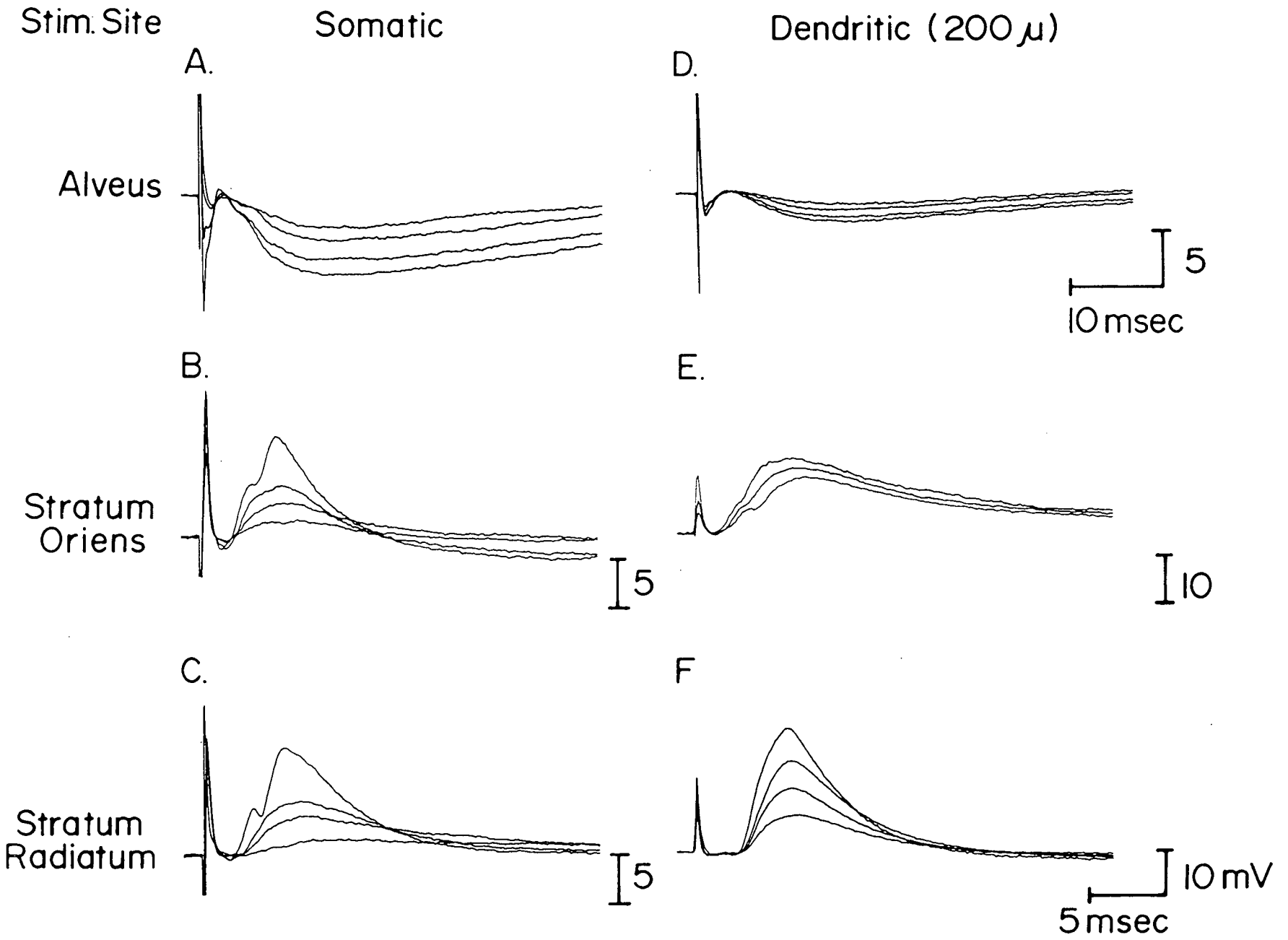
Stim. Site
Somatic
Dendritic (200 μ)
A.
D.
Alveus
5
10 msec
B.
E.
Stratum Oriens
5
10
C.
F
Stratum Radiatum
5
10 mV
5 msec

(n=5; mean +/- sem). The EPSP was of smaller amplitude in the apical dendrite, exhibiting a peak amplitude of 6.4 +/- 1.55mV 200μm from the border of stratum pyramidale (n=11; EPSPs set to spike threshold). Near threshold for spike discharge, a negative-going "notch" was frequently observed on the rising edge of somatic or dendritic EPSPs (Fig 4.4B,E), a response corresponding to reflections of the population spike response in the extracellular space (see Chapter 5).

Stimulation of Schaffer collateral/commissural afferents in stratum radiatum (SR) also evoked a graded excitatory potential in both somata and dendrites of pyramidal neurons (Fig 4.4C,F). This potential had the greatest amplitude in distal dendrites, exhibiting an average value of 21.2 +/- 1.13mV at 200μm distance from the border of stratum pyramidale (n=22; mean +/- sem). The somatic EPSP was of smaller peak amplitude, exhibiting an average value of 12.9 +/- .72mV in somatic impalements (n=34; EPSPs set to spike threshold). Once again, the extracellular population spike could often be observed as a reflection or "notch" on the rising edge of evoked EPSPs (Fig 4.4C; Richardson et al. 1984a; Turner et al. 1984).

Stimulus Evoked Suprathreshold Responses

Stimulus evoked action potential discharge differed markedly from that of current injection in that antidromic or orthodromic stimulation consistently evoked a single all-or-none spike in intracellular recordings of the pyramidal cell. Suprathreshold alvear stimulation evoked a short latency spike in both somatic and dendritic locations (Fig 4.5A,D). These spikes arose directly from baseline with an invariant onset

FIG. 4.5 Characteristic stimulus evoked spike discharge recorded in pyramidal cell somatic (A-C) and apical dendritic (D-F) locations. Spike discharge was evoked by stimulation of the alveus (A,D), stratum oriens (B,E), or stratum radiatum (D,F). Somatic recordings (A-C) were taken from three separate cells while dendritic recordings (D-F) were obtained from a single dendritic impalement (200μm from the border of stratum pyramidale). In each case, recordings are shown for sub- and suprathreshold intensities of stimulation. Note the common voltage and time base calibration of all recordings.

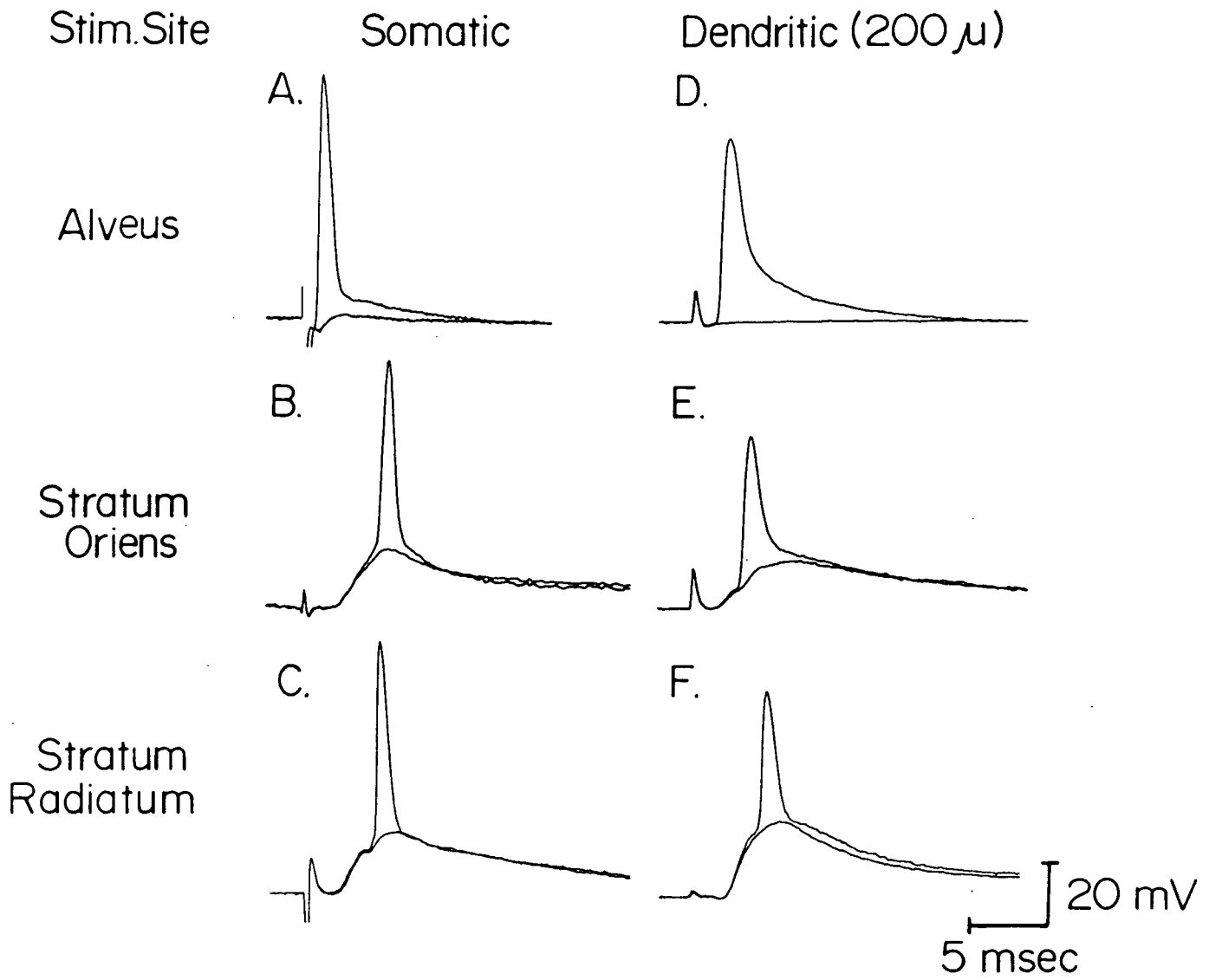
Stim.Site
Somatic
Dendritic (200 μ)
A.
D.
Alveus
B.
E.
Stratum Oriens
C.
F.
Stratum Radiatum
20 mV
5 msec

latency at a given stimulus intensity, representing an antidromic response of the soma and apical dendrites of the pyramidal neuron. Stimulation of stratum oriens (Fig 4.5B,E) or radiatum (Fig 4.5C,F) evoked a single all-or-none spike from an underlying EPSP at all levels of the pyramidal cell. The characteristics of action potentials evoked from each of the three stimulation sites were found to be similar at any given location along the dendro-somatic axis (cf 4.5A-C and D-F). However, as shown in Fig 4.5, spikes recorded at the soma were greater in amplitude and more narrow in halfwidth than those recorded in the apical dendrite.

Some of the properties of synaptically evoked spike discharge recorded from somatic and dendritic locations are illustrated in Fig 4.6. At stimulus intensities near threshold for spike generation, both somatic and dendritic spikes displayed considerable variability in onset latency ("latency jitter"), arising from approximately the peak of the excitatory synaptic potential (Fig 4.6A,B). As stimulus intensity was increased, spikes were evoked with a progressively shorter and less variable latency to discharge (Fig 4.6C,D). In the somatic region, spikes were evoked from a consistent voltage threshold, with spikes arising from a similar level of depolarization regardless of the latency to onset (Fig 4.6A). However, dendritic spike activation differed from that in the soma in displaying no clear voltage threshold for AP generation. This characteristic is clearly illustrated in Fig 4.6B in which spike discharge was evoked at two intensities of stimulation. At the higher stimulus intensity (12V), spikes were evoked from either the peak or the initial falling phase of the EPSP. With 9V

FIG. 4.6 Stratum radiatum evoked spike discharge recorded in pyramidal cell somatic (A,C) and dendritic locations (B,D), shown in each case with several superimposed sweeps. Stimulus intensities were set for threshold (A,B) or suprathreshold (C,D) activation of spike discharge in each location. Similar results were obtained for stratum oriens evoked potentials. All recordings were taken from separate impalements of somata or apical denrites 200um from the border of stratum pyramidale.

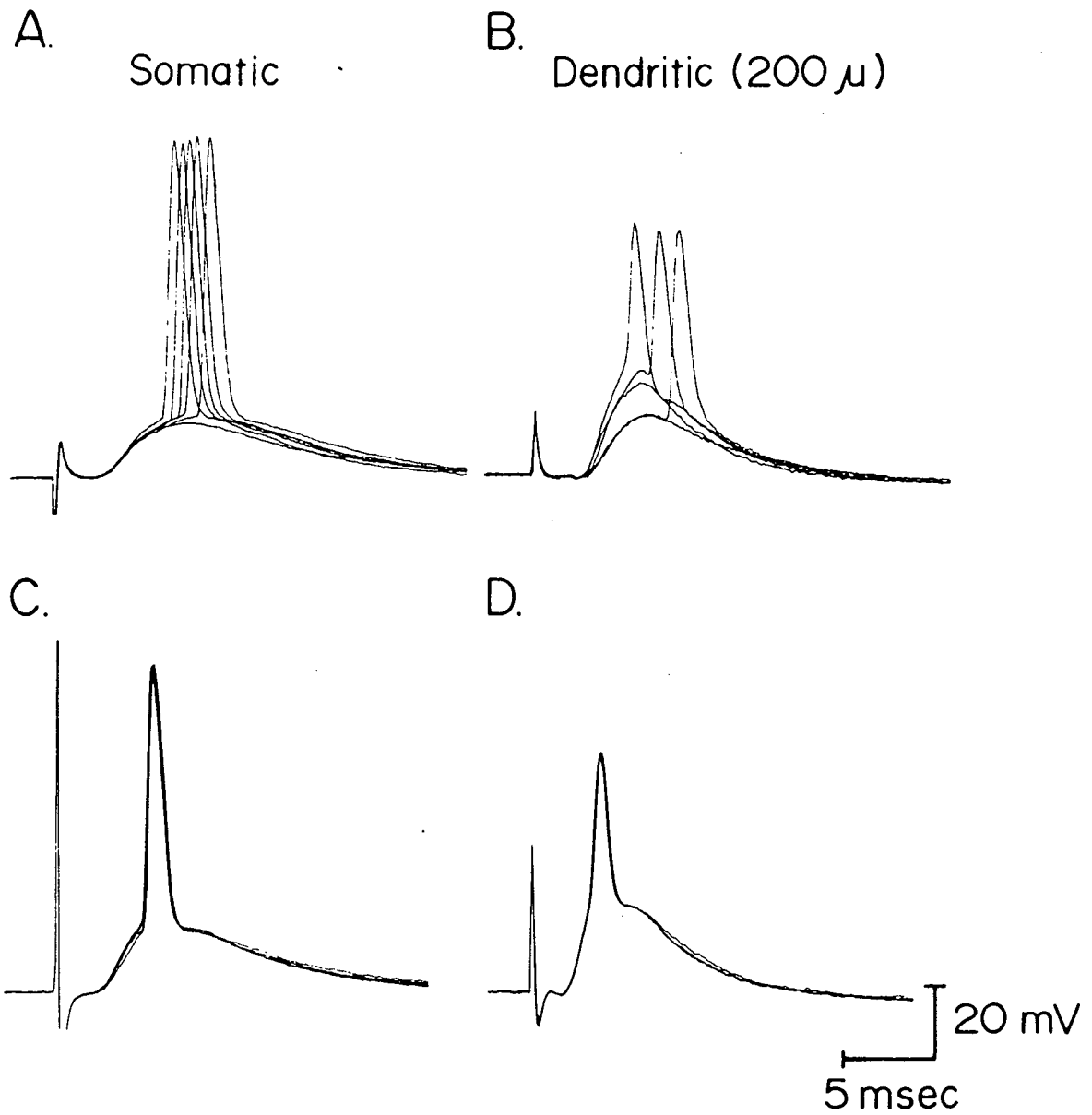
A.
Somatic
B.
Dendritic (200 μ)
C.
D.
20 mV
5 msec

stimulation, a spike could again be evoked, but from a smaller underlying EPSP and at a voltage threshold well below that observed at the 12V intensity.

High frequency stimulation of hippocampal afferent inputs is known to produce a characteristic increase in the rate of rise and amplitude of evoked potentials, a response pattern commonly referred to as "frequency potentiation" (Schwartzkroin 1977; Turner et al. 1984). The somatic and dendritic response to four pulses of a 10Hz stimulus train delivered to stratum radiatum is shown in Fig 4.7. With subthreshold stimulus intensities, repetitive stimulation brought about a potentiation of EPSP amplitude and the generation of a single all-or-none spike at both the somatic and dendritic level. Action potentials were evoked at comparable times during the frequency train and with continued stimulation displayed a shift to a shorter, less variable latency to onset. With prolonged stimulation or with greater frequencies of activation, multiple spike discharge could be evoked in either somatic or dendritic impalements. However, repetitive dendritic spike discharge did not appear to occur prior to the generation of multiple population spikes at the cell layer, a result indicating repetitive activation of spikes in the somatic region (Richardson et al. 1984a; Schwartzkroin and Prince 1980). Therefore, a similar pattern of action potential discharge was found at both the somatic and dendritic level of the pyramidal cell in response to high frequency stimulation of afferent synaptic inputs.

FIG. 4.7 Response of pyramidal cell soma (A) and apical dendrite (B) to 10Hz frequency stimulation of stratum radiatum afferent inputs at subthreshold stimulus intensities. Illustrated are four individual pulses of a ten pulse stimulus train with the last two pulses in either case showing a sub- and suprathreshold example from separate stimulus trains.

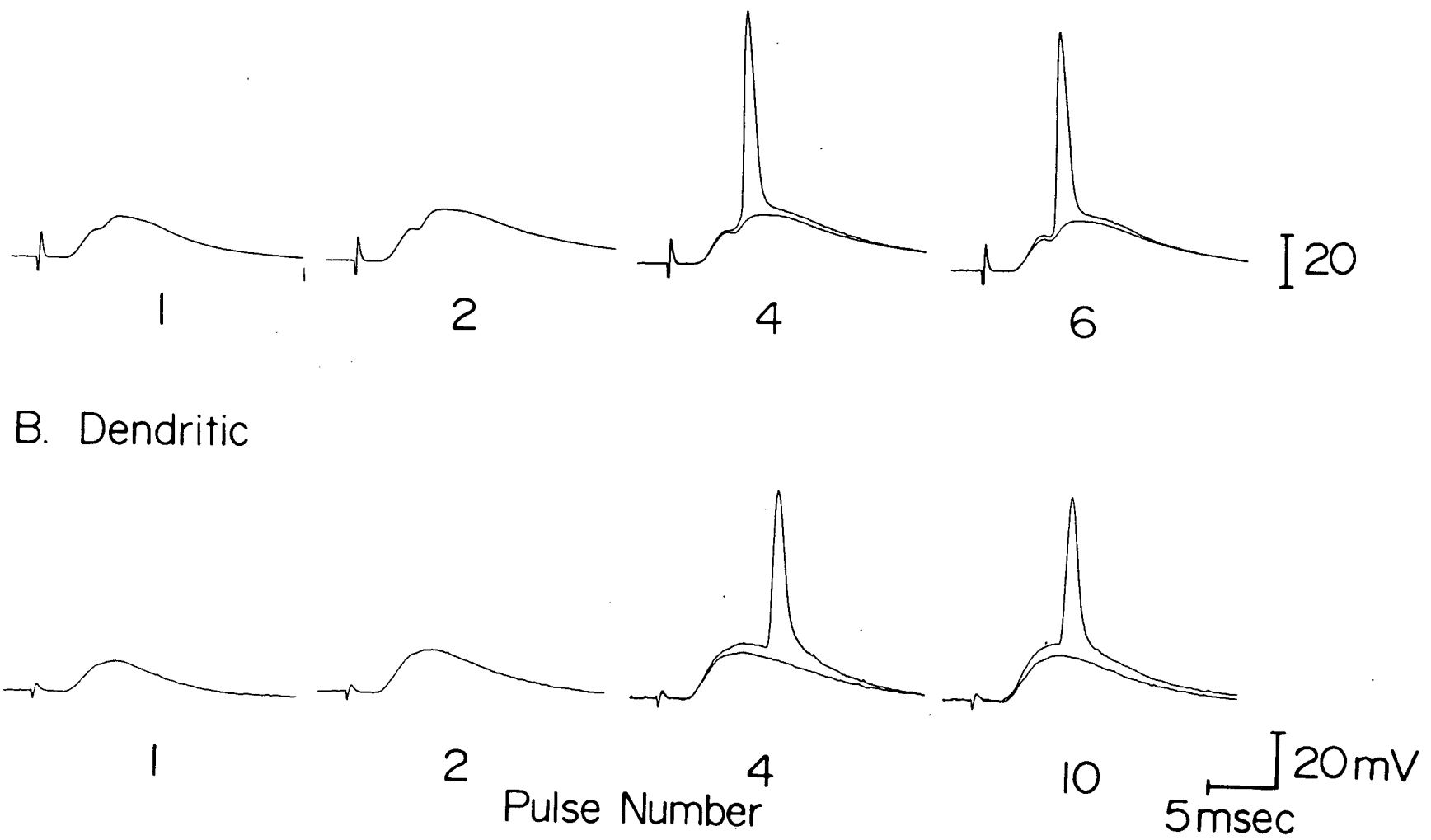
A. Somatic
1
2
4
6
20
B. Dendritic
1
2
4
10
Pulse Number
20mV
5msec

Comparison of Suprathreshold Stimulus and Current Evoked Responses

A characterization of pyramidal cell activity has revealed that depolarizing current evokes a variety of spike responses in the dendritic region, including the repetitive discharge of both large and small amplitude fast spikes, or the generation of a large slow action potential (cf 4.3). However, the most commonly evoked spike is of large amplitude and narrow halfwidth, evoked in a repetitive manner in Type 1 or 2 activity. To determine the similarity between this spike and those evoked through anti- or orthodromic stimulation, the stimulus and current evoked action potential of dendritic membrane was directly compared (Fig 4.8). Upon initial examination, stimulus and current evoked spikes appeared distinctly different in terms of amplitude and halfwidth (Fig 4.8A-C). However, when stimulus evoked spikes were activated upon the same underlying depolarization, all spikes superimposed, revealing a basic similarity between stimulus and current evoked action potential discharge (Fig 4.8D-F). Similar results were obtained in somatic impalements, although the initial difference in amplitude and halfwidth of stimulus and current evoked spikes was not as marked as in dendritic recording locations. In Table 2, a comparison of spike amplitude and halfwidth at the level of the soma and apical dendrites further demonstrates the similarity in waveform of stimulus and current evoked fast spikes of the pyramidal cell.

FIG. 4.8 Comparison of stimulus and current evoked action potential discharge in a pyramidal cell apical dendrite. A-C. Current evoked discharge is shown superimposed upon spikes activated by stimulation of the alveus (A), stratum oriens (B) or stratum radiatum (C). D-F. Stimulus evoked spikes were evoked on the same underlying depolarization as that necessary to elicit current evoked discharge, and a current evoked spike then superimposed for comparison. All potentials are taken from the same dendritic impalement 200μm from the border of stratum pyramidale.

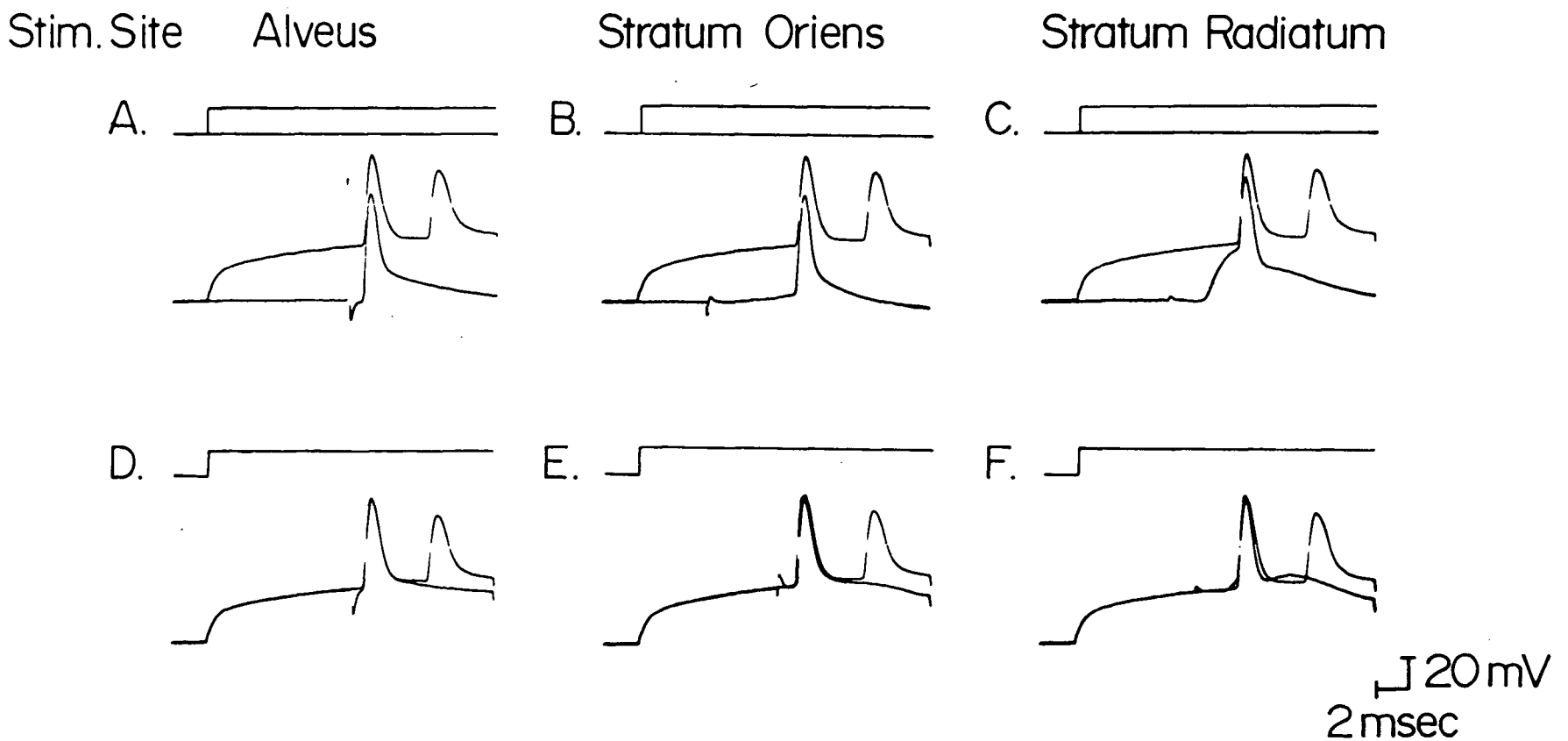
Stim. Site
Alveus
Stratum Oriens
Stratum Radiatum
A.
B.
C.
D.
E.
F.
20 mV
2 msec

TABLE 2 Average amplitude and halfwidth (width at half amplitude) of current and stimulus evoked spikes in pyramidal cell somata and apical dendrites 200μm from the border of stratum pyramidale (mean +/- sem; amplitudes measured from resting membrane potential). Measurements of current evoked spike characteristics were taken from the first spike of either Type 1 or 2 discharge evoked by depolarizing current. Stimulus evoked spikes were evoked by stimulation of the alveus, stratum oriens, or stratum radiatum. The number of impalements for each average are given in brackets. Stimulus evoked spikes at either the somatic or dendritic level were not significantly different according to a one way ANOVA test. Current evoked somatic spike amplitude and current evoked dendritic spike amplitude and halfwidth were found to be significantly different from stimulus evoked spikes. However, this difference can be attributed to the level of membrane depolarization upon which spikes are evoked (see Fig 4.8).

TABLE 2

	SPIKE AMPLITUDE (mV)		SPIKE HALFWIDTH (msec)	
STIMULUS	SOMATIC	DENDRITIC (200 um)	SOMATIC	DENDRITIC (200 um)
CURRENT INJECT.	90.3 ± 2.04 (11)	69.6 ± 3.42 (9)	1.06 ± .051 (6)	1.80 ± .14 (2)
ALVEUS	87.3 ± 2.77 (9)	62.9 ± 2.42 (11)	.96 ± .028 (7)	1.34 ± .069 (11)
STRATUM ORIENS	87.2 ± 4.06 (4)	59.5 ± 2.68 (12)	.84 ± .055 (4)	1.33 ± .066 (12)
STRATUM RADIATUM	90.0 ± 2.36 (9)	65.0 ± .97 (23)	.87 ± .039 (11)	1.17 ± .037 (20)

Spike Pre-Potentials

Somatic recordings of pyramidal neurons have often uncovered the presence of "fast pre-potentials" (FPPs), a name given to a small amplitude all-or-none potential capable of evoking somatic spike discharge (Andersen and Lomo 1966; Knowles and Schwartzkroin 1981b; MacVicar and Dudek 1981; Schwartzkroin 1975; 1977; Spencer and Kandel 1961). These potentials are characterized by a fast rate of rise, a relatively small amplitude, a fast initial decay and a second slower component of decay. Although not systematically examined in the present study, FPPs similar to those observed in the soma were also recorded at the dendritic level.

The characteristics of FPP discharge in pyramidal cell somata and apical dendrites are illustrated in Fig 4.9. Fast pre-potentials were evoked by stimulation of either stratum oriens or radiatum, and "uncovered" through hyperpolarization of the membrane (5-20mV) by current injection (Fig 4.9A,B). In either case, the FPP was evoked in an all-or-none manner near the peak of the EPSP, with action potential discharge arising from the peak of the fast pre-potential. Repetitive stimulation of afferent inputs (10-20Hz) could also evoke FPP discharge on the falling edge of the synaptic potential, with a progressive decrease in the latency to FPP activation during the stimulus train. Depolarizing current injection was also effective in evoking FPPs in both somatic and dendritic locations (Fig 4.9C,D). In several cases, spontaneous FPP discharge was recorded immediately following cellular impalement, during the time in which the cell was greatly depolarized. However, spontaneous fast pre-potentials were also observed at more

FIG. 4.9 Characteristics of fast pre-potential (FPP) discharge in pyramidal cell somata (A,C,E) and apical dendrites (B,D,F). A,B. FPPs underlying stratum radiatum evoked spikes uncovered through membrane hyperpolarization (5-20mV; several sweeps shown in A). C,D. FPP discharge evoked through depolarizing current injection (action potential truncated in C). E,F. Successive sweeps of spontaneous FPP discharge at resting membrane potential.

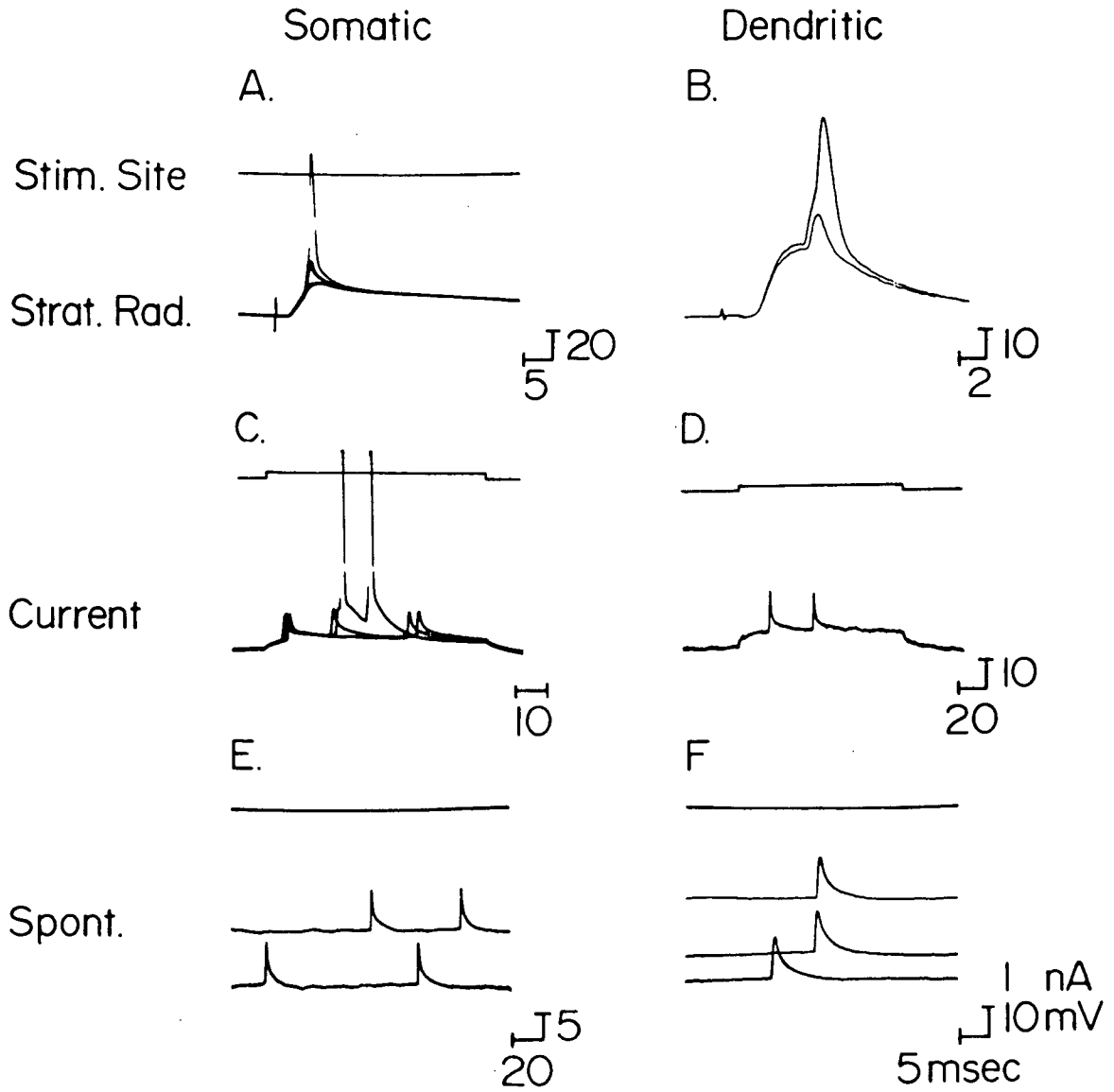
Somatic
Dendritic
A.
B.
Stim. Site
Strat. Rad.
20
5
10
2
C.
D.
Current
1
10
10
20
E.
F
Spont.
5
20
1 nA
10mV
5msec

stable resting potentials, as shown in Fig 4.9E,F. The frequency of spontaneous FPP discharge could be altered with a shift in membrane potential, displaying an increase with depolarization and reduction or blockade with membrane hyperpolarization.

The amplitude of fast pre-potentials varied slightly within a given impalement depending on the resting membrane potential (see Schwartzkroin 1977), but moreso between different pyramidal neurons. However, of the cases documented thus far, no clear difference in the amplitude of evoked FPPs could be found between somatic and dendritic recordings. For instance, of those FPPs evoked through SR stimulation, somatic FPPs displayed an average amplitude of 15 +/- 3.4mV (n=5; mean +/- sem) and dendritic FPPs 14 +/- 1.4mV (n=4; measured from the breakpoint of discharge).

A "pre-potential" was also found to underly antidromic action potential discharge following stimulation of efferent pyramidal cell axons (Fig 4.10). This potential has been previously described in somatic recordings of the pyramidal cell (Spencer and Kandel 1961b), and was thought to represent the activation of a spike in the initial segment region. It is thus referred to as an initial segment or "IS" spike, following the terminology used for the components of spike activation in the spinal motoneuron (Coombs et al. 1957a,b). In many cases, the IS spike underlying the antidromic action potential could be uncovered at the somatic or dendritic level through membrane hyperpolarization (Fig 4.10A,B). Alternatively, a test antidromic stimulus applied 2.0 - 2.4msec following a conditioning antidromic spike could be used in conjunction with membrane hyperpolarization to reveal the IS spike (Fig 4.10C,D).

FIG. 4.10 Initial segment (IS) spikes underlying alvear evoked antidromic spikes in somatic (A,C) and apical dendritic membrane (B,D). IS spikes were uncovered through membrane hyperpolarization (A,B), or through hyperpolarization in conjunction with antidromic paired pulse stimulation (C,D) at condition-test intervals of 2.0 - 2.4 msec. Several sweeps are superimposed in each case. Action potential is truncated in A, and all recordings are taken from separate impalements.

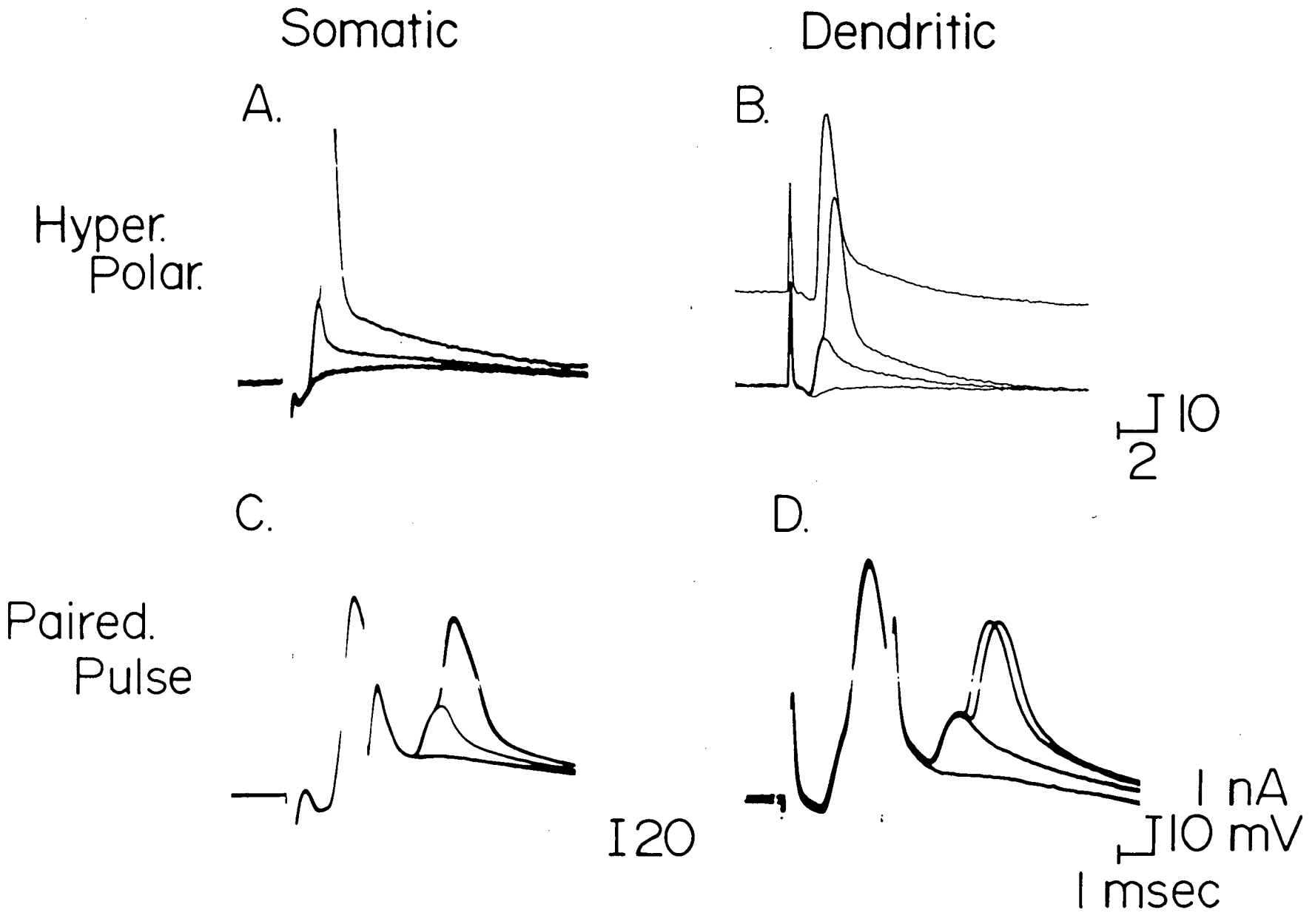
Somatic
Dendritic
A.
B.
Hyper.
Polar.
2
10
C.
D.
Paired.
Pulse
120
1 nA
10 mV
1 msec

The characteristics of this potential were found to be very similar to those of the fast pre-potential (cf 4.9). For instance, the antidromic IS spike displayed a fast rate of rise and a two component decay, including a fast initial fall and a second more prolonged decay to resting potential. Although the amplitude of IS spikes varied somewhat between pyramidal cell impalements, there was no great difference between somatic and dendritic locations, with amplitudes of 19 +/- 2.3mV (n=6; mean +/- sem) in the soma and 21 +/- 3.6mV (n=6) in the dendrite - values rather similar to those of the orthodromically evoked FPP. Antidromically evoked "IS spikes" could in fact be observed in almost all cells exhibiting FPP discharge, with only the means of activation serving to distinguish IS spikes from fast pre-potentials.

4-4. Discussion

The present study has served to further characterize the properties of evoked potentials in somatic and dendritic membranes of the hippocampal pyramidal cell (HPC). One of the more consistent findings was a general similarity in the pattern of evoked activity in somatic and dendritic recording sites. Given the noted exceptions in the absolute value of waveform parameters (ie. spike amplitude and halfwidth), somatic and dendritic membranes were found to exhibit similar membrane properties, synaptic potentials, and both current and stimulus evoked spike discharge.

Membrane Properties and Evoked Synaptic Potentials

The basic characteristics of resting membrane potential and input resistance were found to be comparable in somatic and dendritic impalements, with a similar evoked response to hyperpolarizing or depolarizing current pulse injections at either location. For instance, the dendritic membrane response was linear over a given range of potentials, and displayed anomalous rectification similar to that described for HPC somatic membrane (Brown and Griffith 1983b; Halliwell and Adams 1982; Hotson et al. 1979; Segal and Barker 1984). However, since the pharmacological mechanisms of the dendritic response have not been examined, it should be noted that the above comparison of membrane properties is based largely on the qualitative aspects of evoked activity.

Evoked inhibitory and excitatory synaptic potentials could be recorded at both the somatic and dendritic level of the

pyramidal cell. By comparing the evoked characteristics of these potentials to the results obtained through current-source density analysis (CSD; Chapter 3), some insight into the possible site of origin of these potentials can be gained. For example, stimulation of pyramidal cell axons in the alveus evoked a graded IPSP in both the soma and apical dendritic tree. This potential has been well characterized for HPC somatic membrane, representing a GABA mediated increase in Cl- conductance through the action of recurrent inhibitory interneurons (Allen et al. 1977; Andersen et al. 1969; Dingledine and Langmoen 1980; Knowles and Schwartzkroin 1981a). The principle site of interneuron axonal termination has been localized both anatomically (Cajal 1911; Lorente de No 1934) and electrophysiologically (Leung 1979a,b) to somatic and proximal dendritic membranes of pyramidal neurons. The alvear evoked IPSP in dendritic membrane may thus correspond to a passive electrotonic conduction of inhibitory currents along the dendro-somatic axis. In support of this, current-source density profiles indicate the presence of a long duration current source near the region of stratum pyramidale and a current sink in the dendritic field following the generation of an antidromic population spike (Chapter 3; Leung 1979a,b). A long duration current source is the expected result for current movement associated with the activation of a Cl- conductance at the cell body layer of the pyramidal cell population. The dendritic current sink could thus represent a passive compensatory current flow through pyramidal cell dendritic elements towards the inhibitory current source in stratum pyramidale. In fact, the intradendritic IPSP displayed a longer peak latency than the

somatic inhibitory potential, and was often evoked as a depolarizing potential, a result consistent with an inward movement of current in dendritic regions. The alvear evoked intradendritic IPSP could thus be adequately explained through a passive electrotonic conduction of the active inhibitory potential evoked in the somatic region of the pyramidal cell. Such a process might in fact be expected considering the ability of dendritic excitatory potentials to conduct to the somatic region. However, further work will be required to determine the exact limit of interneuronal synaptic termination along the dendro-somatic axis of the pyramidal cell.

A similar comparison of sink-source relationships and intracellular activity can be applied to excitatory synaptic potentials evoked through stimulation of afferent synaptic inputs. Stratum oriens (SO) stimulation evoked an intracellular EPSP at both the somatic and dendritic level of the pyramidal cell, with the greatest peak amplitude in the region of the cell layer. These results coincide with those obtained through current-source density analysis, in which SO stimulation evoked a large amplitude EPSP and current sink in the basal dendritic field followed by the conduction and decay of synaptic currents through the somata and apical dendrites of the pyramidal cell population. In contrast, stratum radiatum (SR) stimulation evoked the largest EPSP in the apical dendrite and an EPSP of smaller peak amplitude in somatic recordings. These results also agree with those derived from CSD analysis, indicating an apical dendritic site of origin for the SR evoked EPSP, and a subsequent conduction towards the somatic region.

The above data indicate that a synaptic potential evoked

within one given region of the pyramidal cell can conduct through a large extent of the dendro-somatic axis. These results serve to emphasize the short electrotonic length of the pyramidal cell (Brown et al. 1981; Turner 1984; Turner and Schwartzkroin 1980), and may account in part for the similarity in evoked characteristics of somatic and dendritic potentials. It would also imply that the presence of an evoked potential along this axis cannot be taken by itself as evidence for an intrinsic membrane property, and attempts to locate the site of origin of any potential must incorporate additional experimental strategies.

Current Evoked Spikes

Analysis of somatic and dendritic current evoked potentials revealed that spike discharge in response to depolarizing current injection could take a variety of forms, grouped here for the purpose of comparison into three basic patterns (Types 1-3). However, it should be stressed that the grouping of discharge patterns used in the present study is not meant to imply the presence of distinct pyramidal cell types in the CA1 region. Furthermore, the distinction between these patterns is not absolute and some transition or combination of these characteristics can occur, as shown by the occasional change in dendritic spike discharge from Type 2 to Type 3 activity. The presence of three different patterns of current evoked discharge could not be attributed to the quality of cellular impalement, as values of resting potential and input resistance for cells displaying each form of discharge were comparable. In addition, orthodromic stimulation would reliably evoke an EPSP-IPSP

sequence and a single fast spike in both somatic and dendritic impalements regardless of the form of current evoked responses. Therefore, membrane characteristics, synaptic potentials, and stimulus evoked spike discharge appeared to be intact, suggesting that the pattern of current evoked activity was an inherent property of the cell in question and not the result of injury or variability in the quality of the intracellular recording. Rather, pharmacological studies would indicate that the differential pattern of current evoked activity reflects the ionic basis of spike generation in the pyramidal cell soma and apical dendrite.

Previous investigations have shown that fast spikes in both the soma and apical dendrite of pyramidal cells are blocked by the Na+ channel blocker tetrodotoxin (TTX) and are therefore thought to be mediated through voltage-dependent Na+ channels (Hotson and Prince 1980; Schwartzkroin and Slawsky 1977;Wong et al. 1979). In contrast, intermediate and slow spikes of dendritic membrane have been shown to be TTX insensitive, and probably represent regenerative Ca+2 channel activation (Wong et al. 1979). Similarly, the membrane depolarization underlying the initial burst of fast spikes is insensitive to TTX but reduced by Ca+2 channel antagonists (Schwartzkroin and Slawsky 1977; Wong and Prince 1978; Wong et al. 1979).

The distinguishing feature between the three forms of current evoked activity might therefore be the relative contribution of Na+ or Ca+2 channel conductance to AP generation. In this regard, Type 1 discharge was dominated by the generation of fast Na+ spikes, while Type 2 activity was comprised of Na+ spike activation as well as a large underlying

depolarization and the occasional generation of intermediate spikes. Type 2 discharge was also distinct in displaying an afterhyperpolarization following the initial burst of spike discharge, a potential shown to represent a Ca+2-dependent K+ conductance in HPC somatic membrane (Brown and Griffith 1983a; Hotson and Prince 1980). Although not absolute in occurrence, Type 2 discharge appeared to correlate with somatic or dendritic impalements exhibiting anomalous rectification in the depolarizing range of current injection (cf 4.1C,D), a phenomenon related to the activation of a voltage-dependent Ca+2 conductance (Benardo et al. 1982; Hotson et al. 1979). Thus, Type 1 spike discharge would appear to be mediated primarily by Na+ channel conductance, while both Na+ and Ca+2 channel activity contributed to Type 2 discharge. The preponderance of slow spike generation in Type 3 activity would further indicate Ca+2 ions as the principle charge carrier for this form of AP discharge. Of interest is the fact that the distinction between discharge patterns could be made at both the somatic and dendritic level, with Type 1 activity much more commonly recorded in both somatic and dendritic impalements as compared to that of Type 2. Given the similarity in the pattern of evoked activity between somatic and dendritic recording sites, it is thus possible that one form of spike discharge (Type 1 or Type 2) is expressed at both the somatic and dendritic level of a given cell.

Further examination of current evoked responses reveals that potentials thought to indicate the activation of Ca+2 channel conductance were most commonly recorded in dendritic impalements of the pyramidal cell. For instance, the

depolarization underlying the burst of fast spikes in Type 2 discharge was of greater amplitude in dendritic membrane, and Ca+2-dependent intermediate or slow spikes were only observed in dendritic recording locations. These results would suggest a non-uniform distribution of ionic channels along the pyramidal cell axis, with a greater density of Ca+2 channels in dendritic than somatic membrane. Similar conclusions were drawn in previous investigations, but these studies reported that Ca+2-dependent intermediate or slow spikes were readily evoked in dendritic membrane by injection of depolarizing current (Benardo et al. 1982; Wong et al. 1979). In the present study, the intermediate and slow spike could be evoked in the apical dendrite, but these potentials were infrequently observed at all levels of the dendritic tree, being detected in only 8/36 dendrites examined. Instead, the most common form of action potential discharge at both the somatic and dendritic level was that of Na+-dependent spike activation. The apparent difference between these results and those of previous investigators might be attributed to three separate factors. First, previous studies have reported that slow spike generation in the pyramidal cell dendrite is most commonly evoked through injection of depolarizing current in the order of 2nA or greater (Wong et al. 1979). However, current injection of over 1.5nA was not routinely attempted in the present study as such action would often result in loss of the dendritic impalement. Secondly, early investigations of dendritic activity were performed on both CA1 and CA3 pyramidal cells (Wong et al. 1979), the latter of which are known to exhibit more pronounced burst-like behaviour in response to current injection (Wong et al. 1979;

Wong and Prince 1978). Finally, all previous studies on dendritic activity were performed on pyramidal cells of the guinea-pig, while the results of this work were obtained from the rat hippocampus. Of possible relevance to this point is the recent finding that CA1 pyramidal cells of the guinea-pig are not stained immunohistochemically by antibodies specific for Calcium-Binding Protein (CaBP), as is characteristically found for CA1 pyramidal cells of the rat (Dr. K.G. Baimbridge, personal communication; Baimbride and Miller 1982). Although the presence or absence of CaBP may be inconsequential to Ca+2 channel activity, the above results do indicate that rat and guinea-pig pyramidal neurons are not strictly comparable in all respects.

Stimulus Evoked Spikes

The stimulus evoked response of the pyramidal cell differed from that evoked through depolarizing current injection in giving rise to a single all-or-none spike at all levels of the pyramidal cell axis. The alvear evoked spike was evoked directly from baseline with a short onset latency at both somatic and dendritic recording sites. Antidromic spike discharge in the pyramidal cell has been well characterized through laminar profile analyses of extracellular field potentials in both the *in vivo* (Gessi et al. 1966; Leung 1979a,b; Sperti et al. 1967) and *in vitro* preparation (Chapter 3), indicating that the alvear evoked response represents an antidromic spike invasion of somata and apical dendrites of pyramidal cells. Stimulation of stratum oriens or radiatum also evoked a single all-or-none spike arising from the peak of the synaptic depolarization at

both the somatic and dendritic level. Orthodromic spikes displayed similar evoked characteristics at all levels of the dendro-somatic axis, including latency jitter near threshold for AP discharge, and the response to stimulus intensity or repetitive stimulation of the afferent input.

Somatic and dendritic spikes differed characteristically in the exact form of the evoked spike, with somatic spikes exhibiting a larger amplitude and more narrow halfwidth than dendritic spikes. However, at any given level of the cell axis, both alvear and orthodromic spikes were evoked with similar amplitude and halfwidth. Dendritic spikes evoked through stimulation of either stratum oriens or radiatum were thus comparable in waveform to that of a spike antidromically invading the dendritic arborization. AP discharge in somatic and dendritic recording locations also differed in terms of the voltage threshold for spike activation. In the somatic region, orthodromic spikes were evoked at a consistent voltage threshold, as judged by the absolute voltage of the breakpoint of spike discharge. In contrast, dendritic membrane displayed no conspicuous voltage threshold for spike generation, with orthodromically evoked spikes arising at various levels of depolarization from the underlying EPSP. Assuming that dendritic spikes arise through activation of voltage-dependent channels, the above results would suggest that the generator site for the dendritic spike is located distant to the position of the dendritic recording electrode. This site might correspond to one or more locations within the dendritic tree ("hot spots") or to the somatic region of the pyramidal cell. However, the intracellular characteristics of orthodromic spike discharge

would be consistent with results obtained through current-source density analysis (Chapter 3). Laminar profiles of field potentials and current-source density revealed that SO of SR stimulation evoked a single spike response at all levels of the pyramidal cell axis, with the spike conducting from the cell layer through the dendritic field. The intracellular spike would thus be expected to display similar evoked characteristics at the somatic and dendritic level (ie response to stimulus intensity or repetitive stimulation), and to the alvear evoked spike antidromically invading the dendritic arborization. Thus, the intracellular properties of spike discharge are at least in accord with the data obtained from CSD analysis indicating a somatic site of origin for the evoked dendritic spike.

Stimulus Vs. Current Evoked Spikes

A comparison of the stimulus and current evoked response revealed a basic similarity between the characteristics of current evoked Na+-dependent spikes and action potentials evoked through stimulation of afferent or efferent pathways. For instance, depolarizing current evoked similar patterns of activity in both somatic and dendritic locations, with somatic spikes exhibiting a greater amplitude and more narrow halfwidth than those in dendritic recording sites. In addition, the current evoked dendritic spike displayed no consistent voltage threshold for activation, while spike discharge in the somatic region arose from a similar membrane potential for all levels of current injection. In fact, a direct comparison of fast spike discharge revealed that stimulus evoked spikes were comparable to those evoked through curent injection in terms of amplitude

and halfwidth when evoked upon a similar level of membrane depolarization.

The major distinction between stimulus and current evoked spike generation was found in the pattern of AP discharge, with stimulus activation giving rise to a single spike and depolarizing current a repetitive spike discharge. However, these results can be explained by the fact that stimulation of afferent or efferent pathways in the slice is known to result in the recurrent activation of an inhibitory synaptic potential in pyramidal cells capable of suppressing repetitive spike discharge (Andersen et al. 1969; Dingledine and Langmoen 1980). In the presence of appropriate Cl- channel blockers, stimulus activation can also lead to repetitive spike generation at both the somatic and dendritic level (Schwartzkroin and Prince 1980; Wong and Prince 1979). The similarity in evoked characteristics of stimulus and current evoked spikes might then imply a common site of origin for all evoked fast spikes of the pyramidal cell.

Spike Pre-Potentials

The evoked characteristics of fast pre-potentials (FPPs) and antidromic initial segment (IS) spikes recorded in the somatic region of the pyramidal cell have been described by previous investigators (Andersen and Lomo 1966; Kandel et al. 1961; MacVicar and Dudek 1981; Schwartzkroin 1975,1977; Schwartzkroin and Prince 1980; Spencer and Kandel 1961b). The present study extends these findings in reporting the activation of FPPs and "IS" spikes in dendritic recording locations. Previous investigations have drawn a distinction between the FPP and IS spike based upon initial reports that the IS spike was of

greater amplitude than the FPP, and upon an inability to antidromically evoke a fast pre-potential (Kandel et al. 1961; Schwartzkroin 1977; Spencer and Kandel 1961b). However, in the present study, the FPP and IS spike were found to be very similar in waveform, with no great difference in amplitude at any given location.In addition, antidromic activation of the "FPP" has been reported since the first description of these potentials by Spencer and Kandel in 1961 (Knowles and Schwartzkroin 1981b; Schwartzkroin and Prince 1980; Taylor and Dudek 1982). The reported difference in amplitude between these potentials may relate to the fact that the amplitude of the FPP can vary with membrane potential, increasing in amplitude in response to membrane hyperpolarization (Schwartzkroin 1977). In this regard, it is important to note that IS spikes are usually uncovered on a hyperpolarized membrane during antidromic stimulation, while FPPs are observed at all levels of membrane polarization. It is possible therefore that the IS spike and FPP represent "fast pre-potentials" evoked at different levels of resting membrane potential. Therefore, given the similarity in shape and evoked characteristics of the FPP and IS spike, the distinction between these potentials is probably unwarranted, and both will be referred to as fast pre-potentials.

Fast pre-potentials recorded in pyramidal cell somata have been proposed to represent an electrotonically decayed dendritic spike following a failure of active propagation at some point within the dendritic arborization (Andersen and Lomo 1966; Spencer and Kandel 1961b). One would therefore expect to find evidence in dendritic recordings of fast pre-potential-like waveforms intermediate in amplitude between the somatic FPP and

the much larger dendritic spike. However, somatic and dendritic FPPs fell within a similar range of amplitude and could be activated through antidromic stimulation. It would appear therefore that a fast pre-potential in the somatic region may not represent the passive conduction and electrotonic decay of an evoked dendritic spike. Further evidence to support this conclusion will be presented in Chapter 6.

Previous studies have provided evidence that at least some fast pre-potentials represent the electrotonic conduction of a spike across a gap junction between neighboring pyramidal cells (Andrew et al. 1982; MacVicar and Dudek 1981). Support for the presence of gap junctions between pyramidal neurons has come from freeze-fracture studies (Schmalbruch and Jahnsen 1981) and the ability to attain dye-coupling of two or more pyramidal neurons following intracellular injection of Lucifer Yellow into pyramidal cell somata or apical dendrites (Andrew et al. 1982; MacVicar and Dudek 1981). The point of gap junctional contact between pyramidal cells is thought to occur at either the somatic or dendritic level (Andrew et al. 1982; MacVivar and Dudek 1981; Schmalbruch and Jahnsen 1981), and dual impalements of pyramidal cells have shown that spike discharge in one of a pair of electrotonically coupled neurons is reflected in the second as a fast pre-potential (MacVicar and Dudek 1981). Fast pre-potentials recorded in somata and apical dendrites of CA1 pyramidal cells might thus be adequately explained on the basis of electrotonic gap junctions between adjacent pyramidal neurons. Such a mechanism would help to account for the similarity in the evoked characteristics and waveform of somatic and dendritic FPPs, and antidromic activation of the fast

pre-potential at both the somatic and dendritic level. However, the characterization of FPP discharge in dendritic membrane is only at a preliminary stage, and substantially more work will be required to definitively locate the origin(s) of fast pre-potentials in the pyramidal cell.

5-0. EVOKED CHARACTERISTICS OF ACTION POTENTIAL DISCHARGE ALONG THE DENDRO-SOMATIC AXIS OF THE CA1 PYRAMIDAL NEURON

5-1. Introduction

Laminar profile analysis of extracellular field potentials in the CA1 region have indicated a retrograde conduction of a spike response from the cell body layer through the dendritic region, suggesting a somatic site of origin for the evoked dendritic spike in CA1 pyramidal neurons (Chapter 3). The basic properties of spike discharge in the pyramidal cell have also been characterized through intracellular recordings from pyramidal cell somata and apical dendrites (Chapter 4), providing the basis for a comparison of intra- and extracellular spike activity at the somatic and dendritic level. Several of the properties of intracellular spike discharge coincide with the characteristics of extracellular population spike responses recorded in stratum pyramidale and radiatum. For instance, stimulation of afferent or efferent pathways gave rise to a single evoked spike in somatic and dendritic impalements, similar to that observed for extracellular field potentials. In addition, the exact waveform of the intracellular spike differed between somatic and dendritic locations, with the somatic spike exhibiting a greater amplitude and shorter halfwidth than that in the dendrite. Similarly, the extracellular population spike response in stratum pyramidale consisted of a large amplitude negativity while that in stratum radiatum was of smaller amplitude and biphasic in waveform. Furthermore, the lack of voltage threshold of orthodromic intradendritic spikes would

indicate that the spike had originated at a site remote from the recording electrode, as suggested by field potential analysis. However, laminar profiles of extracellular field potentials indicate that the characteristics of the evoked population spike response change in a progressive manner through the dendritic field of the pyramidal cell population. More insight into the properties of spike activation in the pyramidal cell might thus be gained by comparing various parameters of intracellular spike discharge at different sites along the dendro-somatic axis.

Such an analysis would also provide a direct test of the prevailing hypothesis concerning spike generation in the apical dendrite of the pyramidal cell. Previous investigations have assigned the site for generation of a dendritic spike to hot spots of dendritic membrane, possibly located at one or more branchpoints of the dendritic tree (Andersen and Lomo 1966; Spencer and Kandel 1961b). Evidence that dendritic membrane can in fact initiate spike discharge independently of that in the soma has come from intracellular recordings of spike activation in dendrites physically isolated from the cell body by a knife cut across the proximal-mid stratum radiatum (Benardo et al. 1982; Masukawa and Prince 1984). At the somatic level, the dendritic spike is observed in the form of a fast pre-potential, the small amplitude of which suggests a failure of active propagation of the spike within the dendritic tree and a subsequent passive electrotonic conduction to the cell body region (Andersen and Lomo 1966; Spencer and Kandel 1961b). This model of spike activation would predict a change in the characteristics of the intradendritic spike indicative of passive electrotonus, including a decline in amplitude and

increase in both width and onset latency with proximity to the cell body layer. However, this pattern of change in the properties of the dendritic spike are in direct contrast to those observed for the extracellular population spike response on laminar profiles of field potentials in the CA1 region. According to these results, the evoked spike displays a gradual change in waveform and increase in onset latency the greater the recording distance from stratum pyramidale. An analysis of intracellular spike characteristics along the dendro-somatic axis might then provide a means of distinguishing between a somatic or dendritic site of origin for the evoked dendritic spike.

The present study therefore provides a comparative analysis of the properties of action potential discharge along the dendro-somatic axis of the pyramidal cell, including those of amplitude, halfwidth, voltage threshold and onset latency. In view of the fact that current-source density analysis would indicate a somatic site of origin for the dendritic spike, attempts were also made in the present study to record the evoked activity of isolated dendritic elements of the pyramidal cell population.

5-2. Methods

Data was pooled from all intracellular recordings along the dendro-somatic axis of pyramidal neurons and spike amplitude, halfwidth, and voltage threshold measured according to the methods described previously (Chapter 4). Since dual impalements of single pyramidal neurons were not obtained, absolute measurements of spike latency at different regions of the pyramidal cell could not be made. However, an indirect estimate of the latency for spike discharge at the somatic and dendritic level was obtained through a comparison of evoked intracellular spike activity and extracellular field potentials. For these experiments, a low impedance electrode was placed in stratum pyramidale to record the extracellular population spike, and a high impedance intracellular electrode within the apical dendritic region directly below that in the cell layer. Upon obtaining a stable intradendritic impalement, stimulus intensity for each of the three pathways was set to threshold for intradendritic spike generation, and the evoked response recorded simultaneously with that of the population spike in stratum pyramidale. The intradendritic electrode was then withdrawn from the impalement and returned to the depth of the dendritic recording, as monitored by a digital micrometer display of electrode depth (Burleigh Inchworm PZ-550). Extracellular potential waveforms at the cell body and in the region of the dendritic impalement were then collected at the same stimulus intensity for a latency comparison of intra- and extradendritic spike potentials. To avoid any possible change in the extracellular potential over time, threshold intradendritic

responses were usually collected just prior to withdrawal from the recording site. However, if the stimulus intensity of a pathway had been changed before electrode withdrawal, stimulus intensity was set to evoke the same amplitude and latency population spike at the cell layer as that recorded during collection of intradendritic potentials.

In an attempt to assess dendritic activity independently of that in the soma, two dissection techniques were used to place a knife cut in the proximal-mid apical dendritic region in order to separate the cell bodies and apical dendrites of pyramidal neurons. The first method employed a "micro-knife" consisting of a small razor blade chip glued to a thin wooden dowel mounted on a micro-manipulator. Slices were cut immediately following transferral to the recording chamber under observation with a 4X dissecting microscope. The blade was lowered slowly through the slice along the intended line of cut both within stratum radiatum and directly across to the alvear tissue on either side of the cut dendritic region. Small lateral movements along the axis of the blade were often made at the bottom of the cut to obtain a complete separation of slice tissue. In some cases, cuts were extensive enough to allow separation of the cell body region from the remainder of the slice.

In the second method, three to four slices were taken immediately following sectioning on the tissue chopper and placed individually in drops of cold oxygenated medium within a pre-cooled plastic petri dish. The petri dish was then "anchored" with masking tape to the stage of a 3X dissectng microscope to prevent movement during microdissection. Immediately before cutting a slice, the corner of a torn piece

of tissue paper was used to draw away most of the fluid in the drop containing the slice, allowing the slice to rest upon the surface of the petri dish. The tip of a #10 scalpel blade was placed on the petri dish at the edge of the slice and the blade aligned along the intended line of dissection. The blade was held at approximately 45 degrees from vertical so as to watch the progress of the cut and to minimize the possibility of compressive damage to the dendritic region. The blade was then "rolled" along the curved edge across and through the slice in one smooth motion. A few drops of freshly oxygenated cold medium was immediately placed on the cut slice and the procedure repeated for the next slice. In order to avoid hypoxic damage to the tissue, only three to four slices were cut per dissection, quickly transferring them to the recording chamber once cutting was completed. The time required for cutting slices in the above manner (total of 3-5 min) was not found to compromise slice health, as control slices maintained in the petri dish under the same conditions were found to exhibit electrophysiological activity comparable to slices removed directly fron the tissue chopper to the recording chamber.

Slices were allowed a period of at least 45 min for recovery and equilibration to bath conditions. In some cases, the concentration of extracellular calcium in the perfusing medium was elevated from 1.6mM to 2.5-3mM to enhance the recovery of cut tissue elements, as outlined in the procedure of Benardo et al. (1982).

The evoked activity in the CA1 region of dissected slices was examined primarily by extracellular recording techniques in response to stimulation of stratum radiatum inputs. The maximal

somatic and/or dendritic response to SR stimulation (up to 60V stimulus intensity) was recorded at a sequential series of sites extending to either side of the cut from the lateral border of CA2 to the subicular region. When the cut region of stratum pyramidale was still attached to the slice, somatic and dendritic activity was recorded at all points along the CA2-subicular axis (dendritic electrode directly below the somatic recording site). If the excised portion was removed from the slice, somatic and dendritic activity was recorded on either side of the cut region, while dendritic activity was recorded through the entire extent of the cut. In order to achieve maximal stimulation of stratum radiatum afferent inputs, the stimulating electrode was usually moved with the recording electrode to maintain a constant stimulating-recording electrode distance of approximately 400μm. In other cases, the stimulating electrode position in the CA2 region was kept constant while the recording electrode was moved.

The position of the knife cut, location of each recording site, and the maximal evoked somatic or dendritic response at each recording location were noted in a detailed diagram of the slice, and tissue prepared at the end of a recording session for histological analysis. Slices were first placed in a 10% formalin / 1% Ca+2-acetate solution for at least 24 hours and transferred to a 20% sucrose-phosphate buffered saline solution (pH 7.4) 5 hours before sectioning. Slices were individually placed on the flat surface of a pre-cut frozen drop of O.C.T. Compound (Tissue-Tek) on the cutting stage of a cryostat (Tissue-tek; 12-14 degrees centigrade) and 22μm serial sections cut and mounted on glass slides. Slice tissue was then stained

with cresyl violet and microscopically examined to assess the extent of the knife cut at all levels of the slice and the relation of neuronal elements to previously recorded activity.

5-3. Results

Spike Amplitude and Halfwidth

Representative examples of antidromic and orthodromic potentials recorded at the soma and various locations along the apical dendritic tree are illustrated in Fig 5.1. All stimulus evoked spikes were found to exhibit the maximal amplitude and shortest halfwidth at the level of the pyramidal cell body. In the dendritic region, spikes displayed a gradual decline in amplitude and increase in halfwidth with distance from the border of stratum pyramidale (Fig 5.1). The SO evoked EPSP was also largest in the somatic region, declining in amplitude and rate of rise along the apical dendrite (Fig 5.1B). Conversely, the amplitude and rate of rise of the EPSP evoked by SR stimulation was greatest in the region of the apical dendrite, decreasing with proximity to the cell body layer (Fig 5.1C).

Data such as that shown in Fig 5.1 were collected at all levels of the apical dendritic tree and used to calculate the average value of evoked potential characteristics along the dendro-somatic axis (Figs 5.2-5.4). In each case, the average values are plotted against the anatomical distance of the recording site from the border of stratum pyramidale (somatic recordings taken as "0"μm). In Figs 5.2 and 5.4 a scaled schematic diagram of a rat pyramidal neuron and the average values of resting membrane potential or input resistance at each recording site are also provided. These calculations reveal that both antidromic and orthodromic intracellular spikes display a progressive decline in amplitude with distance from the cell body layer (Fig 5.2A-C). However, the change in action potential

FIG 5.1 Oscilloscope traces of typical stimulus evoked action potential discharge recorded in pyramidal cell somata and apical dendrites 65, 165 and 265μm from the border of stratum pyramidale. Spike discharge was evoked by stimulation of the alveus (A), stratum oriens (B) or stratum radiatum (C). Note the gradual change in spike amplitude and halfwidth with recording distance from the cell body layer. In each case, several sweeps are shown superimposed for stimulus intensities near threshold for spike activation. Somatic recordings were taken from three separate cells, while dendritic recordings at each location along the cell axis are from a single dendritic impalement. Note the common voltage and time base calibration for all recordings.

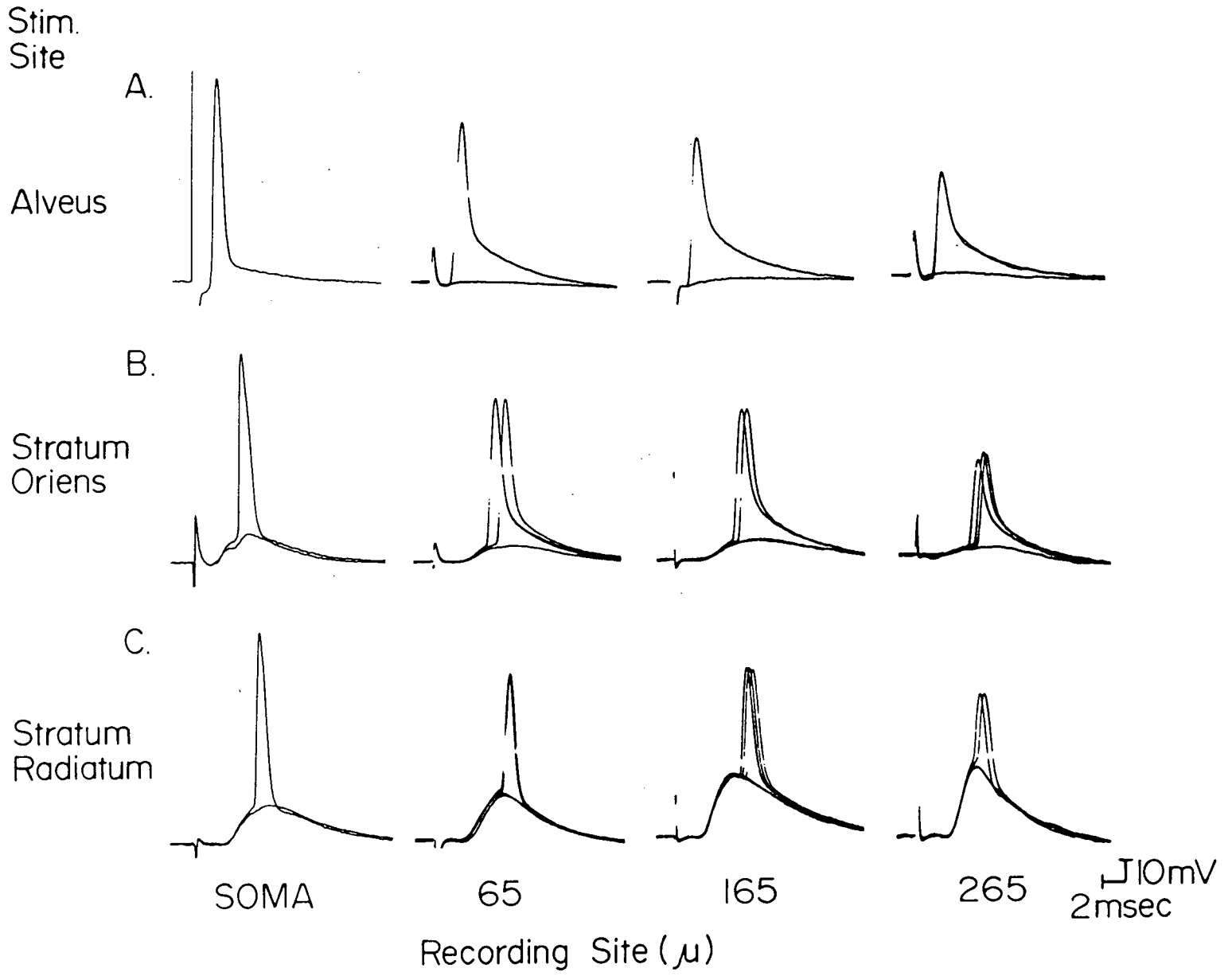
Stim.
Site
A.
Alveus
B.
Stratum
Oriens
C.
Stratum
Radiatum
SOMA
65
165
265
10mV
2msec
Recording Site (μ)

FIG 5.2 Plots of the average amplitude of stimulus evoked spikes recorded in pyramidal cell somata and apical dendrites at varying distances from the border of stratum pyramidale (mean +/- sem; measured from resting membrane potential). Somatic recordings are taken as 0μm distance. Spikes were evoked by stimulation of the alveus (A), stratum oriens (B) or stratum radiatum (C). D. Schematic diagram of the rat pyramidal cell drawn to scale with the border of the alveus and hippocampal fissure denoted by dark lines. Average resting membrane potentials (RMP) for the pyramidal cell impalements in plots A-C are shown in lower part of D. The number of impalements (n) for each point are shown at the base of the graphs. Average values were calculated from the largest evoked spike at each location, and values without standard error bars are those in which the standard error lies within the border of the illustrated point.

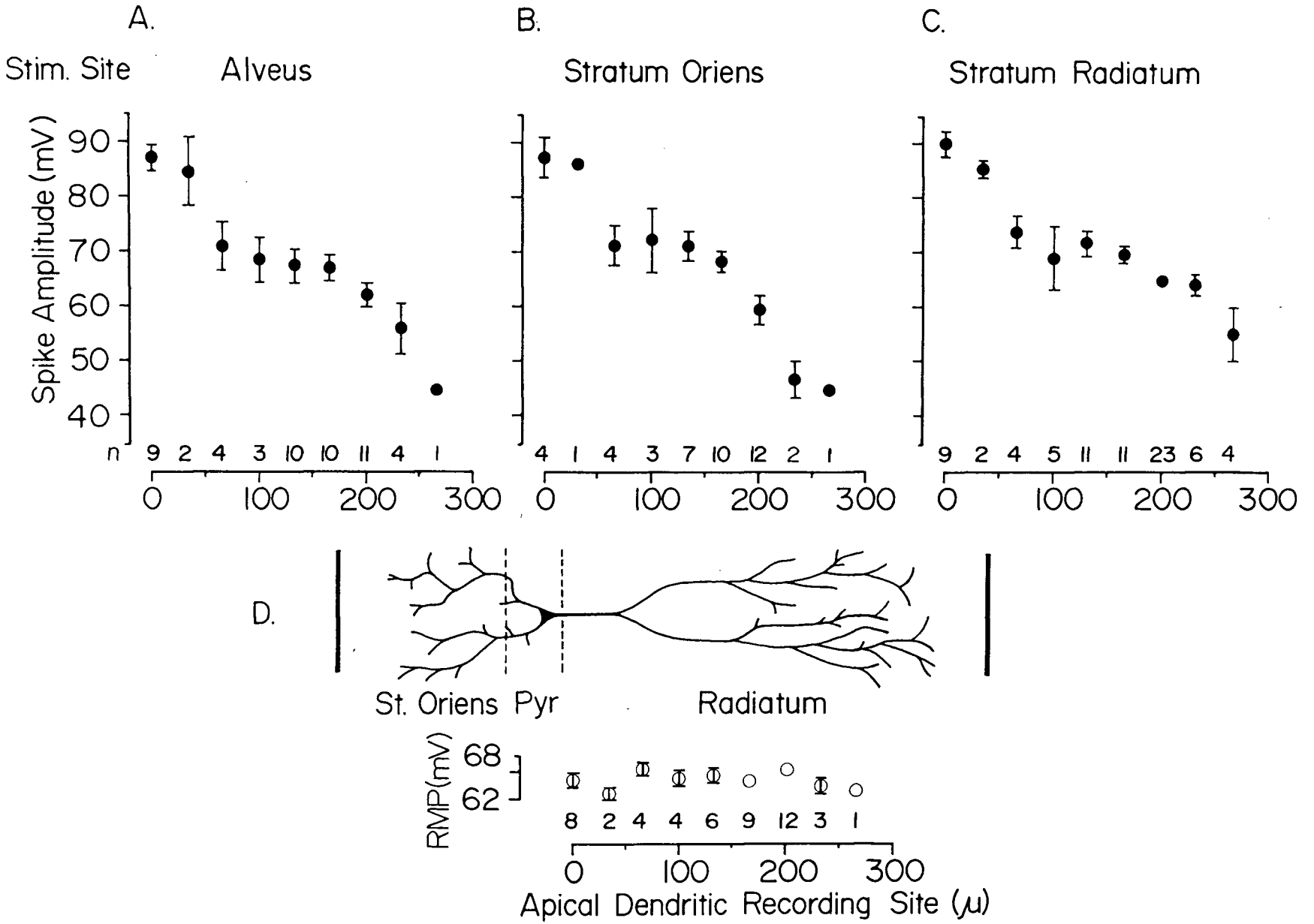
A.
Stim. Site
Alveus
B.
Stratum Oriens
C.
Stratum Radiatum
Spike Amplitude (mV)
90
80
70
60
50
40
n
9 2 4 3 10 10 11 4 1
4 1 4 3 7 10 12 2 1
9 2 4 5 11 11 23 6 4
0
100
200
300
D.
St. Oriens Pyr
Radiatum
RMP(mV)
68
62
8 2 4 4 6 9 12 3 1
Apical Dendritic Recording Site (μ)

amplitude along the dendritic tree occurred in a non-linear manner. A sharp initial drop in spike amplitude was observed within 100um from stratum pyramidale, followed by a "plateau" and a second rapid decline in distal dendritic impalements 150-200um from the cell layer. These results are not due to variability in the quality of dendritic impalements, as the average value of resting membrane potential for each recording location fell within the range of 62-68mV (Fig 5.2D). Rather, a comparison of spike amplitude to a scaled diagram of the pyramidal cell suggests that points of transition in spike configuration correlate to the anatomical location of major branchpoints of the apical dendritic tree.

A progressive increase in spike width with distance along the apical dendrite is also evident in a plot of the average halfwidth of spikes evoked from each of the three stimulation sites (Fig 5.3). Once again, the change in spike halfwidth is similar for both antidromic (Fig 5.3A) and orthodromic spikes (Fig 5.3B,C), with a gradual increase in spike width through the proximal-mid apical dendritic region and a more pronounced increase in distal dendritic locations. Since the majority of these values were obtained from the action potentials in Fig 5.2, the observed change in spike halfwidth cannot be explained on the basis of a variability in resting membrane potential of cellular impalements.

The characteristics of action potentials evoked by injection of depolarizing current also varied according to the recording site along the pyramidal cell axis (Fig 5.4). Representative photographs of the current evoked response (Fig 5.4A) demonstrate that the fast Na+ spike was evoked with the

FIG. 5.3 Plots of the average halfwidth (width at half amplitude) of stimulus evoked spikes recorded in pyramidal cell somata and apical dendrites at varying distances from the border of stratum pyramidale (mean +/- sem; half amplitude measured from resting membrane potential). Somatic recordings are taken as 0um distance. Spikes were evoked by stimulation of the alveus (A), stratum oriens (B) or stratum radiatum (C). The number of impalements (n) for each point are shown at the base of graphs.

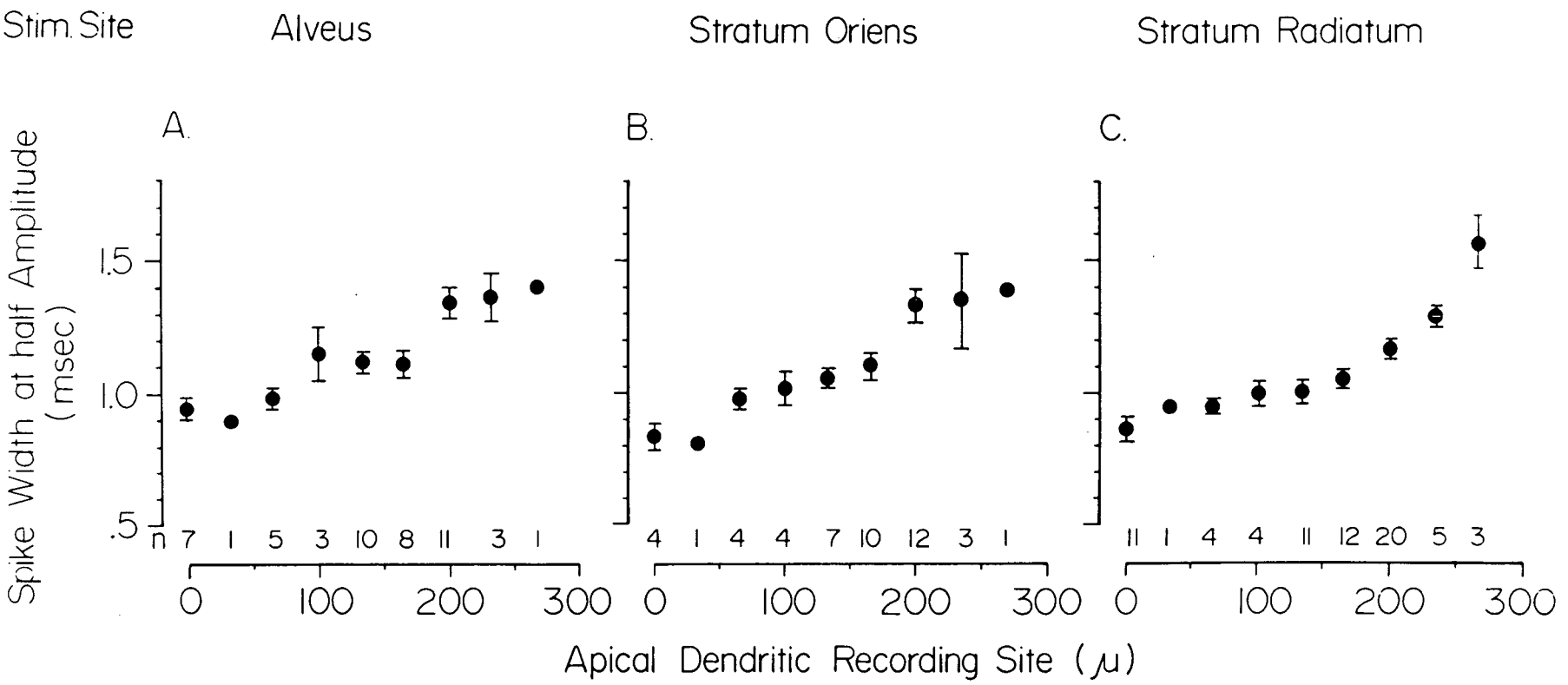
Stim. Site
Alveus
Stratum Oriens
Stratum Radiatum
A.
B.
C.
Spike Width at half Amplitude (msec)
1.5
1.0
.5
n
7 1 5 3 10 8 11 3 1
4 1 4 4 7 10 12 3 1
11 1 4 4 11 12 20 5 3
0
100
200
300
Apical Dendritic Recording Site (μ)

FIG. 5.4 A. Oscilloscope traces of typical current evoked action potential discharge recorded in pyramidal cell somata and apical dendrites 100 and 165μm from the border of stratum pyramidale. B. Plots of the average amplitude (B) and halfwidth (width at half amplitude) of the current evoked spike recorded in pyramidal cell somata and apical dendrites at varying distances from the border of stratum pyramidale (mean +/- sem). Somatic recordings are taken as 0um distance. Amplitudes were measured from resting membrane potential for the first current evoked spike in either Type 1 or Type 2 discharge. The number of impalements (n) for each point are shown at the base of each graph.

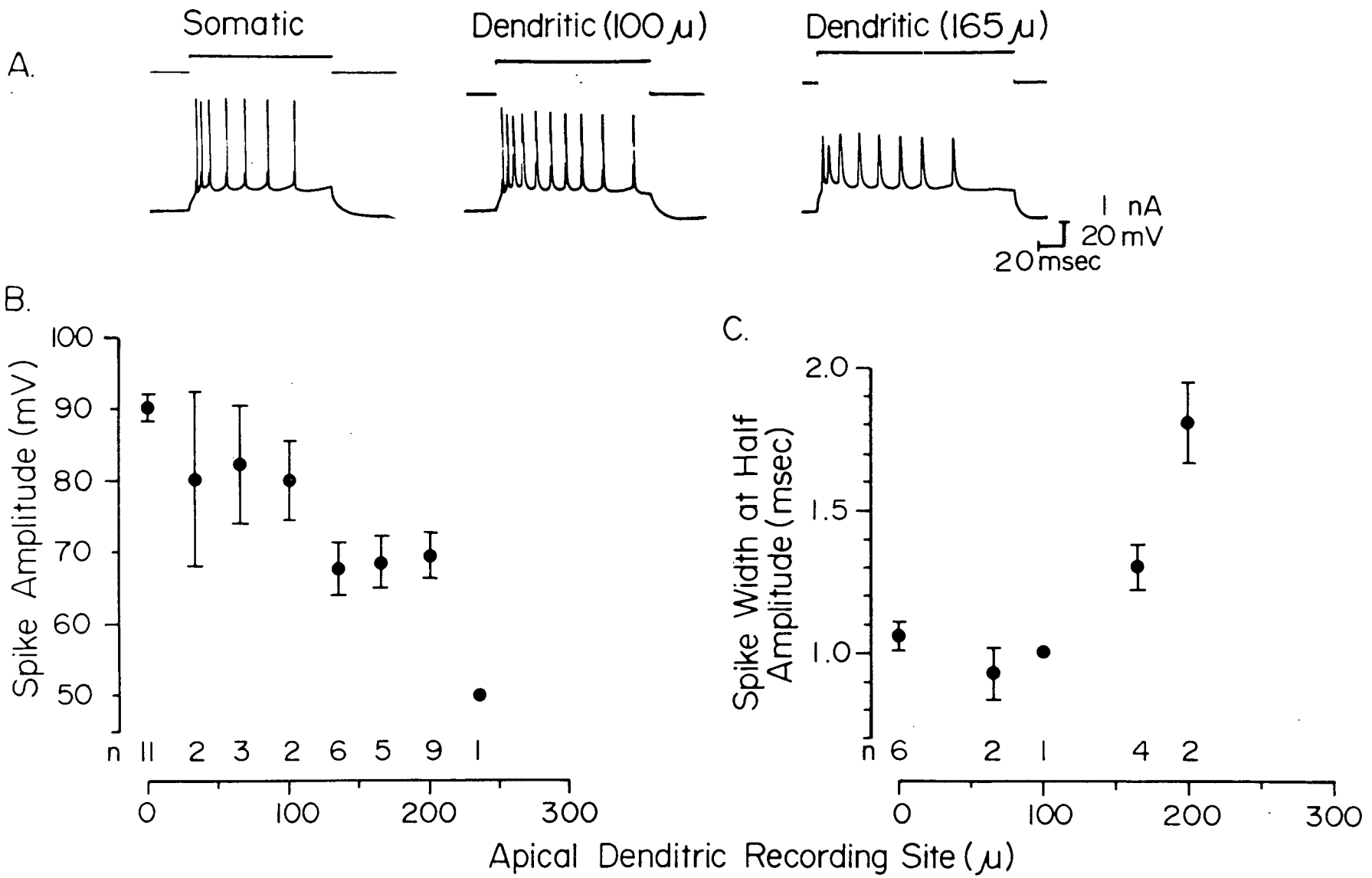
A.
Somatic
Dendritic (100 μ)
Dendritic (165 μ)
1 nA
20 mV
20 msec
B.
Spike Amplitude (mV)
100
90
80
70
60
50
n 11 2 3 2 6 5 9 1
0
100
200
300
C.
Spike Width at Half Amplitude (msec)
2.0
1.5
1.0
n 6 2 1 4 2
0
100
200
300
Apical Denditric Recording Site (μ)

greatest amplitude and shortest halfwidth in the somatic region of the pyramidal cell. Spikes evoked in dendritic recording locations then displayed a decrease in amplitude and increase in halfwidth with distance from the cell layer (Fig 5.4A). Since a similar response was found for spikes evoked in Type 1 or 2 discharge, the first evoked spike in either case was used to calculate the average amplitude and halfwidth of the current evoked spike along the dendro-somatic axis (Fig 5.4B). Although the average values in the plots of Fig 5.4B,C were derived from relatively few cell impalements, the results do indicate a decline in spike amplitude and increase in halfwidth along the apical dendrite, with the greatest change in spike configuration in distal dendritic locations.

Voltage Threshold of Orthodromic Spike Discharge

Voltage threshold for orthodromic spike activation also varied according to the recording position along the dendro-somatic axis of the pyramidal cell (Fig 5.5A). In the case of SR stimulation, spike threshold was found to be lowest in the somatic region, gradually increasing with distance along the apical dendrite. In contrast, spike threshold in response to SO stimulation was greatest at the soma, exhibiting a progressive decrease the greater the distance of the recording site from stratum pyramidale. These results are not due to a variable quality of cellular impalement, as average values of resting membrane potential and input resistance fell within an acceptable range for all recording locations (Fig 5.5C). A variability of dendritic spike threshold for two forms of synaptic input would again suggest that the action potential

FIG 5.5 Plots of the average voltage threshold for spike discharge evoked by stimulation of stratum oriens or stratum radiatum at varying distances along the dendro-somatic axis of the pyramidal cell. Voltage threshold at each location was taken as the average peak amplitude of the evoked EPSP when set to just spike threshold (measured from resting membrane potential). Somatic recordings are taken as 0um distance. B. Schematic diagram of the rat pyramidal neuron drawn to scale below the plots in A. C. Average resting membrane potential (RMP) and input resistance for the impalements shown in A. The number of impalements (n) for stratum radiatum evoked EPSPs are shown at the top of A while others are given at the base of each graph. Average values without standard error bars are those in which the standard error lies within the boundary of the illustrated point.

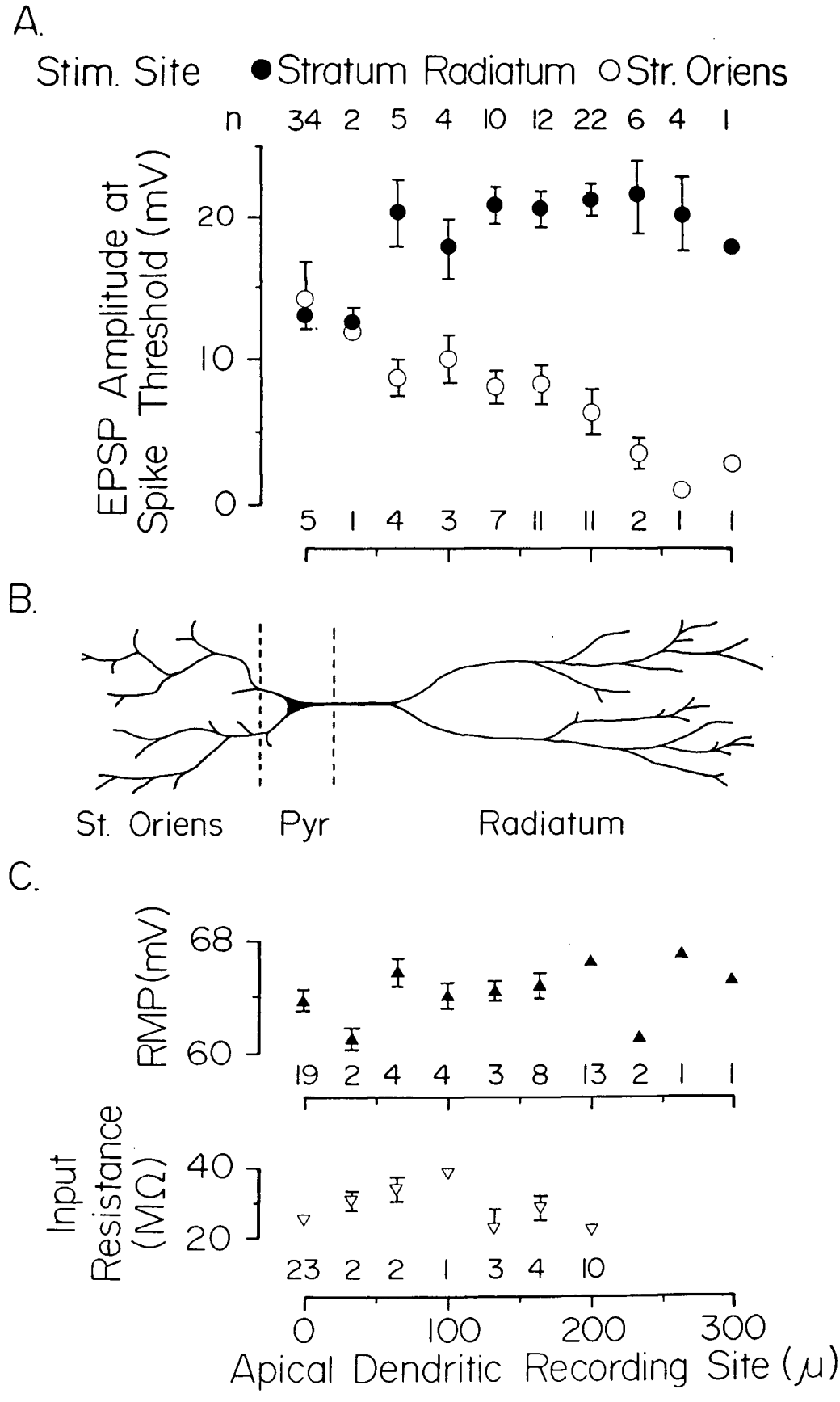
A.
Stim. Site
Stratum Radiatum
Str. Oriens
n
34 2 5 4 10 12 22 6 4 1
EPSP Amplitude at Spike Threshold (mV)
20
10
0
5 1 4 3 7 11 11 2 1 1
B.
St. Oriens
Pyr
Radiatum
C.
RMP (mV)
68
60
19 2 4 4 3 8 13 2 1 1
Input Resistance (MΩ)
40
20
23 2 2 1 3 4 10
0
100
200
300
Apical Dendritic Recording Site (μ)

recorded within an apical dendrite is generated at a site distal to the recording electrode. In this regard, it is worth noting that the only location in which spike threshold for either synaptic input was equivalent was in the region of the pyramidal cell body (Fig 5.5A).

Stimulus Evoked Spike Latency

Since dual impalements of pyramidal cells were not obtained in the present study, spike onset latency could not be measured at different regions of a given pyramidal neuron. In addition, the latency for spike discharge could vary dramatically according to the influence of such factors as latency jitter or stimulus intensity, preventing a direct comparison between separate pyramidal cell impalements. Therefore, it was necessary to estimate the latency for spike discharge by comparing the intracellular response to the latency of evoked extracellular field potentials at both the somatic and dendritic level. Previous studies have shown that intrasomatic spike discharge of CA1 pyramidal cells correlates in time to the negative-going phase or peak of the extracellular population spike response in stratum pyramidale (Richardson et al. 1984; Taylor and Dudek 1984; Turner et al. 1984). The latency of the population spike can thus be used as an indication of the latency of intrasomatic spike generation, and as such, compared to that of spike discharge in the apical dendrite. A second estimate of the latency for dendritic spike activation was obtained by determining the relationship between the intradendritic spike and extracellular waveform in the immediate vicinity of the dendritic impalement (see 5.2 Methods). In this way,

intradendritic AP discharge could be compared to the latency of extradendritic spike waveforms recorded on laminar profiles of extracellular field potentials (Chapter 3).

The relationship between intradendritic spike discharge and extracellular field potentials evoked by stimulation of the alveus, stratum oriens or radiatum is shown in Fig 5.6 (all records obtained from a single dendritic impalement and hippocampal slice). A comparison of intradendritic spike activation to the field potential response recorded at the cell layer revealed that dendritic spikes were evoked at a longer peak latency than the falling edge or peak of the population spike in stratum pyramidale (top two traces in Fig 5.6). The difference in latency between these two responses was found to increase directly with the distance of the dendritic recording site from the border of stratum pyramidale. A comparison of the dendritic spike to the extradendritic field potentials recorded immediately following withdrawal from the impalement is shown in the lowest set of records of Fig 5.6. In each case, intradendritic spikes were found to align with the biphasic positive/negative extracellular spike potential recorded in the dendritic region during suprathreshold stimulation of the pyramidal cell population (Chapter 3). Specifically, the onset of the intradendritic spike corresponded to that of the positive extradendritic potential, while the breakpoint of decay of the spike aligned with the termination of the negative component of the dendritic field potential (denoted by dotted lines in Fig 5.6). While the positive/negative component of the SR evoked extracellular EPSP is not as evident in this particular example, the onset of the positive-going deflection on the extradendritic

FIG. 5.6 A comparison of the latency of intradendritic spike discharge to extracellular field potentials recorded in stratum pyramidale (population spike) and stratum radiatum (extradendritic) immediately following withdrawal from the dendritic impalement. Potentials were evoked by stimulation of the alveus (A), stratum oriens (B) or stratum radiatum (C). Stimulus intensities were set to threshold for intradendritic spike activation (several sweeps shown) and field potentials averaged over 10 successive sweeps. Dotted lines indicate the latency relationship between intradendritic spikes and extradendritic field potentials. Intradendritic recordings were obtained from a single impalement 200um from the border of stratum pyramidale.

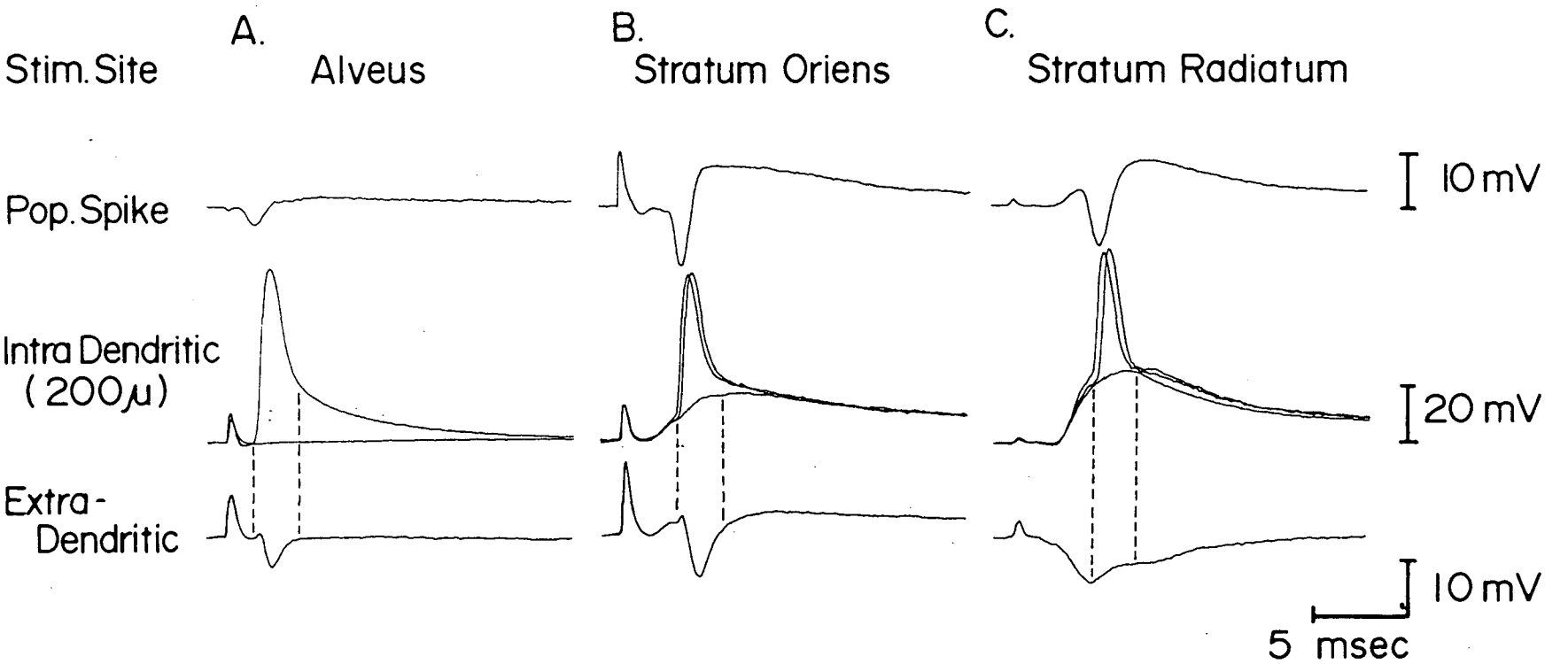
A.
B.
C.
Stim. Site
Alveus
Stratum Oriens
Stratum Radiatum
Pop. Spike
Intra Dendritic
(200μ)
Extra-
Dendritic
10 mV
20 mV
10 mV
5 msec

EPSP can be seen to correspond to the rising edge of the intradendritic spike at this location (Fig 5.6C).

Intradendritic Spike Fractionation

Previous investigators have reported that the evoked dendritic spike of pyramidal neurons could be separated into multiple components, a response referred to as a "fractionation" of the spike waveform (Wong et al. 1979). This result was taken as evidence for spike discharge at regional "hot spots" of dendritic membrane exhibiting a low threshold for spike activation. In the present study, a fractionation of the dendritic spike was occasionally observed in dendritic recording locations 200-300μm from the border of stratum pyramidale. This pattern of spike generation could be evoked by stimulation of the alveus, stratum oriens, or stratum radiatum, with the fractionated spike evoked at a latency beyond the peak of the extracellular population spike at the cell body layer (Fig 5.7A-C). Fractionation of the dendritic spike was related to the latency to spike discharge, with a greater degree of fractionation observed for those spikes evoked well beyond the peak of the population spike or on the falling edge of the intradendritic EPSP.

The fractionated spike appeared to be comprised of two principle all-or-none components. The first was a small potential of 9-25mV amplitude that gave rise to a second, larger spike with an amplitude that could vary with the intensity of stimulation (Fig 5.7A-C). If evoked at just-threshold stimulus intensity, the second component was of small amplitude and clearly distinct in arising from the falling edge of the first

FIG. 5.7 Fractionation of intradendritic spikes recorded 230μm from the border of stratum pyramidale. A-C. Spike discharge evoked through stimulation of the alveus (A), stratum oriens (B) or stratum radiatum (C) is compared to the extracellular population spike response recorded in stratum pyramidale. In each case, several sweeps are superimposed for increasing intensities of stimulation. Note fractionation of spikes into two principle all-or-none components, and the increase in amplitude of the second component at higher stimulus intensities. D,E. Fractionation of the dendritic spike in response to 10Hz repetitive stimulation of the alveus (D) or stratum radiatum (E). During stimulation, the full amplitude dendritic spike increased in peak latency and decreased in amplitude to eventually fractionate into a two component waveform. A slight hyperpolarization of the membrane during the stimulus train is evident. The antidromic response in A was obtained from a separate dendritic impalement from that of B and C.

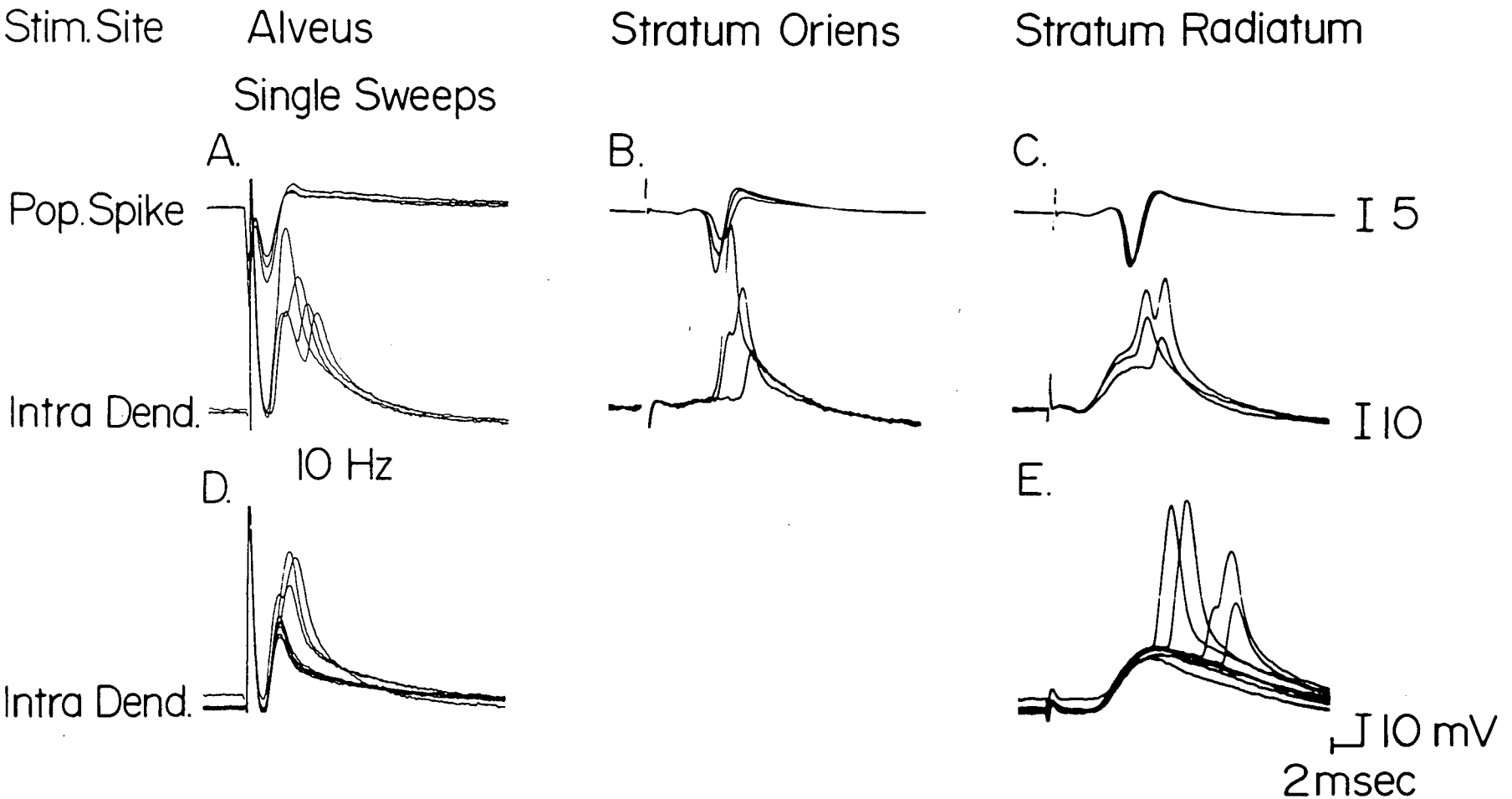
Stim. Site
Alveus
Stratum Oriens
Stratum Radiatum
Single Sweeps
A.
B.
C.
Pop. Spike
Intra Dend.
I 5
I 10
10 Hz
D.
E.
Intra Dend.
10 mV
2msec

potential. As stimulus intensity was increased, the second potential could exhibit the peculiar characteristic of increasing in amplitude, progressively arising with a shorter onset latency until the break between the two components could no longer be discerned (best illustrated for the case of alvear and SO stimulation in Fig 5.7A,B).

Fractionation of the spike could often occur in distal dendritic impalements during repetitive stimulation of efferent or afferent pathways (Fig 5.7D,E). In either case, a dendritic spike evoked in full form on the first pulse would increase slightly in peak latency during the stimulus train, with the second component gradually declining in amplitude to reveal an initial small all-or-none potential. As shown in Fig 5.7D, the second larger potential could be lost during repetitive stimulation, while the first component declined only slightly to be evoked at a comparatively constant amplitude through the majority of the stimulus train.

In the study of Wong et al. (1979), fractionation of the dendritic spike was achieved through hyperpolarization of the membrane during stimulation of stratum radiatum inputs. Similar results could be obtained in the present study, and again the fractionation could be related to the latency of the evoked dendritic spike. In this case, the onset latency for spike discharge in response to SR stimulation would increase with membrane hyperpolarization at both the somatic and dendritic level, with the result that the dendritic spike would exhibit a fractionation into the separate components described above.

Isolation of Apical Dendritic Elements by Knife Cuts in the CA1 Region

In order to determine whether dendritic spike activation could occur independently of that at the soma, attempts were made to physically separate the soma and apical dendrites of CA1 pyramidal cells by a knife cut according to the technique of Benardo et al. (1982). Briefly, this was performed through use of a "micro-knife" consisting of a small razor blade chip glued to a wooden dowel mounted on a micro-manipulator. Slice tissue was cut while resting upon the surface of the nylon net within the recording chamber by lowering the blade across the proximal-mid stratum radiatum under direct microscopic observation (see Methods for details). Initial attempts to cut slice tissue followed this procedure, and SR evoked extracellular field potentials were recorded from within and on either side of the cut to assess the characteristics of evoked dendritic activity. However, several difficulties were encountered in trying to achieve separation of the cell body region without damaging remaining slice tissue. The majority of problems were related to the fact that the nylon net within the recording chamber did not provide adequate support for obtaining a complete cut of the slice. For instance, the net configuration of the nylon fibers supporting the slice would result in only one or a few nylon strands crossing beneath the intended line of cut in the CA1 region, offering little or no background support for which to push the blade against. The pliability of the nylon strands also allowed the net surface to bend beneath the pressure of the blade, requiring further forward advance of the knife with the possibility of compressive damage to surrounding

tissue. In fact, evoked extracellular potentials often displayed evidence of damage to the "intact" regions of a cut slice, including evoked potentials of low amplitude or the repetitive discharge of population spike responses at the cell body layer. Histological analysis revealed that the only means of obtaining complete separation of the cell body layer using this technique was to make small repeated cuts along the axis of the blade at the bottom of the slice. However, this procedure often severed the nylon net supporting the slice, resulting in a sudden loss of net tension and extensive jarring of slice tissue. The inability to successfully section slices in this manner required the development of another technique for cutting the slice prior to placement within the recording chamber. In this case, the slice was placed in a small drop of oxygenated medium within a plastic petri dish and cut by a scalpel blade under microscopic observation. This technique was found to be far superior to that described above, allowing complete and reliable separation of the cell body layer with minimal damage to surrounding neuronal tissue. A thin section (22um) from a hippocampal slice cut in this manner and stained with cresyl violet is shown in Fig 5.8B, demonstrating the excision of pyramidal cell bodies from the apical dendritic region. SR evoked potentials recorded at the indicated locations are shown in Fig 5.8C. A recording electrode placed in stratum pyramidale or radiatum in the intact region of a cut slice revealed that SR evoked potentials were comparable to that of control hippocampal tissue, with maximal evoked EPSPs of 12mV and population spikes of up to 27mV with no evidence of multiple population spike discharge. However, the peak amplitude of the evoked EPSP and population spike progressively declined

FIG. 5.8 Thin sections (22μm) of cresyl violet stained hippocampal tissue from an intact slice and a slice with a knife cut across regio superior for isolation of the apical dendrites from somata of CA1 pyramidal cells. The major subfields of the hippocampal formation are shown in A, including the hippocampal regions of CA1 and CA3, and the dentate gyrus (DG). The stained somata of CA1 pyramidal cells are represented by the dark band of tissue in stratum pyramidale. The diffuse and scattered staining of cells in stratum radiatum can be attributed in large part to glial elements. In B, the removal of pyramidal cell somata by the knife cut is indicated by the loss of stratum pyramidale in CA1. Recording electrode positions are marked in stratum pyramidale (dark triangles) and stratum radiatum (open circles). C. Stratum radiatum evoked potentials recorded at the locations indicated in B from stratum pyramidale and stratum radiatum, moving from left to right. The stimulating electrode was placed in stratum radiatum on the fimbrial side of the recording electrode and moved with the recording electrode to maintain a constant distance of approximately 400μm. D. An enlargement of the stratum radiatum evoked fiber potential recorded in stratum radiatum at the position indicated by the asterisk in B and C.

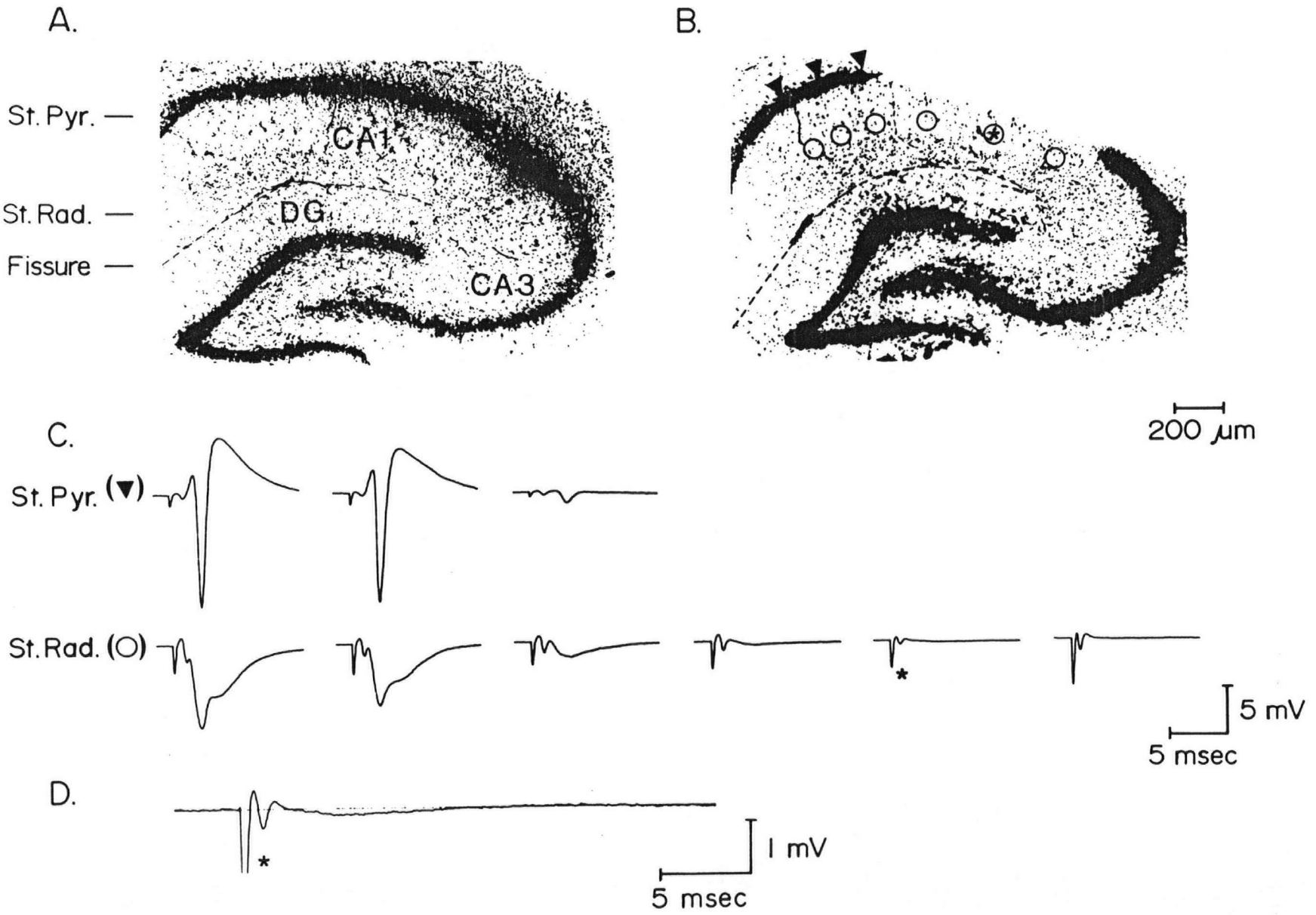
A.
B.
St. Pyr.
St. Rad.
Fissure
CA1
DG
CA3
200 µm
C.
St. Pyr. (▼)
St. Rad. (○)
5 mV
5 msec
D.
1 mV
5 msec

as the recording electrode was moved towards the edge of the cut (Fig 5.8C). A rapid decline in the amplitude of the evoked EPSP in stratum radiatum was then observed within the cut region over approximately 100-150μm from the border of the incision. In almost all slices examined, the maximal amplitude of "EPSPs" evoked beyond this point with stimulus intensities of up to 60V was in the range of 0.2-0.4mV. However, large fiber potentials (up to 4mV) could be evoked and recorded in stratum radiatum along the entire extent of the cut, demonstrating that afferent synaptic projections were still intact (Fig 5.8D). Therefore, the lack of evoked synaptic potentials in stratum radiatum could not be attributed to compressive damage to the dendritic region that might have been sustained during the cutting procedure. In some slices, a postsynaptic potential could be evoked over a limited distance within the cut region of the slice. However, subsequent histological analysis revealed the presence of scattered or displaced pyramidal cell somata at the edge of the incision directly above the position of the evoked activity. The evoked potentials in this case could thus correspond to activity of pyramidal cell dendrites still attached to the cell body region. It appeared therefore, that the vast majority of pyramidal cell apical dendrites had not survived separation from the cell body region, preventing an analysis of spike activation in an isolated dendrite.

5-4. Discussion

Previous studies on the evoked activity of the pyramidal cell have reported evidence for the initial activation of a spike in apical dendritic membrane, with a subsequent electrotonic conduction of the dendritic spike to the somatic region (Andersen et al. 1960; Andersen and Lomo 1966; Cragg and Hamlyn 1955; Schwartzkroin 1977; Spencer and Kandel 1961b). One would thus expect to find evidence in the configuration of the dendritic spike of an electrotonic conduction and decay towards the cell body region. In fact, a comparative intracellular analysis of spike characteristics along the dendro-somatic axis revealed a progressive change in several parameters of spike discharge, including spike amplitude, halfwidth, voltage threshold and latency to onset.

Evoked Characteristics of Spike Discharge Along the Dendro-Somatic Axis

One consequence of an electrotonic conduction of a spike from the dendritic region would be a decrease in amplitude and increase in halfwidth with proximity to the cell body layer. However, spikes evoked from each of the stimulus pathways or through current injection displayed a decrease in amplitude and increase in halfwidth with distance from stratum pyramidale, opposite to that expected for a somatopetal conduction of the dendritic spike.

The initial activation of a spike from a generator zone (hot spot) in dendritic membrane would also predict a low voltage threshold for spike activation at one or more points along the dendro-somatic axis. An analysis of synaptically

evoked spike threshold did reveal a gradual change in the voltage threshold for spike discharge along the pyramidal cell apical dendrite. However, the progression of change in spike threshold was distinctly different for two forms of evoked synaptic depolarization of the pyramidal cell. Voltage threshold for spike discharge in response to SR stimulation was greatest in the mid-distal apical dendrite, declining towards the pyramidal cell layer. In contrast, action potentials evoked by SO stimulation displayed the highest threshold in the cell body, with voltage threshold apparently decreasing with distance along the apical dendrite. A strict interpretation of these results would imply that (1) an apical dendritic spike is most effectively evoked by an EPSP of basal dendritic origin, and (2) that a spike at any given location along the apical dendrite can be evoked at two entirely different voltage thresholds (recall that complementary threshold measurements are taken from the same dendritic impalement; cf 5.1). Neither conclusion would appear to conform to the usual understanding of voltage-dependent activation of spike discharge in neuronal membrane. An alternative explanation for the variability in spike threshold is that a dendritic spike is generated at a site remote from the dendritic recording location. In fact, the only location in the pyramidal cell in which spike discharge was evoked from a consistent voltage threshold was in the region of the cell body layer. The above results might then be explained by the initial activation of a spike in the somatic region, and a subsequent retrograde spike invasion of dendritic membrane. An action potential conducting back through the dendritic tree would then superimpose upon the coincident level of

depolarization within the apical dendrite, giving rise to an apparent lack of voltage threshold in dendritic locations.

The results obtained in an analysis of the latency for spike discharge also contradict the concept of initial spike activation in dendritic locations of the pyramidal cell. Although strict measures of spike latency were not obtained, a comparison of the intradendritic spike to extracellular field potentials provides an indirect estimate of the latency for spike discharge at different levels of the dendro-somatic axis. Should dendritic spike activation precede that at the somatic level, one would expect the dendritic spike to be evoked at a shorter latency than the population spike in stratum pyramidale, a potential reflecting the average latency for somatic spike discharge. However, intradendritic spikes were evoked beyond the peak of the population spike at the cell layer, suggesting that spikes recorded in dendritic locations were evoked subsequent to that in the somatic region. Furthermore, intradendritic spikes aligned with the extradendritic positive/negative potential recorded in stratum radiatum following suprathreshold activation of the pyramidal cell population. As described in Chapter 3, this potential was found through current-source density analysis to conduct with increasing latency through the dendritic region with distance from the cell body layer.

Therefore, the characteristics of evoked dendritic spike amplitude, halfwidth, and onset latency along the dendro-somatic axis of the pyramidal cell are directly opposed to the expected result for the initial activation of a spike from within the dendritic arborization. In addition, an analysis of the voltage threshold for spike activation in the dendrite did not reveal

regions of dendritic membrane exhibiting a low voltage threshold for spike discharge (hot spots). In fact, the only consistent voltage threshold for spike discharge in response to either synaptic or current evoked depolarizations was found in the region of the cell body layer. Although dendritic "hot spots" may have been isolated or remote to the dendritic impalements obtained, all data are consistent with the initial activation of a spike in the somatic region of the pyramidal cell, and a subsequent retrograde conduction of the spike through the dendritic arborization.

Some of the strongest evidence for this interpretation comes from the close correlation of intracellular spike discharge to the spike components of extracellular field potentials at all levels of the dendro-somatic axis. For instance, the onset latency of dendritic spikes evoked from all three pathways corresponded to the field potential waveform shown through current-source density analysis to conduct from the cell body layer. The correlation between intra- and extracellular spike potentials is further noted in the pattern of transition in spike configuration along the dendro-somatic axis. At approximately 100μm from stratum pyramidale, the extracellular spike component changed from a negative-going population spike to a positive/negative dendritic potential (Chapter 3). This location corresponds to the approximate point at which intradendritic spikes exhibit a decrease in amplitude and increase in halfwidth with respect to spikes recorded in the somatic region of the pyramidal cell. Similarly, the loss of the negative component of the extracellular dendritic spike in distal stratum radiatum correlates to the second rapid decline

in amplitude and increase in halfwidth of the intradendritic spike. Anatomical measurements of the rat pyramidal cell indicate that these points of transition correspond to the approximate location of major branchpoints of the apical dendritic structure (Chapter 3). The change in spike configuration in proximal stratum radiatum may then correspond to a conduction of the spike past the point of bifurcation of the proximal dendritic shaft. Similarly, the change in spike characteristics in distal stratum radiatum may indicate spike conduction past secondary dendritic branchpoints in distal dendritic regions. An alteration in action potential waveform is in fact the expected result for the case of a spike conducting past the branchpoint of a neuronal structure (Goldstein and Rall 1974). However, regardless of the mechanism underlying the change in spike characteristics along the dendro-somatic axis, the close correlation between intra- and extracellular spike properties indicate that results obtained from field potential profiles are representative of the activity in individual pyramidal cell elements. Intracellular data would thus support the conclusions derived form current-source density analysis, indicating a retrograde spike conduction through the apical dendritic region (Chapter 3).

Dendritic Spike Fractionation

Beyond approximately 200μm from the border of stratum pyramidale (approximately half the distance to the hippocampal fissure), dendritic spikes could exhibit a "fractionation" in waveform. Spike fractionation has previously been taken as evidence for multiple sites of spike generation in dendritic

membrane (Wong et al. 1979). In the present study, spike fractionation was observed for dendritic spikes evoked through both antidromic or orthodromic stimulation, with all components of the fractionated spike evoked beyond the peak of the population spike recorded in stratum pyramidale. Thus, it would appear that fractionated dendritic spikes had been evoked subsequent to AP discharge at the cell body layer. These results also indicate that an antidromic spike conducting from the somatic region can exhibit a fractionation of waveform similar to that observed for orthodromic spike discharge. Thus, the fractionation of an orthodromic spike does not necessarily indicate the presence of multiple sites for spike activation in the apical dendrite. However, these results cannot rule out the possible presence of dendritic hot spots, as retrograde spike activation of a low threshold dendritic region might be "reflected" in neighboring dendritic branches as a fractionated spike (Parnas 1979).

Close examination of this phenomenon revealed that a fractionated spike could be separated into essentially two components - a small all-or-none potential of relatively constant amplitude, and a second spike of variable amplitude. The basic form of the "fractionated" spike thus resembles the case of a fast pre-potential underlying the activation of a second larger spike (cf 4.9 and 4.10). In fact, fractionated spikes displayed similar evoked characteristics to that of FPP discharge, being uncovered through membrane hyperpolarization or repetitive stimulation. However, fractionation of the spike was also strongly correlated to the latency of spike activation, a parameter of AP discharge directly related to the recording

distance from stratum pyramidale. A greater fractionation of the spike was found at comparatively long latencies to onset, with more separation of spike components when evoked upon the falling edge of the EPSP. It is important to note that spikes evoked at this latency fall close to the approximate time for activation of the inhibitory postsynaptic conductance observed at the cell body region (Dingledine and Langmoen 1980) or perhaps in dendritic membrane (Alger and Nicoll 1984). Fractionation of the evoked spike may thus correspond to an inhibition of spike amplitude as a retrogradely conducted dendritic spike shifts in peak latency to within the time of inhibitory current movements along the dendro-somatic axis. Such a mechanism could explain the correlation between spike fractionation and recording distance from the cell layer, as well as the intensity dependence of the amplitude of a fractionated spike. However, further work is required to identify the factors responsible for spike fractionation, and to assess the similarity of this form of spike activation to FPP discharge.

Evoked Activity of Isolated Apical Dendrites

In order to determine whether an action potential could be evoked in dendritic membrane independently of that at the cell body, attempts were made to isolate apical dendrites from the cell body layer by placing a knife cut in the CA1 region. To accomplish this, a technique was developed by which the cut would ensure a complete and reliable separation of pyramidal cell somata and apical dendrites, as confirmed through subsequent thin sectioning and histological analysis of slice tissue. An analysis of evoked activity in cut slices revealed

minimal damage to pyramidal cell structures outside the region of the cut or to afferent fibers projecting through the dendritic field under the cut. In contrast, little or no postsynaptic activity could be recorded from isolated dendritic elements beyond approximately 150um from the border of the knife cut. Anatomical measurements would indicate that this distance is within the range of lateral branching of the pyramidal cell apical dendrite (Chapter 3). Evoked activity at the edge of a cut could then correspond to dendritic structures attached to the cell bodies of pyramidal cells in the intact portion of stratum pyramidale. In fact, in the few slices demonstrating evoked activity within the region of the cut, histological analysis revealed the presence of pyramidal cell somata at the edge of the cut above the location of the evoked potential. The results would thus indicate that most if not all isolated apical dendrites had not survived separation from the cell body region.

Previous investigators have reported obtaining an isolation of apical dendrites and somata of pyramidal cells, and have recorded action potential discharge from within the "isolated" dendrite (Benardo et al. 1982; Masukawa and Prince 1984). However, the technique used in these studies for cutting the slice could not be successfully employed in the present work, and proved to be inadequate or at least unreliable in obtaining complete separation of dendritic structures from the cell body region. It may thus be possible that dendritic recordings in these studies were obtained from "intact" dendrites still attached to somata not removed by the knife cut. Considering the difficulties associated with this technique, the demonstration of evoked activity from within an isolated dendrite would

require additional anatomical confirmation of cell body loss through injection of a suitable cell stain. Therefore, using the techniques presently available, it would appear that pyramidal cell dendrites cannot survive separation from the cell body region, and the possibility of dendritic spike activation independent of that in the cell body has not yet been adequately tested.

The present study has further characterized the properties of action potential discharge in somatic and dendritic membranes of the CA1 pyramidal cell. A detailed analysis of spike activity has demonstrated a gradual change in the properties of spike amplitude, halfwidth, voltage threshold and onset latency along the pyramidal cell dendro-somatic axis. However, the direction of change in these characteristics is directly opposed to the results predicted by a model of spike generation within the dendritic arborization. The intracellular characteristics of spike discharge thus coincide with the results obtained through current-source density analysis (Chapter 3), indicating that the initial site for Na+ spike generation in the pyramidal neuron is in the region of the soma-axon hillock. Action potential discharge in dendritic membrane then follows that in the soma as the result of a retrograde spike invasion of the dendritic arborization.

6-0. GENERAL SUMMARY AND DISCUSSION

The Site of Origin of Pyramidal Cell Dendritic Spikes

The present study has served to identify the site of origin of evoked dendritic spikes in CA1 pyramidal neurons of mammalian hippocampus. A comprehensive analysis of field potentials, current-source density, and intracellular activity indicate that the initial site of spike discharge in the pyramidal cell for both antidromic or orthodromic stimulation is in the region of the soma-axon hillock. Evoked spikes in dendritic locations then arise through a retrograde conduction of the spike from the cell layer through the dendritic arborization. Furthermore, the similarity in the characteristics of Na+ spikes evoked by depolarizing current to those evoked by anti- or orthodromic stimulation may indicate a somatic site of origin for all evoked Na+ spikes recorded in the pyramidal cell dendrite.

These results are directly opposed to the existing hypothesis regarding dendritic spike activation in the pyramidal cell. According to this model, dendritic spikes are evoked from within the dendritic tree at regional "hot spots" of membrane exhibiting a low threshold for spike discharge (Andersen and Lomo 1966; Spencer and Kandel 1961b; Traub and Llinas 1979; Wong et al. 1979). As a result, synaptic depolarization can give rise to the initial activation of a spike at the dendritic level that electrotonically conducts to the cell body to appear in the soma as a fast pre-potential (Andersen and Lomo 1966; Schwartzkroin 1977; Wong et al. 1979). A spike evoked within the dendrite can thus summate with synaptic currents, increasing the probability for AP discharge at the axon hillock. Several results of the

present study argue against the validity of the above hypothesis. For instance, current-source density analysis revealed that the shortest latency current sink was evoked in the soma-axon hillock region of pyramidal cells, and not in dendritic locations. In addition, the observed change in the configuration of the intracellular spike along the dendritic axis was opposite to that predicted for the electrotonic conduction of a spike from the dendrite to the cell body. Finally, intradendritic spikes were evoked following the peak of the population spike recorded in stratum pyramidale, and aligned with the extradendritic field potential shown through CSD analysis to conduct from the cell body layer. Therefore, the evidence does not support the contention of a dendritic site of origin for spikes recorded at the dendritic level of the pyramidal cell. Rather, the results indicate that evoked dendritic spikes arise through a retrograde invasion of the dendrite by a spike initiated in the region of the soma-axon hillock.

Implications of the Present Study

The findings presented in this work question our current understanding of pyramidal cell physiology. For instance, the fact that the dendritic spike is evoked following that at the cell body implies immediately that dendritic spike activation does not contribute directly to the generation of a spike in the axon hillock. The retrograde conduction of a spike from the cell layer also indicates that a fast pre-potential does not reflect the electrotonic decay of a spike from the dendrite towards the pyramidal cell body. In fact, FPPs of similar amplitude and

waveform were recorded at both the somatic and dendritic level, and the change in configuration of the spike along the dendrite was opposite to that predicted for a somatopetal decay of an action potential arising from within the dendritic tree. Although the mechanism underlying FPP discharge was not determined, alternative explanations have been proposed in previous studies, including the electrotonic conduction of a spike across a gap junction located at either the somatic or dendritic level (Andrew et al. 1982; MacVicar and Dudek 1981).

The results also press for a critical evaluation of the evidence for low threshold hot spots for Na+ spike activation in dendritic membrane of the pyramidal cell. Dendritic hot spots were originally proposed to account for the apparent dendritic site of origin of spikes in the pyramidal cell, and the interpretation that somatic fast pre-potentials represent an electrotonically decayed dendritic spike (Andersen and Lomo 1966; Spencer and Kandel 1961b). A fractionation of the dendritic spike was taken as further evidence for multiple sites of spike generation in dendritic regions (Wong et al. 1979). However, as discussed above, spikes were found to originate at the somatic level of the pyramidal cell, and the retrograde conduction and configuration of the spike along the dendro-somatic axis suggest that the somatic FPP does not represent a dendritic spike. In addition, fractionated spikes were evoked following the peak of the population spike in stratum pyramidale and by antidromic stimulation, suggesting that the fractionated spike had arisen subsequent to spike discharge at the cell body layer. Furthermore, spike discharge at dendritic hot spots was not detected on current-source

density profiles, and measurement of the voltage threshold for spike discharge along the dendro-somatic axis did not reveal regions of particularly low threshold for spike activation in the apical dendrite. It might be argued that generation of a spike at a dendritic hot spot only occurs during periods of intense activation, such as that found during epileptiform discharge of the pyramidal cell population. However, preliminary analysis of multiple population spike discharge has revealed a similar pattern of spike activation as that found under normal conditions, with each spike in the burst originating at the cell body layer. It is possible that spike discharge at a dendritic hot spot was simply not detected in the present study. Nevertheless, alternative explanations can be offered for data supporting the existence of hot spots in dendritic membrane. Therefore, it may not be necessary to invoke the special characteristic of dendritic hot spots to account for certain aspects of pyramidal cell physiology.

The properties of the evoked dendritic spike would further question the possible means of conduction of a spike along the dendro-somatic axis. Previous investigations have shown a blockade of the pyramidal cell apical dendritic spike through application of tetrodotoxin (TTX) or QX-314 injection (Benardo et al. 1982; Wong et al. 1979), suggesting that the dendritic spike is actively generated through a voltage-dependent Na+ conductance. However, the results of the present study can also be explained on the basis of a passive electrotonic conduction of the spike along the dendritic axis. As discussed in Chapter 3, the invasion of the dendritic region by a current source/sink could be interpreted as a passive depolarization and subsequent

active spike generation as a spike conducted towards the recording location. However, a biphasic positive/negative potential and current source/sink would also be expected for capacitance current flow associated with the electrotonic conduction of a high frequency component (ie a spike) along membrane with a comparatively long time constant (Nobles 1966). The gradual change in waveform of the spike through the dendritic field would then be a function of the rate of rise and decay of the intracellular spike at each location. Passive electrotonus could thus account for the biphasic postive/negative spike potential conducting through the dendritic region on laminar profiles of extracellular field potentials. The presence of a current sink in the proximal stratum radiatum may however indicate an active propagation of the spike through the proximal dendritic region.

Intracellular data would also support the contention of a passive electrotonic decay of the spike through the majority of the dendritic arborization. Intracellular spikes declined in amplitude and increased in halfwidth with distance from the cell layer, and displayed a single consistent voltage threshold only at the level of the pyramidal cell body. The lack of a voltage threshold for spike activation in the dendrite could be explained by an electrotoniclly conducted spike superimposing upon the existing level of depolarization at any point along the cell axis. In fact, the amplitude of the dendritic spike could be altered with the level of membrane polarization, suggesting no clear reversal potential for the dendritic spike (see Fig 4.8). The evidence for a Na+-dependence of dendritic spike discharge may relate to the methods used in applying Na+ channel

blockers. In the study in which TTX was applied to dendritic membrane, the drug was perfused across the entire slice (Wong et al. 1979), and blockade of the dendritic spike may have occurred secondarily to inhibition of somatic spike discharge. Similarly, injection of the anesthetic QX-314 into a dendritic impalement (Benardo et al. 1982) cannot necessarily be taken as evidence for a blockade of the spike at the dendritic level, as the drug may have diffused to the region of the soma-axon hillock (or proximal dendrite). A test for the ionic basis of the dendritic spike may therefore require a more selective application of Na+ channel blockers to dendritic membrane of the pyramidal cell.

The Possible Significance of Dendritic Spikes to Pyramidal Cell Function

The retrograde conduction of a spike through the dendritic arborization could be of important consequence to pyramidal cell function. For instance, the large depolarization induced by a spike invading the dendrite would rapidly depolarize the majority of the dendritic structure over a short period of time. Through activation of intrinsic voltage-dependent channels unrelated to spike discharge, such a depolarization could serve to increase the effective length constant of the cell, enhancing the transfer of synaptic currents to the cell layer (Llinas and Sugimori 1984). Alternatively, a spike conducting through the region of afferent termination might also limit the time course of synaptic depolarization by reducing the driving force for inward synaptic currents. The retrograde invasion of a spike will certainly influence the form of extracellular potentials along the cell axis, altering the shape of the extracellular

voltage gradient in the CA1 region (Richardson et al. 1984b). The dendritic spike will therefore modify the characteristics of extracellular current flow, and will be an important consideration in determining the ephaptic influence of field potentials upon the pyramidal cell at both the somatic and dendritic level (Richardson et al. 1984a,b; Turner et al. 1984).

The retrograde conduction of the spike through the dendrite might also contribute to the multiple spike discharge of pyramidal cells thought characteristic of epileptiform activity. Under normal conditions, pyramidal cell discharge evoked by stimulation of afferent or efferent pathways is restricted to single spike activation by a recurrent inhibitory feedback system (Andersen et al. 1969; Dingledine and Langmoen 1980; Schwartzkroin and Prince 1980). However, in the presence of pharmacological agents known to block the action of inhibitory synaptic inputs, synaptic depolarization can elicit a large paroxysmal depolarizing shift (PDS) capable of evoking repetitive somatic spike activation (Schwartzkroin and Prince 1980; Schwartzkroin and Wyler 1979). The PDS is Ca+2-dependent, and thought to arise in part from the activation of voltage-dependent Ca+2 channels in dendritic membrane (Schwartzkroin and Prince 1980; Schwartzkroin and Wyler 1979; Wong and Prince 1979). In fact, previous work has shown that activation of a dendritic Na+ spike by antidromic stimulation under these conditions gives rise to Ca+2 spike discharge at the dendritic level(Schwartzkroin and Prince 1980). Therefore, one function of the inhibitory feedback network to the pyramidal cell may be to prevent the activation of dendritic Ca+2 spikes by the Na+ spike conducting through the dendrite from the region

of the cell layer.

The present study has demonstrated that dendritic spikes of the pyramidal cell arise through a retrograde invasion of the dendrite by a spike initiated in the region of the soma-axon hillock, a finding that will require major revisions in our present concept of pyramidal cell physiology. A similar pattern of activity has been shown to exist in other CNS neurons, including the dentate granule cell (Jefferys 1979), cerebellar Purkinje cell (Llinas 1975; Llinas and Sugimori 1980a,b), and the Mauthner cell of the goldfish (Furshpan and Furakawa 1962). The properties of Na+ spike discharge in the pyramidal cell are thus comparable to a diverse group of cell types, and elucidation of the role of dendritic spikes in determining pyramidal cell activity may have widespread implications to our basic understanding of neuronal function.

REFERENCES

ALGER, B.E. AND NICOLL, R.A. (1982) Feed-forward dendritic inhibition in rat hippocampal pyramidal cells studied in vitro. J. Physiol. London 328: 105-123.

ALLEN, G.I., ECCLES, J., NICOLL, R.A., OSHIMA, T. AND RUBIA, F.J. (1977) The ionic mechanisms concerned in generating the IPSPs of hippocampal pyramidal cells. Proc. R. Soc. Lond. B 198: 363-384.

ANDERSEN, P. (1959) Interhippocampal impulses. I. Origin, course and distribution in cat, rabbit and rat. Acta physiol. scand. 47: 63-90.

ANDERSEN. P. (1960) Interhippocampal impulses. II. Apical dendritic activation of CA1 neurons. Acta physiol. scand. 48: 178-208.

ANDERSEN, P., BLACKSTAD, T.W. AND LOMO, T. (1966a) Location and identification of excitatory synapses on hippocampal pyramidal cells. Exp. Brain Res. 1: 236-248.

ANDERSEN, P., BLISS, T.V.P. AND SKREDE, K.K. (1971a) Lamellar organization of hippocampal excitatory pathways. Exp. Brain Res. 13: 222-238.

ANDERSEN, P., BLISS, T.V.P. AND SKREDE, K.K. (1971b) Unit analysis of hippocampal population spikes. Exp. Brain Res. 13: 208-221.

ANDERSEN, P., BRULAND, H. AND KAADA, B. (1961) Activation of the field CA1 of the hippocampus by septal stimulation. Acta physiol scand. 51: 29-40.

ANDERSEN, P. ECCLES, J.C., LOYNING, Y. (1964) Location of postsynaptic inhibitory synapses on hippocampal pyramids. J. Neurophysiol. 27: 592-607.

ANDERSEN, P., GROSS, G.N., LOMO, T. AND SVEEN, O. (1969) Participation of inhibitory and excitatory interneurons in the control of hippocampal cortical output. In: The Interneuron, edited by M.A.B. Brazier. Berkely: Univ. Calif. Press, p. 415-465.

ANDERSEN, P., HOLMQVIST, B. AND VOORHOEVE, P.E. (1966b) Excitatory synapses on hippocampal apical dendrites activated by entorhinal stimulation. Acta physiol. scand. 66: 461-472.

ANDERSEN, P. AND LOMO, T. (1966) Mode of activation of hippocampal pyramidal cells by excitatory synapses on dendrites. Exp. Brain Res. 2: 247-260.

ANDREW, R.D., TAYLOR, C.P., SNOW, R.W. AND DUDEK, F.E. (1982) Coupling in rat hippocampal slices: dye transfer between CA1 pyramidal cells. Brain Res. Bull. 8: 211-222.

ANGEVINE, J.B.Jr. (1975) Development of the hippocampal region. In: The Hippocampus Vol. 1: Structure and Development, edited by R.L. Isaacson and K.H. Pribram, New York: Plenum Press, p. 61-94.

ASHWOOD, T.J., LANCASTER, B. AND WHEAL, H.V. (1984) In vivo and in vitro studies on interneurons in the rat hippocampus: possible mediators of feed-forward inhibition. Brain Res. 293: 279-291.

BAIMBRIDGE, K.G. AND MILLER, J.J. (1982) Immunohistochemical localization of Calcium-Binding Protein in the cerebellum, hippocampal formation and olfactory bulb of the rat. Brain Res. 245: 223-229.

BENARDO, L.S., MASUKAWA, L.M. AND PRINCE, D.A. (1982) Electrophysiology of isolated hippocampal dendrites. J. Neurosci. 2: 1614-1622.

BLACKSTAD, T.W. (1956) Commissural connections of the hippocampal region in the rat, with special reference to their mode of termination. J. Comp. Neurol. 105: 417-538.

BROWN, T.H., FRICKE, R.A. AND PERKEL, D.H. (1981) Passive electrical constants in three classes of hippocampal neurons. J. Neurophysiol. 46: 812-827.

BROWN, D.A. AND GRIFFITH, W.H. (1983a) Calcium-activated outward current in voltage-clamped hippocampal neurons of the guinea-pig. J. Physiol. London 337: 287-301.

BROWN, D.A. AND GRIFFITH, W.H. (1983b) Persistent slow calcium current in voltage-clamped hippocampal neurons of the guinea-pig. J. Physiol. London 337: 303-320.

CAJAL, S. RAMON y (1911) Histologie du systeme nerveaux de l'homme et des vertebres. A. Maloine. Paris. Vol II.

COOMBS, J.S., CURTIS, D.R. AND ECCLES, J.C. (1957a) The interpretation of spike potentials of motoneurons. J. Physiol. London 139: 198-231.

COOMBS, J.S., CURTIS, D.R. AND ECCLES, J.C. (1957b) The generation of impulses in motoneurons. J. Physiol. London 139: 232-249.

CRAGG, B.G. AND HAMLYN, L.H. (1955) Action potentials of the pyramidal neurons in the hippocampus of the rabbit. J. Physiol. London 129: 608-627.

DINGLEDINE, R. AND LANGMOEN, I.A. (1980) Conductance changes and inhibitory actions of hippocampal recurrent IPSPs. Brain Res. 185: 277-287.

EDWARDS, C. AND OTTOSON, D. (1958) The site of impulse initiation in a nerve cell of a crustacean stretch receptor. J. Physiol. London 143: 138-148.

EKEROT, By. C.F. AND OSCARRSON, O. (1981) Prolonged depolarization elicited in Purkinje cell dendrites by climbing fiber impulses in the cat. J. Physiol. London 318: 207-221.

EULER, C. von, AND GREEN, J.D. (1960) Activity in single hippocampal pyramids. Acta physiol scand. 48: 95-109.

EULER, C. von, GREEN, J.D. AND RICCI, G. (1958) The role of hippocampal dendrites in evoked responses and after-discharges. Acta physiol scand. 42: 87-111.

FREEMAN, J.A. AND NICHOLSON, C. (1975) Experimental optimization of current source-density technique for Anuran cerebellum. J. Neurophysiol. 38: 369-382.

FREEMAN, J.A. AND STONE, J. (1969) A technique for current density analysis of field potentials and its application to the frog cerebellum. In: Neurobiology of Cerebellar Evolution and Development, edited by R.Llinas. American Medical Association, p. 421-430.

FUJITA, Y. AND SAKATA, H. (1962) Electrophysiological properties of CA1 and CA2 apical dendrites of rabbit hippocampus. J. Neurophysiol. 25: 209-222.

FURSHPAN, E.J. AND FURUKAWA, T. (1962) Intracellular and extracellular responses of the several regions of the Mauthner cell of the goldfish. J. Neurophysiol. 25: 732-771.

GESSI, T. SPERTI, L. AND VOLTA, F. (1966) Local response of the hippocampal cortex to direct stimulation in the guinea-pig. Arch. Sci. Biol. 50: 20-40.

GLOOR, P. VERA, C.L. AND SPERTI, L. (1963) Electrophysiological studies of hippocampal neurons. I. Configuration and laminar analysis of the "resing" potential gradient, of the main-transient response to perforant path, fimbrial and mossy fiber volleys and of "spontaneous" activity. Electroencephalogr. Clin. Neurophysiol. 15: 353-378.

GOLDSTEIN, S.S. AND RALL, W. (1974) Changes of action potential shape and velocity for changing core conductor geometry. Biophys. J. 14: 731-757.

GREEN, J.D. AND MAXWELL, D.S. (1961) Hippocampal electrical activity. I. Morphological aspects. Electroencephalogr. clin. Neurophysiol. 13: 837-846.

GREEN, J.D., MAXWELL, D.S. AND PETSCH, H. (1961) Hippocampal electrical activity. III. Unitary events and genesis of slow waves. Electroencephalogr. Clin. Neurophysiol. 13: 854-867.

HABERLY, L.B. AND SHEPHERD, G.M. (1973) Current-source analysis of summed evoked potentials in Opossum Prepyriform cortex. J. Neurophysiol. 36: 789-802.

HALLIWELL, J.V. AND ADAMS, P.R. (1982) Voltage-clamp analysis of muscarinic excitation in hippocampal neurons. Brain Res. 250: 71-92.

HOTSON, J.R. AND PRINCE, D.A. (1980) A calcium-activated hyperpolarization follows repetitive firing in hippocampal neurons. J. Neurophysiol. 43: 409-419.

HOTSON, J.R., PRINCE, D.A. AND SCHWARTZKROIN, P.A. (1979) Anomalous inward rectification in hippocampal neurons. J. Neurophysiol. 42: 889-895.

JEFFERYS, J.G.R. (1979) Initiation and spread of action potentials in granule cells maintained in vitro in slices of guinea-pig hippocampus. J. Physiol. London 289: 375-388.

JEFFERYS, J.G.R. (1984) Current flow through hippocampal slices. Soc. Neurosci. Abstr. 14: 1074.

KADO, R.T. (1973) Aplysia giant cell: soma axon voltage clamp current differences. Science 182: 843-845.

KANDEL, E.R. AND SPENCER, W.A. (1961) Electrophysiology of hippocampal neurons. II. After-potentials and repetitive firing. J. Neurophysiol. 24: 243-259.

KANDEL, E.R., SPENCER, W.A. AND BRINLEY, F.J. Jr. (1961) Electrophysiology of hippocampal neurons. I. Sequential invasion and synaptic organization. J. Neurophysiol. 24: 225-242.

KNOWLES, W.D. AND SCHWARTZKROIN, P.A. (1981a) Local circuit synaptic interactions in hippocampal brain slices. J. Neurosci. 1: 318-322.

KNOWLES, W.D. AND SCHWARTZKROIN, P.A. (1981b) Axonal ramifications of hippocampal CA1 pyramidal cells. J. Neurosci. 1: 1236-1241.

LEUNG, L.S. (1979a) Potentials evoked by alvear tract in hippocampal CA1 region of rats. I. Topographical projection, component analysis, and correlation with unit activities. J. Neurophysiol. 42: 1557-1570.

LEUNG, L.S. (1979b) Potentials evoked by alvear tract in hippocampal CA1 region of rats. II. Spatial field analysis. J. Neurophysiol. 42: 1571-1589.

LEUNG, L.S. (1979c) Orthodromic activation of hippocampal CA1 region of the rat. Brain Res. 176: 49-63.

LLINAS, R. (1975) Electroresponsive properties of dendrites in central neurons. Adv. Neurol. 12: 1-13.

LLINAS, R. AND NICHOLSON, C. (1971) Electrophysiological properties of dendrites and somata in Alligator hippocampal Purkinje cells. J. Neurophysiol. 34: 532-551.

LLINAS, R. AND SUGIMORI, M. (1980a) Electrophysiological properties of *in vitro* Purkinje cell somata in mammalian cerebellar slices. J. Physiol. London 305: 171-195.

LLINAS, R. AND SUGIMORI M. (1980b) Electrophysiological properties of *in vitro* Purkinje cell dendrites in mammalian cerebellar slices. J. Physiol. London 305: 197-213.

LLINAS, R. AND SUGIMORI, M. (1984) Simultaneous intracellular somatic and dendritic recordings from Purkinje cells *in vitro:* dynamic soma-dendritic coupling. Soc. Neurosci. Abstr. 14: 659.

LORENTE de NO, R. (1934) Studies on the structure of the cerebral cortex. II. Continuation of the study of the Ammonic System. J. Psychol. Neurol. (Lpz.) 46: 113-177.

MacVICAR, B.A. AND DUDEK, F.E. (1981) Electrotonic coupling between pyramidal cells: a direct demonstration in rat hippocampal slices. Science 213: 782-785.

MASUKAWA, L.M. AND PRINCE, D.A. (1984) Synaptic control of excitability in isolated dendrites of hippocampal neurons. J. Neurosci. 4: 217-227.

MITZDORF, U. (1980) Justification of the assumption of constant resistivity used in current source-density calculations. J. Physiol. London 304: 216-220.

MITZDORF, U. (1985) Current-source density method and application in cat cerebral cortex: investigation of evoked potentials and EEG phenomenon. Physiol. Rev. 65: 37-100.

NICHOLSON, C. (1973) Theoretical analysis of field potentials in anisotropic ensembles of neuronal elements. IEEE Trans. Biomed. Eng. BME-20: 278-288.

NICHOLSON, C. AND FREEMAN, J.A. (1975) Theory of current source-density analysis and determination of conductivity tensor for Anuran cerebellum. J. Neurophysiol. 38: 356-368.

NICHOLSON, C. AND LLINAS, R. (1971) Field potentials in the Alligator cerebellum and theory of their relationship to Purkinje cell dendritic spikes. J. Neurophysiol. 34: 509-531.

NOBLE, D. (1966) Applications of Hodgkin-Huxley equations to excitable tissues. Physiol. Rev. 46: 1-50.

PARNAS, I. (1979) Propagation in nonuniform neurites: Form and Function in Axons. In: The Neurosciences: Fourth Study Program, edited by F.O.Schmidt and F.G.Worden. Cambridge, MA:MIT Press, p. 499-512.

PITTS, W. (1952) Investigations on synaptic transmission. In: Cybernetics, Trans. Ninth Conf., edited by H. von Foerster. New York: Josiah Macy, p. 159-162.

RAISMAN, G., COWAN, W.M. AND POWELL, T.P.S. (1965) The extrinsic afferent, commissural and association fibres of the hippocampus. Brain Res. 88: 963-998.

RICHARDSON, T.L., TURNER, R.W. AND MILLER J.J. (1984a) Extracellular fields influence transmembrane potentials and synchronization of hippocampal neuronal activity. Brain Res. 294: 255-262.

RICHARDSON, T.L., TURNER, R.W. AND MILLER J.J. (1984b) Extracellular voltage gradients and ephaptic interactions in the hippocampal formation. Soc. Neurosci. Abstr. 14, 204.

RINGHAM, G.L. (1971) Origin of nerve impulse in slowly adapting stretch receptor of crayfish. J. Neurophysiol. 34: 773-784.

SCHAFFER, K. (1892) Beitrag zum Histologie der Ammonshornformation. Archiv. fur Mikroskopische Anatomie 39: 611-632.

SCHMALBRUCH, H. AND JAHNSEN, H. (1981) Gap junctions on CA3 pyramidal cells of guinea-pig hippocampus shown by freeze-fracture. Brain Res. 217: 175-178.

SCHWARTZKROIN, P.A. (1975) Characteristics of CA1 neurons recorded intracellularly in the hippocampal <u>in vitro</u> slice preparation. Brain Res. 85: 423-436.

SCHWARTZKROIN, P.A. (1977) Further characteristics of hippocampal CA1 cells *in vitro.* Brain Res. 128: 53-68.

SCHWARTZKROIN, P.A. AND MATHERS, L.H. (1978) Physiological and morphological identification of a nonpyramidal hippocampal cell type. Brain Res. 157: 1-10.

SCHWARTZKROIN, P.A. AND PRINCE, D.A. (1980) Changes in excitatory and inhibitory synaptic potentials leading to epileptogenic activity. Brain Res. 183: 61-76.

SCHWARTZKROIN, P.A. AND SLAWSKY, M. (1977) Probable calcium spikes in hippocampal neurons. Brain Res. 135: 157-161.

SCHWARTZKROIN, P.A. AND WYLER, A.R. (1979) Mechanisms underlying epileptiform burst discharge. Ann. Neurol. 7: 95-107.

SEGAL, M. AND BARKER, J.L. (1984) Rat hippocampal neurons in culture: potassium conductances. J. Neurophysiol. 51: 1409-1433.

SKREDE, K.K AND WESTGAARD, R.H. (1971) The transverse hippocampal slice: a well-defined cortical structure maintained *in vitro.* Brain Res. 35: 589-593.

SMITH, T.G., Jr. (1983) Sites of action potential generation in cultured vertebrate neurons. Brain Res. 288: 381-383.

SMITH, T.G., Jr., FUTAMACHI, K. AND EHRENSTEIN, G. (1982) Site of action potential generation in a giant neuron of *Aplysia californica.* Brain Res. 242: 184-189.

SOMOGYI, P., NUNZI, M.G. AND SMITH, A.D. (1983) A new type of specific interneuron in the monkey hippocampus forming synapses with the axon initial segments of pyramidal cells. Brain Res. 259: 137-142.

SPENCER, W.A. AND KANDEL, E.R. (1961a) Elecrophysiology of hippocampal neurons. III. Firing level and time constant. J. Neurophysiol. 24: 260-271.

SPENCER, W.A. AND KANDEL, E.R. (1961b) Electrophysiology of hippocampal neurons. IV. Fast pre-potentials. J. Neurophysiol. 24: 272-285.

SPERTI, L., GESSI, T. AND VOLTA, F. (1967) Extracellular potential field of antidromically activated CA1 pyramidal neurons. Brain Res. 3: 343-361.

TAYLOR, C.P. AND DUDEK, F.E. (1984) Excitation of hippocampal pyramidal cells by an electrical field effect. J. Neurophysiol. 52: 126-142.

TIELEN, A.M., LOPES da SILVA, F.H. AND MOLLEVANGER, W.J. (1981) Differential conduction velocities in perforant path fibres in guinea-pig. Exp. Brain Res. 42: 231-233.

TOMBOL, T., BABOSA, M., HAJDU, F. AND SOMOGYI, Gy. (1979) Interneurons: an electron microscopic study of the cat's hippocampal formation, II. Acta Morphologica Acad. Sci. Hung. 27: 297-313.

TRAUB, R.D. AND LLINAS, R. (1979) Hippocampal pyramidal cells: significance of dendritic ionic conductance for neuronal function and epileptogenesis. J. Neurophysiol. 42: 476-496.

TURNER, D.A. (1984) Segmental cable evaluation of somatic transients in hippocampal neurons (CA1, CA3, and Dentate). Biophys. J. 46: 73-84.

TURNER, D.A. AND SCHWARTZKROIN, P.A. (1980) Steady-state electrotonic analysis of intracellularly stained hippocampal neurons. J. Neurophysiol. 44: 184-199.

TURNER, R.W., BAIMBRIDGE, K.G. AND MILLER, J.J. (1982) Calcium-induced long-term potentiation in the hippocampus. J. Neurosci. 7: 1411-1416.

TURNER, R.W., RICHARDSON, T.L. AND MILLER, J.J. (1984) Ephaptic interactions contribute to paired pulse and frequency potentiation of hippocampal field potentials. Exp. Brain Res. 54: 567-570.

WESTRUM, L.E. AND BLACKSTAD, T.W. (1962) An electron microscopic study of the stratum radiatum of the rat hippocampus (Regio Superior, CA1) with particular emphasis on synaptology. J. Comp. Neurol. 119: 281-309.

WONG, R.K.S. AND PRINCE, D.A. (1978) Participation of calcium spikes during intrinsic burst firing in hippocampal neurons. Brain Res. 159: 385-390.

WONG, R.K.S. AND PRINCE, D.A. (1979) Dendritic mechanisms underlying penicillin-induced epileptiform activity. Science 204: 1228-1231.

WONG, R.K.S., PRINCE, D.A. AND BASBAUM, A.I. (1979) Intradendritic recordings from hippocampal neurons. Proc. Natl. Acad. Sci. USA 76: 986-990.